
بسم الله الرحمن الرحيم

مجلة جامعة الملك عبدالعزيز: العلوم الهندسية، م ٣٢ ع ٢، ١٠٠ صفحة (١٤٤٤هـ/٢٠٢٢م) ردمد ١٠٤٧-١٣١٩
رقم الإيداع : ٠٣٠٠ / ١٤

مجلة جامعة الملك عبد العزيز

العلوم الهندسية

المجلد ٣٢ العدد ٢
٢٠٢٢م

مركز النشر العلمي
جامعة الملك عبد العزيز
ص ب : ٨٠٢٠٠ ـ جدة : ٢١٥٨٩
المملكة العربية السعودية
http://spc.kau.edu.sa

مجلة جامعة الملك عبدالعزيز: العلوم الهندسية، م ٣٢ ع ٢، ١٠٠ صفحة (١٤٤٤هـ/٢٠٢٢م) ردمد ١٠٤٧-١٣١٩
رقم الإيداع : ٠٣٠٠ / ١٤

المحتويات

الصفحة

القسم العربي

تأثيرات حركة المكبس على الطاقة الناتجة من آلات دورة ستيرلينغ

ماجد معلا الحازمي

الهندسة الميكانيكية، جامعة الملك عبد العزيز

جدة، المملكة العربية السعودية

مستخلص. تستخدم هذه الورقة نموذجًا بسيطًا لتقدير الطاقة المنتجة من محرك ستيرلينغ عند إعطاء المكابس حركة مستمرة بنمط محدد وتردد ثابت وانزياح طور متغير لنسب درجة حرارة تشغيلية مختلفة. تم فحص نمطين للحركة المستمرة ، الجيبية والجيبية المعدلة ، ضد الحركة المتقطعة للدورة المثالية. الطاقة الناتجة من المحركات ذات المكابس المتحركة باستمرار أقل من الطاقة الناتجة من الدورة المثالية. تنخفض نسبة الطاقة مع زيادة نسبة درجة الحرارة. أعلى طاقة منتجة بنسبة درجة حرارة ١,٥ ، هي ٩٧٪ من الدورة المثالية وتحدث عند تحول طور قدره ٨١ درجة. يعمل التشغيل عند ±١٠ درجة من أعلى حالة تغيير طور الطاقة على تقليل طاقة المنتجة بنسبة ٥-٧٪. بالنسبة للحركة الجيبية المعدلة ، تكون أعلى طاقة منتجة ٨٨٪ عندما يكون تغيير الطور ٥٥ درجة. يعمل التشغيل عند رجات من أقصى حالة تغيير طور الطاقة على تقليل طاقة المنتجة بنسبة ٢٪. علاوة على ذلك ، عند فرق الطور المتسبب في أعلى طاقة منتجة، تنخفض نسبة الطاقة من ٩٧٪ إلى ٩٣٪ ، للحركة الجيبية حيث تتغير نسبة درجة حرارة الدورة من ١,٥ إلى ٣. أما بالنسبة للحركة الجيبية المعدلة فإن الطاقة المنتجة تنخفض من ٨٨٪ إلى ٧٨ ٪ من قيمتها العليا.

[20] **Červenka L.,** Idealization of the real Stirling cycle, MECCA Journal of Middle European construction and design of cars, Vol. 14 No. 03 (2016).

[21] **Briggs M. H.** Improving power density of free-piston Stirling engines, 14th International Energy Conversion Engineering Conference, July 25-27, Salt Lake City, Utah USA, (2016), https://doi.org/10.2514/6.2016-5016.

[22] **Gopal, V.K**, "Active Stirling Engine ", PhD Theses University of Canterbury. Electrical and Computer Engineering, New Zealand.

[23] **Craun M., Bamieh, B**. Control-Oriented Modeling of the Dynamics of Stirling Engine Regenerators, Journal of dynamic systems, measurement, and control, ASME Transactions, 140(4): 041001, Paper No: DS-15-1652 (2018) https://doi.org/10.1115/1.4037838

[24] **Masser, R.; Khodja, A**.; Scheunert, M.; Schwalbe, K.; Fischer, A.; Paul, R.; Hoffmann, K.H. Optimized Piston Motion for an Alpha-Type Stirling Engine. Entropy, 22, 700 (2020).

[25] **Podešva J, Poruba Z.** "The Stirling engine mechanism optimization." Perspectives in Science. 1 (7):341-6, (2016).

[26] **Scheunert, M., Masser, R., Khodja, A., Paul, R., Schwalbe, K., Fischer, A. and Hoffmann, K.H**., Power-optimized sinusoidal piston motion and its performance gain for an Alpha-type Stirling engine with limited regeneration. Energies, 13(17), p.4564. (2020) doi:10.3390/en13174564

[27] **Gussoli M.K., de Oliveira JC, Higa M.** Investigation on volume variation for alpha Stirling engines on isothermal model. Revista de Engenharia Térmica. 19 (2):10-6 (2020).

[28] **Nicol-Seto, M. and Nobes, D**., Experimental evaluation of piston motion modification to improve the thermodynamic power output of a low temperature gamma Stirling engine, E3S Web of Conferences 313, 04002, 19th International Stirling Engine Conference, (2021)

University of California; Berkeley, (2016).

[5] **Lu, D., Bai, Y., Zhao, Y., Dong, X., Gong, M., Luo, E., Chen, G., Xu, Q. and Shen, J.**, Experimental investigations of an absorption heat pump prototype with intermediate process for residential district heating. Energy Conversion and Management, 204, p. 112323 (2020).

[6] **Urieli I., and Berchowitz D.M.,** Stirling cycle engine analysis, A. Hilger, (1984).

[7] **Hu JY, Luo EC, Dai W, and Zhang LM.** Parameter sensitivity analysis of duplex Stirling coolers. Applied Energy.190:1039-46 (2017).

[8] **Pan QW, and Wang RZ.** Study on boundary conditions of adsorption heat pump systems using different working pairs for heating application. Energy Conversion and Management, 154:322–35 (2017).

[9] **Doğan B., Ozturk M.M., and Erbay L.B.,** Effect of working fluid on the performance of the duplex Stirling refrigerator. Journal of Cleaner Production,189:98–107 (2018).

[10] **Li X, Liu B, Yu G, Dai, W., Hu, J., Luo, E. and Li, H.** Experimental validation and numeric optimization of a resonance tube-coupled duplex Stirling cooler. Applied Energy, 207:604–12 (2017).

[11] **Chen, H., and Longtin, J.P.,** Performance analysis of a free-piston Vuilleumier heat pump with dwell-based motion. Applied Thermal Engineering, 140:553–63 (2018).

[12] **Wong, H. M., and S. Y. Goh**. Experimental comparison of sinusoidal motion and non-sinusoidal motion of rise-dwell-fall-dwell in a Stirling engine. Journal of Mechanical Engineering and Sciences 14, (3): 6971-6981 (2020).

[13] **Li RJ, Grosu L, Queiros-Condé D.** Losses effect on the performance of a Gamma type Stirling engine, Energy Conversion Management, 114:28–37 (2016).

[14] **Liao C, Jiang T, Hofbauer P, Ye W, Liu J, Luo B, and Huang Y.** Simplified model and analysis for the performance of Hofbauer-Vuilleumier heat pump. International Journal of Refrigeration. 1 (103) 126-34 (2019).

[15] **Shang, S., Li, X., Wu, W., Wang, B. and Shi, W.**, Energy-saving analysis of a hybrid power-driven heat pump system. Applied Thermal Engineering, 123, pp.1050-1059 (2017).

[16] **Dogkas, G. and Rogdakis, E.,** A review on Vuilleumier machines. Thermal Science and Engineering Progress, 8: 340-354 (2018).

[17] **Hèyihin, A.G., Awanto, C., Anjorin, M. and Lanzetta, F.,** Thermodynamic analysis of the Stirling Duplex machine. In Advanced Engineering Forum. 30:. 80-91. Trans Tech Publications Ltd (2018).

[18] **Guo, T., Jiang, T., Zou, P., Luo, B., Hofbauer, P., Liu, J. and Huang, Y.,** Analytical model for Vuilleumier cycle. International Journal of Refrigeration, 113:126-135. (2020).

[19] **Ranieri, S., Prado, G.A. and MacDonald, B.D**., Efficiency reduction in Stirling engines resulting from sinusoidal motion. Energies, 11(11), p.2887. (2018).

https://doi.org/10.3390/en11112887

Conclusions

The piston motion effect on the power output from a Stirling cycle machine is evaluated. The power produced when the pistons have continuous motion is lower than the power produced from the ideal cycle for all operational temperature ratios. The power ratio decreases as the temperature ratio increases. For a temperature ratio of 1.5, the highest produced power is 97% of the ideal cycle and occurs that occurs and phase-shift of 81°. Operating at ±10° off the highest power phase shift condition reduces the output power by 5-7%. For modified sinusoidal motion, the highest output power is 88% when the phase shift is 55°. Operating at ±10° off the maximum power phase shift condition reduces the output power by 2%. Moreover, at the highest output phase shift condition, the power output ratio drops from 97% to 93%, for sinusoidal motion as the cycle temperature ratio changes from 1.5 to 3. For modified sinusoidal motion, the output power drops from 88% to 78% at the highest phase shift condition.

Nomenclature

A	Cross sectional Area of the working space
B_1&B_2	Parameters describing the modified motion pattern Eq.(22)-(23)
c_p	Fluid specific heat at constant pressure
c_v	Fluid specific heat at constant volume
M	Total mass of the working fluid filling the machine
m	Mass of the working fluid inside each compartment of the machine
P	Pressure
Q	Heat
R	Gas constant
S	Entropy
T	Temperature
V	Volume
x	Position of the pistons
W	Work

Symbol

α	Phase shift
γ	Specific heat ratio
ω	Frequency

Subscripts

c	Compression space
e	Expansion space
dc	Dead volume compression side
de	Dead volume expansion side
in	Inlet
out	Outlet
h	Heat exchanger at hot side
k	Heat exchanger at cold side

References

[1] **She X., Cong L., and Nie B.**, Energy-efficient and-economic technologies for air conditioning with vapor compression refrigeration: a comprehensive review. Applied Energy, 232:157–86 (2018).

[2] **Abas N., Kalair A.R., and Khan N.**, Natural and synthetic refrigerants, global warming: a review. Renewable and Sustainable Energy Reviews, 90:557–69 (2018).

[3] Sadovskaia K, Bogdanov D, Honkapuro S, and Breyer, C. Power transmission and distribution losses–A model based on available empirical data and future trends for all countries globally. International Journal of Electrical Power and Energy Systems. 107:98–109 (2019).

[4] **He M.M.** Stirling engine for solar thermal electric generation.

Operating at ±10° of the maximum power phase shift condition reduces the output power by 2%.

Moreover, at the highest output phase shift condition, the power output ratio drops from 97% to 93%, as the cycle temperature ratio changes from 1.5 to 3, for sinusoidal motion pattern. For modified sinusoidal motion, the output power drops from 88% to 78% at the highest phase shift condition

.

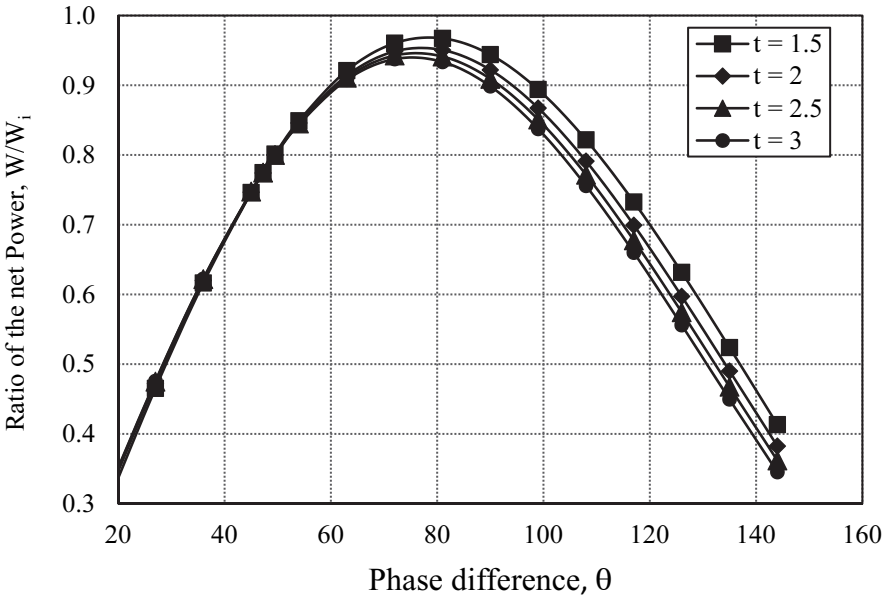

Figure 5. Variation of output power with phase shift for different temperature ratios (Sinusoidal motion).

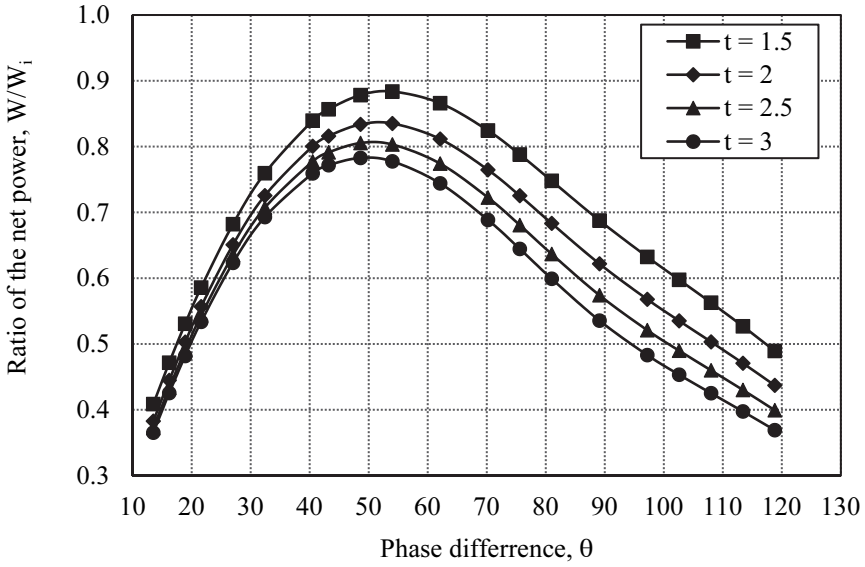

Figure 6. Variation of output power with phase shift for different temperature ratios (Modified motion).

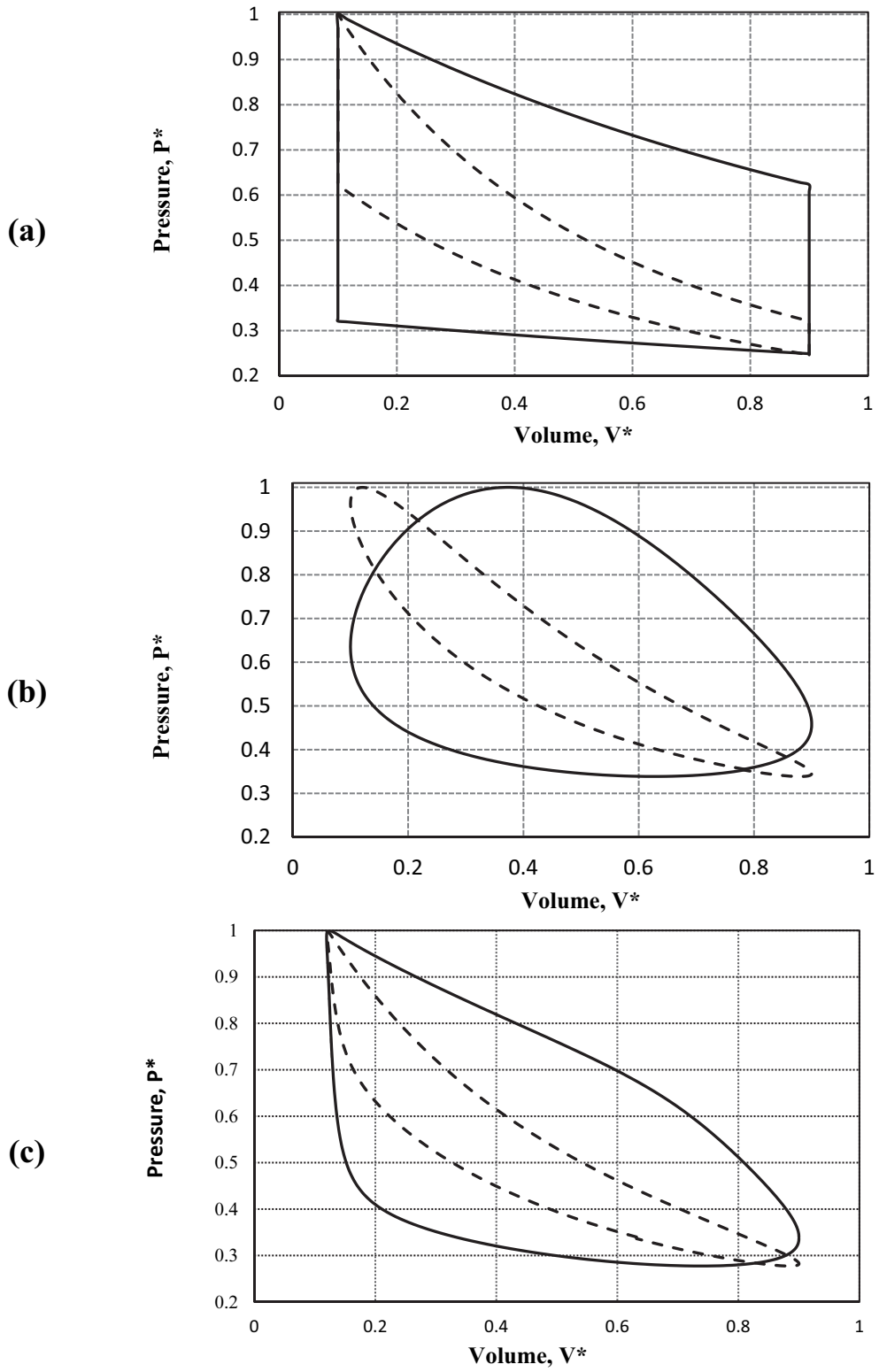

Figure 4. The Stirling cycle as P V plot fir the three piston's motions
(__ compression, _ _ _ compression)

Similarly, Fig. 6 shows the power output ratio when the piston has the modified motion given by Eqs. (22)-(23) and Fig. 3 (c). The highest output power reached is 88% of the power from an ideal cycle and obtained a phase shift of 55^{o}.

(a)

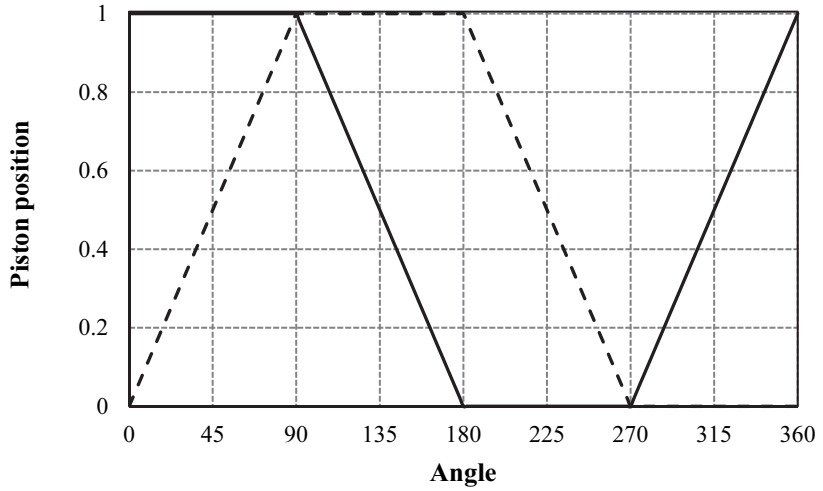

(b)

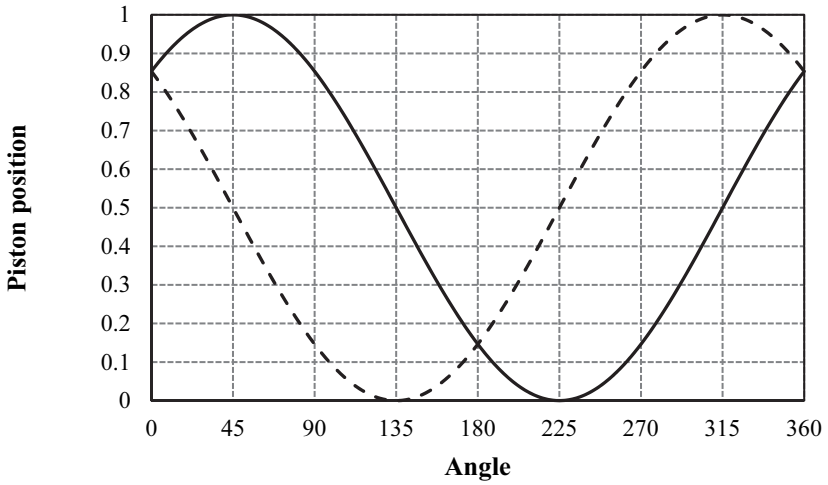

(c)

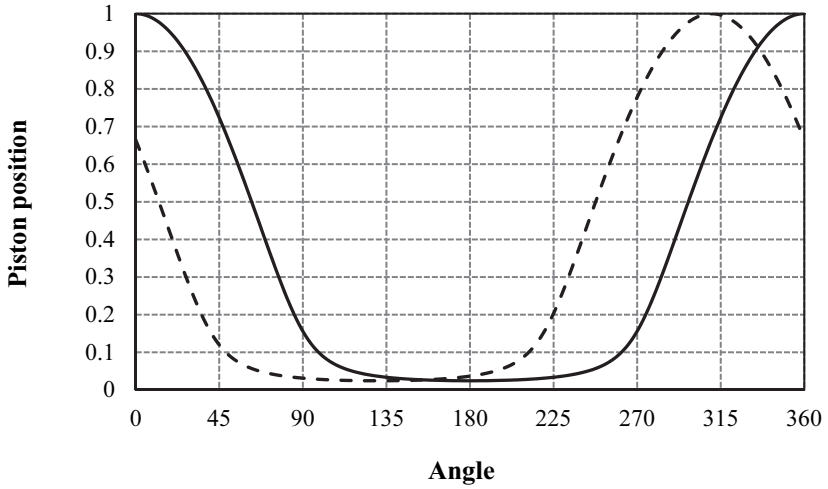

Figure 3. The three examined piston's motions
(__ compression, _ _ _ compression)

$$dP = \frac{-\gamma P\left(\frac{dV_c}{T_c}+\frac{dV_e}{T_e}\right)}{\frac{V_c}{T_c}+\gamma\left(\frac{V_{hc}}{T_{hc}}+\frac{V_r}{T_r}+\frac{V_e}{T_e}\right)+\frac{V_e}{T_e}} \quad (14)$$

The change in the temperature of the fluid inside the compression and expansion spaces can be related to the change in the mass, volume, and pressure through the ideal gas law as

$$\left.\begin{aligned} dT_c &= T_c\left(\frac{dP}{P}+\frac{dV_c}{V_c}-\frac{dm_c}{m_c}\right)\\ dT_e &= T_e\left(\frac{dP}{P}+\frac{dV_e}{V_e}-\frac{dm_e}{m_e}\right)\end{aligned}\right\} \quad (15)$$

The above analysis shows how the properties of the working fluid are related and calculated once the motion of each piston is known. The expansion and compression work can then be evaluated as

$$\left.\begin{aligned} dW_c &= PdV_c\\ dW_e &= PdV_e\\ dw &= dW_c + dW_e\end{aligned}\right\} \quad (16)$$

$$W = W_c + W_e \quad (17)$$

Results and discussions

The model presented above yields the power output from Stirling engine when the motion of the pistons is defined. The model power output is evaluated for three different motion patterns given by Eqs. (18)-(23). Equations (18) and (19) show the first pattern, it is the discontinues motion of the ideal Stirling cycle. This motion is plotted in a dimensionless scale in Fig 3 (a) for the compression piston, x_{1c}, and the expansion piston x_{1e}.

$$x_{1c} = \begin{cases} 1 & 0 \le t \le \frac{\pi}{2\omega}\\ 2-2\frac{\omega t}{\pi} & \frac{\pi}{2\omega} \le t \le \frac{\pi}{\omega}\\ 0 & \frac{\pi}{\omega} \le t \le \frac{3\pi}{2\omega}\\ 2\frac{\omega t}{\pi}-3 & \frac{3\pi}{2\omega} \le t \le \frac{\pi}{\omega}\end{cases} \quad (18)$$

$$x_{1e} = \begin{cases} \frac{2\omega}{\pi}t & 0 \le t \le \frac{\pi}{2\omega}\\ 1 & \frac{\pi}{2\omega} \le t \le \frac{\pi}{\omega}\\ 3-2\frac{\omega t}{\pi} & \frac{\pi}{\omega} \le t \le \frac{3\pi}{2\omega}\\ 0 & \frac{3\pi}{2\omega} \le t \le \frac{\pi}{\omega}\end{cases} \quad (19)$$

Similarly, equations (20) and (21) show the second motion pattern, it is a typical continuous sinusoidal motion as plotted in a dimensionless scale in Fig 3 (b) with a phase shift, α, between the compression piston, x_{2c}, and the expansion piston x_{2e}.

$$x_{2c} = 1 + \cos(\omega t) \quad (20)$$

$$x_{2e} = 1 + \cos(\omega t + \alpha) \quad (21)$$

Similarly, equations (22) and (23) show the third motion pattern, it is a modified sinusoidal motion. It consists of two sin functions combined by two constants B_1 and B_2 as plotted in a dimensionless scale in Fig 3 (c) with a phase shift, α, between the compression piston, x_{3c}, and the expansion piston x_{3e}.

$$x_{3c} = \frac{B_1\cos(\omega t)+\sqrt{\left(B_2^2-B_1^2\sin^2(\omega t)\right)}}{B_1+B_2} \quad (22)$$

$$x_{3e} = \frac{B_1\cos(\omega t+\alpha)+\sqrt{\left(B_2^2-B_1^2\sin^2(\omega t+\alpha)\right)}}{B_1+B_2} \quad (23)$$

where B_1 and B_2 are constant parameters to define the piston's motion profile and the dwelling duration (angle) [25].

Figure 3 shows the position of the pistons during a full working cycle for discontinuous ideal pattern as well as for the two continuous motions with a specified phase shift between the compression and expansion pistons. Similarly, Fig. 4 shows the Stirling cycle resulted from such motions, plotted on the P-V diagram, at the highest work output condition.

Figure 5 shows the power output for the sinusoidal motion, Eqs. (20)-(21) and Fig. 3 (b), as a ratio to the power produced by an ideal cycle operating at the same temperature ratio, t. The results show that low temperature ratios bring the output power closer to the output of ideal cycle for all phase shift angles. The highest output power reached is 97% of the ideal cycle, it occurs at a phase shift, α, of 81°. Moreover, the output power changes with the phase shift. Operating at ±10° of the maximum power phase shift condition reduces the output power by 5-7%.

$$\left.\begin{aligned} x_c(t) &= f_c(t) \\ x_e(t) &= f_e(t+\alpha) \end{aligned}\right\} \quad (1)$$

The volume of each working space depends on the piston position as,

$$\left.\begin{aligned} V_c(t) &= A_c\, x_c(t) + V_{dc} \\ V_e(t) &= A_e\, x_e(t) + V_{de} \end{aligned}\right\} \quad (2)$$

Note that A_c and A_e are the cross-sectional areas of the compression and expansion spaces, respectively, similarly, V_{dc} and V_{de} are the dead volumes in the compression and expansion spaces, respectively. Although the mass of the working fluid in each compartment changes during operation, the total mass filling up all the compartments of the Engine is constant,

$$M_{tot} = m_c + m_k + m_r + m_h + m_e \quad (3)$$

But dM_{tot}=0 Therefore,

$$dm_c + dm_k + dm_r + dm_h + dm_e = 0 \quad (4)$$

The ideal gas law relates the mass of the fluid occupying each compartment of the engine to the volume, pressure and temperature of each compartment as follows,

$$\left.\begin{aligned} m_c &= \frac{P\,V_c}{R\,T_c} \\ m_k &= \frac{P\,V_k}{R\,T_k} \\ m_r &= \frac{P\,V_r}{R\,(T_e - T_c)\,ln\left(\frac{T_e}{T_c}\right)} \\ m_h &= \frac{P\,V_h}{R\,T_h} \\ m_e &= \frac{P\,V_e}{R\,T_e} \end{aligned}\right\} \quad (5)$$

Substituting the relations from Eq. (5) into Eq. (3) yields,

$$M_{tot} = \frac{P\,V_c}{R\,T_c} + \frac{P\,V_k}{R\,T_k} + \frac{P\,V_r}{R\,(T_e - T_c)\,ln\left(\frac{T_e}{T_c}\right)} + \frac{P\,V_h}{R\,T_h} + \frac{P\,V_e}{R\,T_e} \quad (6)$$

To obtain the mass flow rate entering or leaving each compartment, one may use the first law of thermodynamics in the differential form. In the absence of the variations in kinetic and potential energy, and assuming the working fluid to be an ideal gas the first law of thermodynamics in the differential form is

$$dE_{cv} = \delta Q - \delta W + dH_{in} - dH_{out} \quad (7)$$

The heat exchangers, the regenerator, and each working space, at every instant, either receive or deliver fluid, moreover, the compression space is adiabatic, and the work is a boundary work $W = P\,dV$, therefore the first law of thermodynamics, Eq. (7), becomes,

$$c_v\; d(m_c T_c) = -P\,dV_c + c_p\,T_c\,dm_c \quad (8)$$

Note that for ideal gas $m\,T = \frac{P\,V}{R}$, therefor Eq (8) can be rewritten as

$$\frac{c_v}{R}\,[P\,dV_c + V_c\,dP] = -P\,dV_c + c_p\,T_c\,dm_c \quad (9)$$

Rearranging Eq. (9), the change in the mass inside the compression space becomes

$$dm_c = \frac{\frac{V_c}{\gamma}dP + P\,dV_c}{RT_c} \quad (10)$$

Similarly, the change in the mass in the expansion space is,

$$dm_e = \frac{\frac{V_e}{\gamma}dP + P\,dV_e}{RT_e} \quad (11)$$

The volume and the temperature of each heat exchanger and the regenerator are fixed, therefore the ideal gas law gives the change in the mass inside them as

$$\left.\begin{aligned} dm_k &= \frac{V_k}{RT_k}dP \\ dm_r &= \frac{V_r}{RT_r}dP \\ dm_h &= \frac{V_h}{RT_h}dP \end{aligned}\right\} \quad (12)$$

The mass balance on the heat exchangers gives,

$$\left.\begin{aligned} m_{ck} &= -dm_c \\ m_{kr} &= m_{ck} - dm_c \\ m_{eh} &= dm_e \\ m_{rh} &= m_{he} - dm_h \end{aligned}\right\} \quad (13)$$

Substituting from Eqs. (10)-(13) into Eq.(4), the change in the pressure in the machine is,

cycle output power may increase when the pistons motion adjusted to a modified type of a sinusoidal motions. An optimum performance should balance between maximizing the output power and the overall performance [24-25]. A way to minimize the deviation between the sinusoidal and the discontinuous motion to control the phase shift between the motion of the compression piston and the expansion piston [26-28].

The aim of the present paper is to show the effect of the motion pattern on the performance of a Stirling engine. The heat addition and heat rejection in Stirling cycle occur along isothermal processes, therefore, the power output is chosen to be the performance indicator to compare effect of different motion patterns. The two pistons are given are prescribed motion with a fixed frequency and a phase shift. Two different motion patterns, sinusoidal and modified sinusoidal, are examined against the discontinuous motion of the ideal cycle, at different operational temperature ratios and different angles of phase shifts.

2. Analysis

Figure 2 shows a schematic of a Stirling engine that consists of an expansion space, a hot heat exchanger, a regenerator, a cold heat exchanger, and a compression space. The expansion and compression spaces are called working spaces. Each working space is a piston moving inside a cylindrical chamber and encloses ideal gas as the working fluid. As the pistons move the fluid transfers from one expansion spaces through the two heat exchangers and the regenerator until it reaches the other working space.

In details, as pistons move, the volume and the pressure in each compartment of the machine change. The pressure difference causes the mass to move from one side of the machine to the other. Urieli and Berchowitz [6] presented a simple model for these changes, based on which a theoretical model to relate the machine performance is presented below. The analysis assumes that the working is ideal gas, perfect regenerator, isothermal heat exchangers, and adiabatic hot and the cold working spaces.

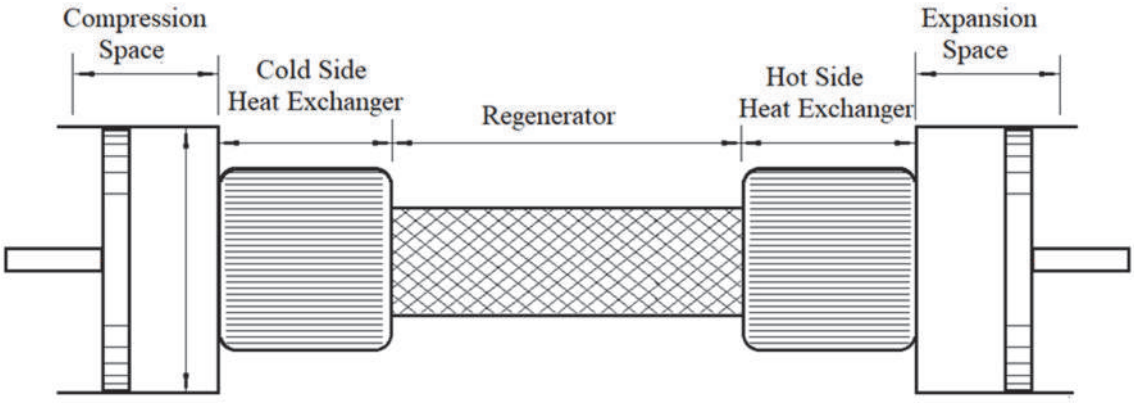

Figure 2. Schematic of a typical Stirling Engine

The model starts by describing the motion, x_c and x_e of the compression and expansion pistons, respectively, as a function of time. There is a time lag (phase shift), α, between the motion of the two pistons, Eq. (1).

between the two working spaces absorbs and rejects heat as it moves between the two working spaces.

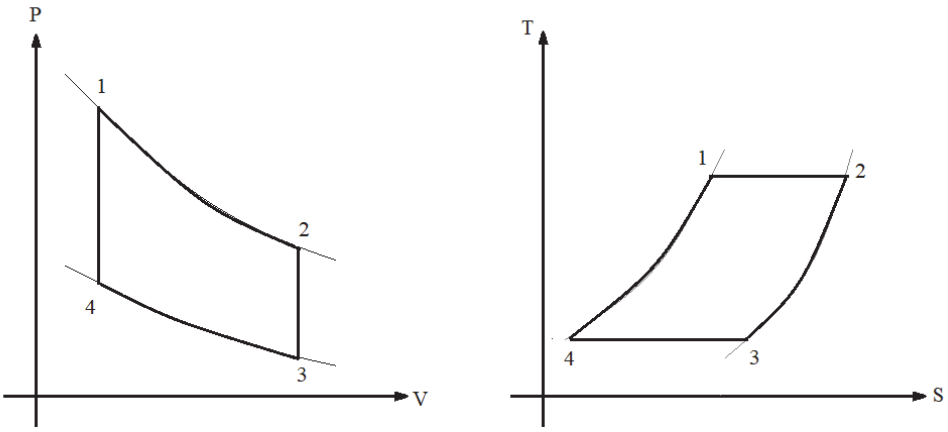

(a) (b)

Figure 1 Stirling Cycle, (a) PV diagram, (b) TS diagram

Efforts to improve the performance of Stirling machines never stop, several attempts have been reported in the literature [7-11]. These include optimizing operating temperature and pressure ratios [7-8], comparing different working fluids [9], examining the effect of the ratio of the dead volume and the details of the piston motion [10-12]. Results of both experimental and analytical studies on the performance of Stirling engines [13], Stirling heat pumps [14-15], and Stirling liquefiers and coolers [16-18] are available.

The pistons of the ideal Stirling cycle have a discontinues motion, the pistons in real Stirling machines, however, move in continuous motion. Discontinues motion is difficult to maintain, therefore, sinusoidal motion is usually the chosen pattern. Although Sinusoidal motion is easy to maintain, it yields a lower performance compared to discontinuous motion. This is expected because the pistons speed in sinusoidal motion is slower near the cylinder's two dead centers and faster near the middle of the stroke. This does not happen in the discontinuous motion. The difference in the motion pattern determines the change in the mass flow rate of the working fluid entering to and leaving (or dwelling) the working spaces the ultimately affects the performance of the machine because. The details the motion of the pistons along with the type of the thermal process determine the changes in temperature and pressures of the working fluid throughout the different states of the cycle, and therefore, the shape of the thermodynamic cycle.

Ranieri et al [19] reported a 65% reduction in the efficiency when the pistons of an alpha type Stirling engine have a sinusoidal motion. Červenka [20] reported a power drop by 82% when pistons move in sinusoidal motion compared to the discontinuous motion of the ideal cycle. Briggs [21] achieved 14% power increase by manipulated electrically the sinusoidal volume change of a free-piston Stirling engine. By using a linear electric motor Gopal [22] reported a 15% increase in efficiency. Craun and Bemiah [23] reported that a non-sinusoidal motion enhances the performance of the Stirling engine by 40% more than to sinusoidal motion. Masser et al [24] reported that the

JKAU: Eng. Sci., Vol. **32** No. 2, pp: 89 – 100 (1444 A.H. / 2022 A.D.)
Doi: 10.4197/Eng. 32-2.7

Effects of Piston motion on the power generated by Stirling cycle machines

Majed M. Alhazmy*

Mechanical Engineering, King Abdulaziz University, Jeddah, Saudi Arabia

Abstract. This paper uses a simple model to estimate the power output of Stirling engine when giving the pistons a continuous motion with a prescribed pattern, fixed frequency, and a variable phase shift for different operational temperature ratios. Two continuous motions patterns, sinusoidal and modified sinusoidal, have been examined against the discontinuous motion of the ideal cycle. The power produced from engines having continuously moving pistons is lower than the power produced from the ideal cycle. The power ratio decreases as the temperature ratio increases. the highest produced power with a temperature ratio of 1.5, is 97% of the ideal cycle and it occurs at a phase-shift of 81°. Operating at ±10° off the highest power phase shift condition reduces the output power by 5-7%. For modified sinusoidal motion, the highest output power is 88% when the phase shift is 55°. Operating at ±10° off the maximum power phase shift condition reduces the output power by 2%. Moreover, at the highest output phase shift condition, the power output ratio drops from 97% to 93%, for sinusoidal motion as the cycle temperature ratio changes from 1.5 to 3. For modified sinusoidal motion, the output power drops from 88% to 78% at the highest phase shift condition.

Keywords. Stirling machines, Piston's discontinuous motion, Piston's continuous motion Performance of Stirling machines

1. Introduction

Oil high prices, pollution control, and global warming reducing policies call for replacing the traditional power systems with environmentally safe power sources [1-3]. Stirling cycle machines operated by solar energy or waste heat are promising future solutions for engines [4] and coolers [5]. Stirling machines are regenerative closed cycle machines that have low noise levels and high efficiency and can operate at low temperatures or at elevated temperatures [6].

Figure 1 shows an ideal Stirling cycle that consists of four reversible processes performed by inviscid ideal working fluid. The four processes of the Stirling cycle are isochoric heat addition, isothermal expansion, isochoric heat rejection and isothermal compression. Figure 2 shows a schematic of the Stirling machine. The machine has two pistons each is contained inside a separate isothermal cylinder. The piston-cylinder arrangement is called working space that is maintained at a specific temperature. The two cylinders are connected by an ideal regenerator. The working fluid shuttles

* Corresponding author: mhazmy@kau.edu.sa

تدهور أنابيب المكثف في محطة طاقة نووية معرضة لظروف عملية قاسية

ضياء شجاع العثماني

الهندسة النووية، جامعة الملك عبد العزيز

جدة المملكة العربية السعودية

مستخلص. تستخدم أنابيب الألمنيوم والنحاس في المكثفات والمبادلات الحرارية لمحطات الطاقة النووية منذ زمن بعيد بسبب حقيقة أن هذه المادة أرخص نسبيًا. لكن سجل فشل الأنبوب يشير إلى معدل فشل أعلى مع هذه المادة. من المشاكل الشائعة جدا تسرب أنابيب المكثف النحاسية. عادة مع التشغيل الممتد للمكثفات لمدة ٢٠ عامًا أو نحو ذلك، يمكن للمرء أن يتوقع استبدال حوالي ١٥-٢٠ ٪ من أنابيب المكثف بسبب التسرب .يكشف تحليل فشل الأنابيب أن أنابيب المنطقة المركزية عانت من هجوم تآكل الأمونيا بينما عانت المناطق المتبقية من التآكل الداخلي والتآكل ورواسب الكائنات البحرية. على الرغم من أن تركيز الأمونيا والأكسجين منخفض بدرجة كافية لإحداث أي تآكل للأنابيب، إلا أن التركيز العالي من الأمونيا والأكسجين يمكن أن يتطور في أقسام تبريد الهواء في المكثفات، مما قد يتسبب في تآكل سبائك النحاس .أحد الأسباب المهمة لتسرب أنابيب المكثف هو التآكل الأموني. ومع ذلك، يمكن تقليل هذا التآكل الأموني عن طريق التحكم في درجة الحرارة جنبًا إلى جنب مع طرق الوقاية المختلفة من التآكل. يُلاحظ أنه مع زيادة درجة الحرارة، يزداد معدل التآكل. ومع ذلك، فإن الاتجاه الأخير نحو جميع المركبات المتطايرة التي تستخدم مركبات الأمونيا والأمونيا للتحكم في كيمياء مياه التغذية في محطة الطاقة النووية، يبرز الحاجة إلى الاختيار الدقيق لسبائك أنابيب المكثف المقاومة للتآكل. يستخدم الهيدرازين بشكل شائع في نظام محطات توليد الطاقة البخارية لإزالة O2 وضبط درجة الحموضة وتقليل معدل تآكل الفولاذ. يتم إذابة هذه المواد الكيميائية بسهولة في مياه تغذية الغلايات .الطريقة الحالية المستخدمة في مكثفات محطة توليد الكهرباء هي الحماية الكاثودية القربانية .(SCP) أيضًا، تم إجراء عدد من التجارب في المعمل لحماية التآكل باستخدامSCP ، وكذلك الحماية الكاثودية للتيار القسري (ICCP) ، أي بتطبيق تيار صغير أقل من ١ .mA / dm2وجد أن ICCP أفضل بكثير من .SCP على ما يبدو، تم العثور على Zn على أنه مادة أنود مناسبة تستخدم في.ICCP

الكلمات المفتاحية: المكثفات، محطات الطاقة النووية ، تسرب الأنابيب ، التآكل ، الحماية الكاثودية القربانية، ملخص تنفيذي

[16] **Kear, G., Barker, B., Stokes, K. and Walsh, F**. Electrochemical corrosion behavior of 90-10 CuNi alloy in chloride-based electrolytes, J. Appl. Electro chem. 34 (2004) 659–669.

[17] **Campbell, S.A., Radford, G.J.W., Tuck, C.D.S. and Barker, B.D**. Corrosion and galvanic compatibility studies of a high-strength copper-nickel alloy, Corrosion 58 (2002) 57-71. 57–71.

[18] **Alfantazi, A.M., Ahmed, T.M. and Tromans, D.** Corrosion behavior of copper alloys in chloride media, Mater. Des. 30 (2009) 2425–2430.

[19] **El-Aziz, A.M., Hoyer, R., Kibler, L.A. and Kolb, D.M.** Potential of zero free charge of Pd overlayers on Pt(111), Electrochim. Acta 51 (2006) 2518–2522.

[20] **Morad, M.S. and Sarhan, A.A.O**. Application of some ferrocene derivatives in the field of corrosion inhibition, Corros. Sci. 50 (2008) 744–753.

Engineering Failure Analysis 109 (2020) 104390.

[3] **Rezaei, M., Mahidashti, Z., Eftekhari, S. and Abdi, E**. A corrosion failure analysis of heat exchanger tubes operating in petrochemical refinery, Engineering Failure Analysis 119 (2021) 105011.

[4] **Rao, T.S. and Bera, S**. Protective layer dissolution by chlorine and corrosion of aluminum brass condenser tubes of a nuclear power plant, Engineering Failure Analysis 123 (2021) 105307.

[5] **Sun, B., Ye, T., Feng, Q., Yao, J. and Wei, M**. Accelerated degradation test and predictive failure analysis of B10 copper-nickel alloy under marine environmental conditions, Materials 8 (2015) 6029–6042.

[6] **Traverso, P. and Canepa, E**. A review of studies on corrosion of metals and alloys in deep-sea environment, Ocean. Eng. 87 (2014) 10–15.

[7] **Zhang, T., Yang, Y., Shao, Y., Meng, G. and Wang, F**. A stochastic analysis of the effect of Hydrostatic pressure on the pit corrosion of Fe–20Cr alloy, Electr ochim. Acta 54 (2009) 3915–3922.

[8] **Liu, B., Zhang, T., Shao, Y.W., Meng, G.Z., Liu, J.T. and Wang, F.H.** Effect of hydrostatic Presse on the corrosion behavior of pure nickel, Int. J. Electro chem. Sci. 7 (2012) 1864–83.

[9] **Yang, Y.G., Zhang, T., Shao, Y.W., Meng, G.Z. and Wang, F.H**. New understanding of the effect of hydrostatic pressure on the corrosion of Ni-Cr-Mo-V high strength steel, Corros. Sci. 73 (2013) 250–261.

[10] **Wang, Z.Y., Cong, Y. and Zhang, T**. Effect of hydrostatic pressure on the pitting corrosion behavior of 316L stainless steel, Int. J. Electro chem. Sci. 9 (2014) 778–798.

[11] **Badawy, W.A., Ismail, K.M. and Fathi, A.M.** Effect of Ni content on the corrosion behavior of Cu–Ni alloys in neutral chloride solutions, Electro chim. Acta 50 (2005) 3603–3608.

[12] **Ma, A., Jiang, S., Zheng, Y. and Ke, W.** Corrosion product film formed on the 90/10 copper–nickel tube in natural seawater: composition/structure and formation mechanism, Corros. Sci. 91 (2015) 245–261.

[13] **Mansfeld, F., Liu,G., Xiao, H., Tsai, C. and Little, B**. The corrosion behavior of copper alloys, stainless steels and titanium in seawater, Corros. Sci. 36 (1994) 2063–2095.

[14] **Cao, C.N. and Zhang, J.Q.** An Introduction to Electrochemical Impedance Spectroscopy, Science press, China, 2002.

[15] **Assis, S.L., Wolynec, S. and Costa, I**. Corrosion characterization of titanium alloys by electrochemical techniques, Electro chim. Acta 51 (2006) 1815–1819.

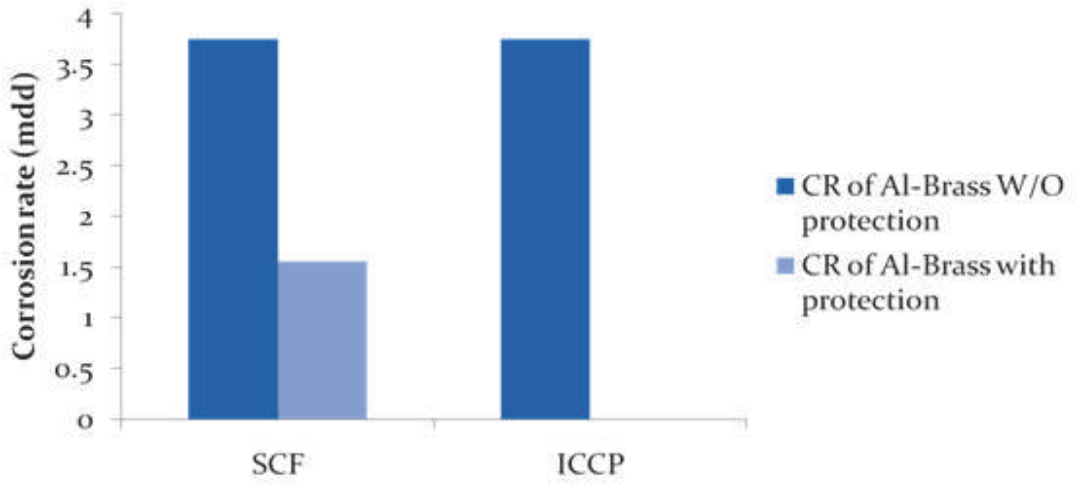

Figure 5: Comparison between SCP and ICCP

If ICCP were to compare with SCP, then it can be seen that ICCP is much better than SCP (Figure 5), with negligible corrosion rate in the case of ICCP. It was found that the condenser tubes had the corrosion deposit because of biopolymer/slime formation and stress corrosion cracking in presence of ammonia. Copper alloys also exhibits the Erosion corrosion mechanism until the water flow in the tube reaches the critical velocity which then accelerates the erosion. The normal protective film on Al-brass is not formed in the presence of chlorine.

4. Conclusions

It is concluded that the initially corrosion rate was high, so more protection against ammonical corrosion was required at the start. Ammonical corrosion increase with increase in temperature, so temperature should be controlled to minimize ammonical corrosion. The air ejection system must be efficient to remove ammonia in air cooler zone. By comparing sacrificial cathodic protection (SCP) and impressed current cathodic protection (ICCP), it is concluded impressed current cathodic protection is better. Small amount of current will be required in impressed current cathodic protection i.e. only less than 1mA/dm^2. Zn is suitable anode material used in impressed current cathodic protection. By adding alloy elements such as Be metal, corrosion resistance properties of Al-Brass can be increased.

References

[1] **Hu, S., Liu, L., Cui, Ying, Y. and Fuhui, W.** Influence of hydrostatic pressure on the corrosion behavior of 90/10 copper nickel alloy tube under alternating dry and wet condition, Corros. Sci. 146 (2019) 202-212.

[2] **Jawwad, K.A. and Mohamed, I.K**. The combined effects of surface texture, flow patterns and water chemistry on corrosion mechanisms of stainless steel condenser tubes,

SCP is efficient method to reduce ammonical corrosion, as shown in Figure 5. In this case, the Al-Brass material act as cathode, while Zn act as anode. So, Al-Brass material is protected, while Zn corroded [20], see Table 6. ICCP is an excellent method to reduce corrosion. In this case, a DC current is applied externally with the help of power supply. Only less than 1 mA/dm^2 is required (Table 7).

Table 6: Sacrificial cathodic protection

Exp. No.	Time (hrs)	Coupon No.	Surface Area (dm2)	Initial Weight (g)	Final Weight (g)	Corrosion Rate (mdd)
1	3.20	01 (Al-Brass)	0.22	9.0933	9.0922	1.56
		4 (Zn)	0.15	4.8170	4.8130	8.33
2	90	01 (Al-Brass)	0.22	9.0587	9.0594	!
		2 (Zn)	0.15	8.5112	8.4066	7.75

Table 7: Impressed Current Cathodic Protection

Exp. No.	Current (mA)	Coupon No.	Surface Area (dm2)	Initial Weight (g)	Final Weight (g)	Wt. deposited (mg)
1	14.5	07 (Al-Brass)	0.11	4.3161	4.3262	10.1
		4 (Zn)	0.15	8.1470	8.1140	33
2	9	07 (Al-Brass)	0.11	----------	----------	----------
		2 (Zn)	0.15	7.8773	7.8546	22.7
3	3.0	07 (Al-Brass)	0.11	4.2243	4.2236	6
		06 (Zn)	0.15	8.0498	8.0366	13.2
4	1.0	07 (Al-Brass)	0.11	4.2047	4.2043	4
		04 (Zn)	0.15	4.7341	4.7285	5.6

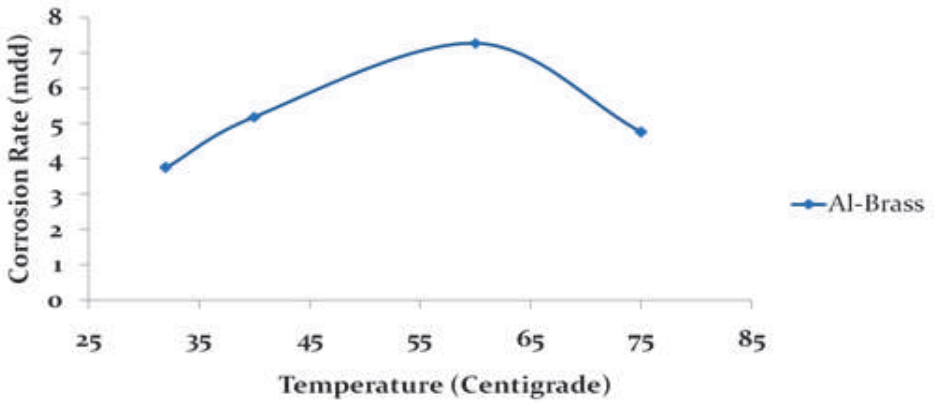

Figure 2: Corrosion rate vs temperature

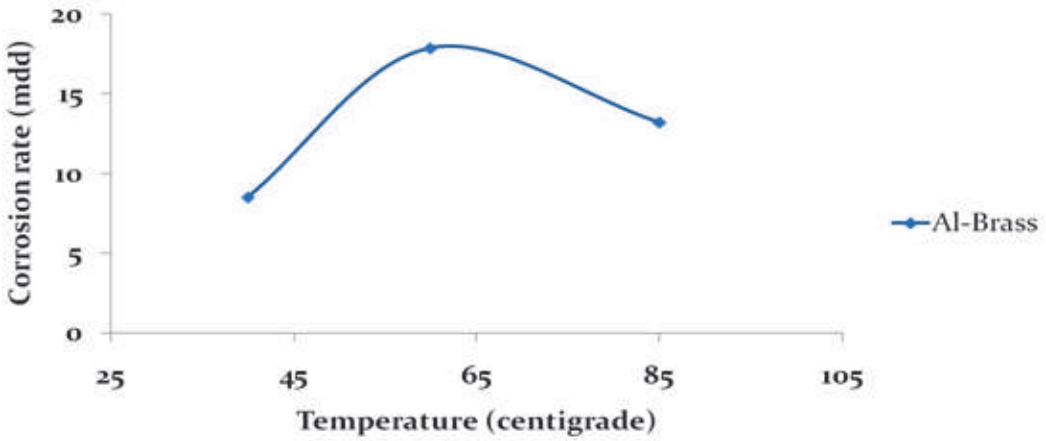

Figure 3: Corrosion rate vs temperature (Close to atmosphere: CTA)

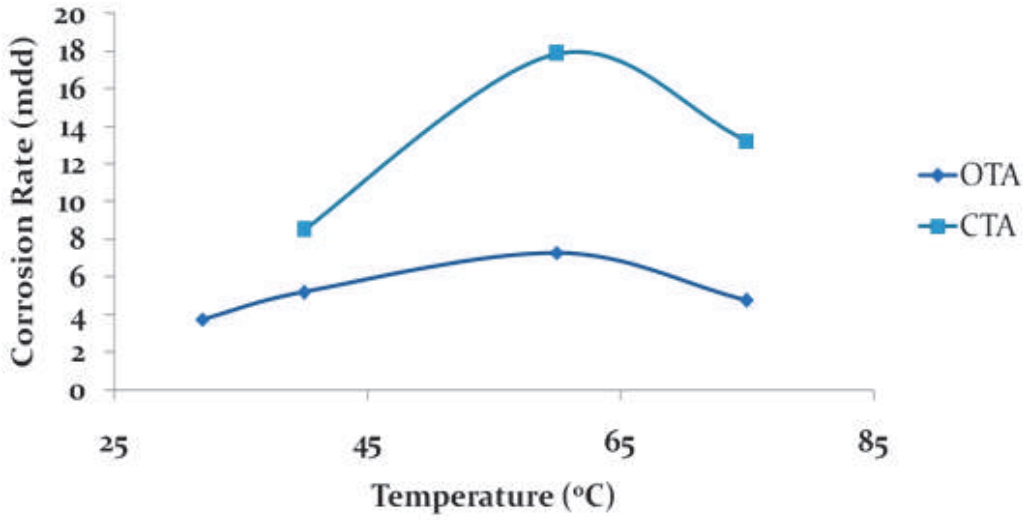

Figure 4: Comparison of OTA and CTA

determined by using weight loss method. Experiments also conducted to determine effect of impressed current cathodic protection (ICCP) on corrosion rate of Al-Brass material. The specimens were placed in beakers containing 10% ammonical solutions for different time. Al-Brass (used as cathode, material to be protected) was connected to negative terminal of battery, while positive terminal is connected with Zn metal (used as anode) as done by a number of authors [15-18]. These specimens were weighed and surface area was measured. Then it is dried and weighed again. Then corrosion rate was determined by using weight loss method.

3. Results and Discussion

The effect of corrosion rate was studied, and it was found that the initially corrosion rate increases due to absence of oxide layer, and then decreases due to formation of oxide layer as shown in Figure 1.

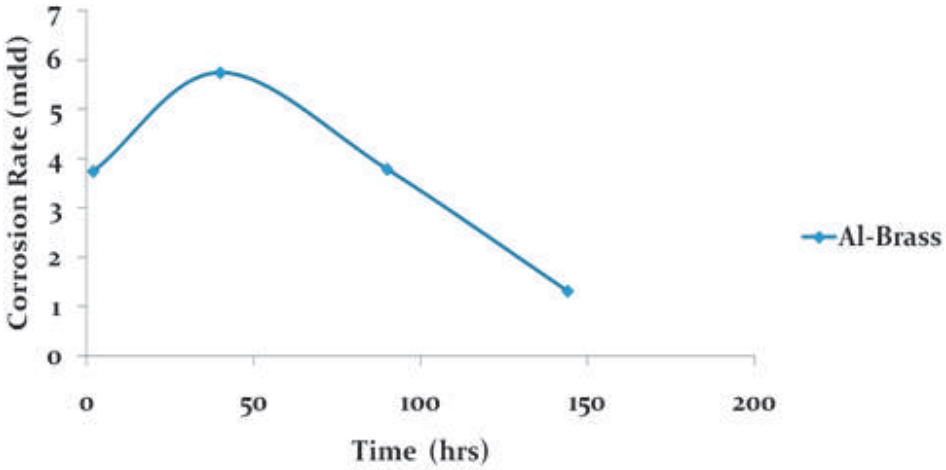

Figure 1: Corrosion rate vs time

An increase in temperature will tend to stimulate corrosive attack by increasing the rate of electrochemical reactions and diffusion processes. For a constant humidity, an increase in temperature would therefore lead to a higher corrosion rate as shown in Figure 2. Raising the temperature will, however, generally lead to a decrease in relative humidity and more rapid evaporation of the surface electrolyte [19-21].

For closed air spaces, such as indoor atmospheres, it has been pointed out that the increase in relative humidity associated with an increase in temperature will cause more corrosion rate (Figure 3). Comparison between corrosion rate of open to atmosphere (OTA) and closed to atmosphere (CTA). In case of OTA, there is less corrosion rate because of decrease in humidity than CTA (Figure 4).

emery paper. Then specimens were weighed and surface area was measured. Then specimens were placed in beakers containing 10% ammonical solutions. Then these beakers were placed in water bath for different temperature (32°C, 40°C, 60°C, 80°). Then it is dried and weighed again. Then corrosion rate was determined by using weight loss method (Table 4).

Table 4: Effect of temperature on Al-Brass Materials when open to atmosphere

Experiment #	Coupon #	Temperature C	Initial weight (W1) gm	Final Weight W2 (gm)	Time of Dip (Hr)	Corrosion Rate mdd
1	6	32	9.9828	9.9810	2	3.75
2	3	40	11.7987	11.7945	3	5.19
3	3	60	12.1411	12.1304	5.45	7.27
4	3	80	11.9147	11.9079	5.30	4.75

Experiments to determine effect of temperature (close to atmosphere) on corrosion rate of Al-Brass material. The specimens were cleaned and polished by emery paper. Then specimens were weighed and surface area was measured. Then specimens were placed in beakers containing 10% ammonical solutions. These beakers are closed so that dissolved oxygen can not come out the solution. Then these beakers were placed in water bath for different temperature (32 ^{0}C, 40 ^{0}C, 60 ^{0}C, 80 ^{0}C). Then it is dried and weighed again. Then corrosion rate was determined by using weight loss method (Table 5).

Table 5: Effect of temperature on Al-Brass Materials when close to atmosphere

Experiment #	Coupon #		Temperature C	Initial weight (W1) gm	Final Weight W2 (gm)	Time of Dip (Hr)	Corrosion Rate Mdd
1	6		40	9.8340	9.8321	3	2.64
2	4		60	11.9521	11.9258	5.45	17.87
3	6		80	9.9114	9.9040	5.15	5.99
4	4		80	11.5485	11.5378	3	13.21

Experiments to determine effect of sacrificial cathodic protection (SCP) on corrosion rate of Al-Brass material. The specimens were cleaned and polished by emery paper. Al-Brass (used as cathode, material to be protected) was placed along with Zn metal which is used as anode. These specimens were weighed and surface area was measured. Then specimens were placed in beakers containing 10% ammonical solutions for different time. Then it is dried and weighed again. Then corrosion rate was

Table 2: Surface areas of coupons

No.	L_{avg}	W_{avg}	T_{avg}	*S.A* (cm^2)	*S.A* (dm^2)
1	3.7	2.76	0.12	21.9744	0.219744
2	3.483333	3.413333	0.12	25.43476	0.254348
3	3.64	3.473333	0.12	26.99307	0.269931
4	3.716667	3.456667	0.12	27.41616	0.274162
5	3.696667	3.456667	0.12	27.27309	0.272731
6	3.55	3.15	0.12	23.973	0.23973

By using following formula, surface area was obtained (Table 2).

$$S.A = 2 \times (L \times W + W \times H + H \times L)$$

To find out corrosion rate of Al-Brass, "Weight loss method" was adopted, and the corrosion rate was calculated using the following formula:

$$\text{Corrosion rate} = \text{Wt. loss} / (\text{surface Area} \times \text{Immersion Time})$$

Experiments were conducted to determine effect of time on corrosion rate of Al- Brass material. Also experiments to determine effect of temperature (open to atmosphere) on corrosion rate of Al-Brass material and same was repeated to determine effect of temperature (close to atmosphere) on corrosion rate of Al-Brass material. The effect of sacrificial cathodic protection (SCP) on corrosion rate of Al-Brass material was also investigated. Studies were also done to determine effect of ICCP on corrosion rate of Al-Brass material. The specimens were cleaned and polished by emery paper. Then specimens were weighed and surface area was measured. Then specimens were placed in 10% ammonical solutions for different time. Then it is dried and weighed again. Then corrosion rate in milligram per square decimeter (mdd) was determined by using weight loss method. Table 3 summarizes the experimental methodology for corrosion rate for Al-Brass materials when open to atmosphere.

Table 3: Corrosion rate for Al-Brass Materials when open to atmosphere

Experiment #	Coupon #	Initial weight (W1) gm	Final Weight W2 (gm)	Time of Dip (Hr)	Corrosion Rate mdd
1	6	9.9810	9.9810	2	3.75
2	3	12.0679	12.0058	40	5.75
3	4	11.8603	11.7668	90	3.79
4	3	11.7126	11.6615	143	1.32

Experiments were conducted to determine effect of temperature (open to atmosphere) on corrosion rate of Al-Brass material. The specimens were cleaned and polished by

with passage of time, experiments are performed for various time [6]. Experiments are also done to know the effect of temperature of ammonical corrosion of Al-Brass material. It is seen that, with the increase in temperature, corrosion rate increases. A study was conducted to determine the feasibility of cathodic protection of Al-Brass material with Zn metal. A laboratory cell was used to determine required current density for Al-Brass material using SCP. Also effective of Impressed Current Cathodic Protection (ICCP) is compared with sacrificial cathodic protection (SCP). It is seen that ICCP is more effective than SCP [8].

Ammonical Corrosion and its Prevention Aluminum-Brass tubes are being used in condensers and heat exchangers since long time because of the fact that this material is relatively cheaper [9]. But the tube failure history indicates a higher failure rate with this material. The problems are being resolved by studying and implementing the recommendations from plant to plant. Failure analysis of tubes removed from west water box reveals that central zone tubes (air cooler zone) suffered ammonia corrosion attack (on outside tubes) while remaining zones suffered internal erosion-corrosion and deposits of marine organism [10.11].

In power plant condensers, the ammonia attack has been observed in air cooler zone on external surface of condenser tubes on the hot well side. The severe grooving is found, more prominently at support plate with wall thickness reduction of more than 50%. The source of ammonia is from the breakdown of hydrazine (added to boiler feed water) dissolved in the condensed water in the air cooling zone. This ammonia trickles down the tube support plates creating groove-like corrosion. This is owing to poor resistance of Aluminum Brass against any ammonia present. This ammonical corrosion can be prevented by following ways [12-14].

2. Materials and Methods

At laboratory scale, the electrolysis process is used to study the condenser tube corrosion. By using this process we can determine the effectiveness of ICCP, and compare to that of SCP. Required surface area of sample was determined with the help of Vernier caliper and following readings were obtained (Table 1);

Table 1: Dimensions of coupons

No.	*L1*	*L2*	*L3*	*W1*	*W2*	*W3*	*T1*	*T2*	T3
1	3.68	3.72	3.7	2.72	2.78	2.78	0.12	0.12	0.12
2	3.5	3.45	3.5	3.42	3.42	3.4	0.12	0.12	0.12
3	3.62	3.65	3.65	3.48	3.46	3.48	0.12	0.12	0.12
4	3.68	3.71	3.76	3.48	3.44	3.45	0.12	0.12	0.12
5	3.68	3.71	3.7	3.48	3.44	3.45	0.12	0.12	0.12
6	3.55	3.55	3.55	3.15	3.15	3.15	0.12	0.12	0.12

JKAU: Eng. Sci., Vol. **32** No. 2, pp: 77 – 87 (1444 A.H. / 2022 A.D.)
Doi: 10.4197/Eng. 32-2.6

Degradation of Condenser Tubes of a Nuclear Power Plant Exposed to Harsh Process Conditions

Dheya Sh. Al-Othmani[1]
Nuclear Engineering, King Abdulaziz University, Jeddah, Saudi Arabia

Abstract. Nuclear Power Plants condensers face various problems during their lifetime. One of very common problem is the leakage of Al-brass condenser tubes. Usually with the extended operation of condensers for 20 year or so, one can expect replacement of about 15-20% of condenser tubes due to leakage. One of the significant reasons of leakages of condenser tubes is ammonical corrosion. This ammonical corrosion can be minimized by controlling temperature along with various prevention method of corrosion. Current method used in power plant condensers is Sacrificial Cathodic Protection (SCP). A number of experiments were performed in the lab to protect corrosion by using SCP as well as the Impressed Current Cathodic Protection (ICCP). It was found that the ICCP is much better than SCP.

Keywords: condensers, nuclear power plants, leakages of tubes, corrosion, sacrificial cathodic protection,

1. Introduction

The recent trend toward all volatile compound using ammonia and ammonia compounds to control feed water chemistry in nuclear power plant, accentuates, the need for careful selection of corrosion resistance condenser tube alloys. Hydrazine is commonly employed in steam generator power plant system to scavenge O_2, adjust PH and reduce the corrosion rate of steel. These chemicals are readily dissolved in boiler feed water [1,2]. In contrast to ammonia, they do not tend to concentrate in subcooled condensate in air cooler section of steam condenser. This hydrazine can breakdown to some extent ammonia with the result of ammonia concentration at somewhat lower level than occurs with straight ammonia injection [3].

Aluminum-Brass tubes are being used in condensers and heat exchangers since long time because of the fact that this material is relatively cheaper. But the tube failure history indicates a higher failure rate with this material [4]. The problems are being resolved by studying and implementing the recommendations to different power plants. Failure analysis of tubes removed from west water box of condensers reveals that central zone tubes (air cooler zone) suffered ammonia corrosion attack (on outside tubes) while remaining zones suffered internal erosion-corrosion and deposits of marine organism [5].

The concentration of ammonia and oxygen is sufficiently low to cause any corrosion. However high concentration of ammonia and oxygen can develop in air cooler sections of condensers, which can cause corrosion of copper alloys. To know the corrosion rate

[1] Corresponding author: **dothmany@kau.edu.sa**

تقييم جودة الملابس والقفازات المستخدمة في مستشفيات المملكة العربية السعودية

عبدالحليم محمود سامي[١] ، علي محمد ال عوض[٢]

[١]قسم هندسة الانتاج والتصميم الميكانيكي، كلية الهندسة،جامعة المنيا،جمهورية مصر العربية

[٢]قسم الهندسة الصناعية ، كلية الهندسة ، جامعة جازان، المملكة العربية السعودية

مستخلص. يستخدم الأطباء في المستشفيات غازات التخدير أثناء العمليات وبعض هذه الغازات قابلة للانفجار. و إذا تسرب الغاز إلى الهواء فإن شرارة صغيرة من الشحنة الساكنة قد تجعله ينفجر. لذا فإنه من الضروري تقليل أو تجنب الشحنات الاستاتيكيه في غرف العمليات والغرف الأخرى. يهدف العمل الحالي إلى التحقق من جودة المنسوجات في المستشفيات من حيث الشحنة الكهروستاتيكية الناتجة عن التلامس والفصل، ويمكن تحقيق ذلك من خلال دراسة انزلاق قفازات اللاتكس للأطباء والممرضات وغيرهم من العاملين في المستشفيات ضد منسوجات الملابس في ظروف العمل الجافة.

بناءً على النتائج فإنه كمية الشحنات الساكنة التي يتم جمعها على سطح النسيج ستحدد جودته. حيث تتميز افضل أنواع المنسوجات بأقل قيمة للشحنات الإستاتيكية، وتتولد الشحنات الاستاتيكية عندما تتراكم خلال انزلاق القفازات على المنسوجات والملابس. و في الظروف الجافة ، كانت القيمة الأكبر للشحنة الساكنة ٢٤٠ فولت ، كما هو موضح في الملابس التي يرتديها الأطباء في غرف العمليات. و من أجل العمل الآمن في أماكن العمل المختلفة فإنه من الضروري حقًا أن نولي اهتمام دقيق للتفاصيل التي تؤثر على الأداء من أجل تحسين بيئة العمل للعاملين في اماكن الرعاية الصحية. حيث يُنصح بشدة باتباع سياسات إدارة الجودة واختيار المنسوجات والملابس بناءً على الشحن الكهروستاتيكي. و يعد أداء اليد والقفازات أمرًا بالغ الأهمية لأخصائيي الرعاية الصحية. كما أنه يحتاج صانعو القفازات وإدارة المستشفى وموظفو الرعاية الصحية إلى أن يكونوا أكثر وعياً بخصائص القفازات. و توصي هذه الدراسة باختيار المنسوجات والملابس بناءً على الشحنات الكهروستاتيكية لضمان الجودة والعمل الآمن في أماكن العمل المختلفة.

الكلمات الرئيسية: الجودة ، المنسوجات ، القفازات ، الشحنات الاستاتيكية

Properties of Fiber-forming Polymers, *Materials Science (Medžiagotyra*) 16(1), 72–75, (2010).

[20] Ameer A. K., Samy A. M. and Bakry M., Measurements of Electric Static Charge Generated From Sliding of Cotton Against Clothes Textile, *Solid State Technology*, ISSN: 0038-111X Vol. 63, No. 4,p.p 7834:7842, (2020).

Bilz, S., Sigrist, S., Brandle, M., Benz, C., Henzen, C., Mattman, S., Thomann, R., Brand, C., Rutishauser, J., Aujesky, D., Rodondi, N., Donze, J., Stanga, Z. and Mueller, B, Individualised Nutritional Support in Medical Inpatients at Nutritional Risk: A Randomised Clinical Trial, 393(10188), 2312–2321, (2019).

[5] Mäkinen, M., Meinander, H., Luible, C. and Magnenat-Thalmann, N., Influence of Physical Parameters on Fabric Hand, *Proceedings of the HAPTEX'05 Workshop on Haptic and Tactile Perception of Deformable Objects*, Hanover, December, (2005).

[6] Bensaid, S., Osselin, J-F., Schacher, L. and Adolphe, D. The Effect of Pattern Construction on the Tactile Feeling Evaluated Through Sensory Analysis, *The Textile Institute,* 97(2,) 137-145, (2006).

[7] Das, A. and Ishtiaque, S.M, Technology and Management, Comfort Characteristics of Fabrics Containing Twist-less and Hollow Fibrous Assemblies in Weft, *Journal of Textile and Apparel*, 3, p.p 1-7,(2004).

[8] Zhao, Y., Yin, L., Ikiz, Y., Sato, T., Yu, Q., Zhang, Z., Zhu, K. and Li, Q., A Study on Customer's Preference Towards Summer Shirt Fabric, *Journal of Engineered Fiber and Fabrics*, volume 15 , p.p 1-7, (2020).

[9] Mäkinen, M., Meinander, H., Luible, C. and Magnenat-Thalmann, N. (2005). Influence of Physical Parameters on Fabric Hand, *Proceedings of the HAPTEX'05 Workshop on Haptic and Tactile Perception of Deformable Objects*, Hanover, December, (2005).

[10] Bensaid, S., Osselin, J-F., Schacher, L. & Adolphe, D. (2006). The Effect of Pattern Construction on the Tactile Feeling Evaluated Through Sensory Analysis, *The Textile Institute*, 97(2), 137–145, (2006).

[11] Pan, N., Yen, K.C., Zhao, S.T, Yang, S.R. (1988). A New Approach to the Objective Evaluation of Fabric Handle from Mechanical Properties, Part I; Objective Measure for Total Handle, *Textile Research Journal*, 58, 438-444, (1988).

[12] Kim, J.O. and Slaten B.L. (1999). Objective Evaluation of Fabric Hand Part I: Relationships of Fabric Hand by the Extraction Method and Related Physical and Surface Properties, *Textile Research Journal*, 69 (1), 59–67, (1999).

[13] Lüttgens, G. Collection of Accidents Caused by Static Electricity, *Journal of Electrostatics* 16(2–3), 247–255, (1985).

[14] Alekseeva, L. V. Theoretical Aspects of Predicting the Electrostatic Properties of Textile Materials, *Fibre Chemistry,* 39(3), 225–226, (2007).

[15] Mahltig, B., Textor, T., Nanosols and Textiles. *World Scientific,* book, ISBN 9814470260, 9789814470261, page 224, , (2008).

[16] EN 1149-1:2006. Protective Clothing – Electrostatic Properties – Part 1: Test Method for Measurement of Surface Resistivity, (2006).

[17] EN 1149-2:2006. Protective Clothing – Electrostatic Properties – Part 2: Test Method for Measurement of the Electrical Resistance through a Material (Vertical Resistance), (2006).

[18] EN 1149-3:2006. Protective Clothing – Electrostatic Properties – Part 3: Test Methods for Measurement of Charge Decay, (2006).

[19] Stankutė, R., Grinevičiūtė, D., Gutauskas, M., Žebrauskas, S. and Varnaitė, S. Evaluation of Electrostatic

elastane. When cotton fabric is slid against various garments, the amounts of static charge vary on the composition of the various fibres in the apparel [20].

At moist working circumstances, a larger amount of static charge was measured, indicating that the water was well conductive. It is possible to propose the usage of cotton clothing in various healthcare settings based on this finding.

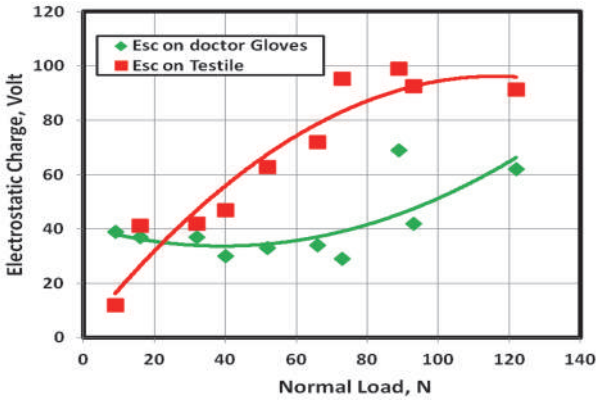

Fig. 16. Electrostatic charges generated from sliding of doctor's gloves against blue clothes for doctor's in operating theatres, dry condition

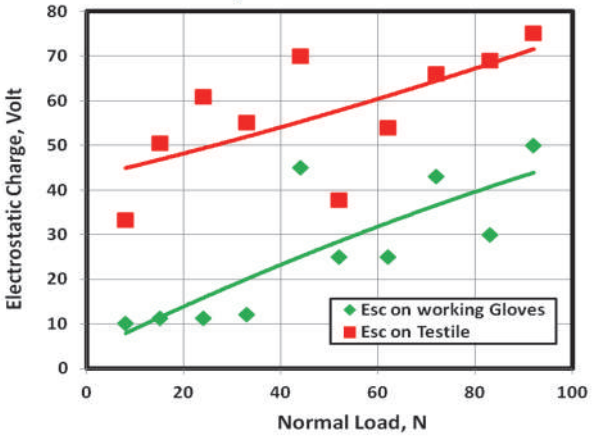

Fig. 17. Electrostatic charges generated from sliding of doctor's gloves against blue clothes for worker's in operating theatres, dry condition

4 Conclusions

1. To achieve effective work, the performance of gloves and garments must be reevaluated at medical institutions using quality management concepts. The amount of static charge collected on the textile surface determines its quality.
2. The finest grade textiles have the lowest static charge values. More than the gloves, the static charge created when sliding the gloves accumulates on the material and clothing.
3. In dry conditions, the larger value of static charge was 240 volts, as shown on yellow clothing worn by physicians in operating theatres.
4. For safe working in various workplaces, by following quality management policies and selecting textiles and clothing based on electrostatic charge is pstrongly advised.
5. In order to improve the work place for healthcare workers, it is crucial to give the nuances that affect performance enough consideration. Hand and glove performance is extremely important for health care professionals.
6. Glove makers, hospital administration, and health-care personnel all need to be better aware of the issues surrounding gloves. There is a need for procedures and tools that can detect issues with medical gloves.

Acknowledgment

I would like to acknowledge the undergraduate students: Hussain Naseeb, Haitham Jali, Khaled Moraya and Naif Hakami for their efforts during some parts of data collection. I would also like to thanks the training center at Jazan health affairs.

References

[1] Holdstock Technical Services, A Review of Electrostatic Standards, *Journal of Electrostatics*, 115, 103652, (2022).

[2] Liover-Segovia P., Domínguez-Lagunilla M., Fuster-Roig V. and Quijano-López A, Electrostatics Comfort in Buildings and Offices: Some Experiences and Basic Rules, *Journal of Electrostatics*, 115, 103650, (2022).

[3] Zheng, V., Cao, B., Zheng, Y., Xie, X. and Yang, Q. Collaborative Filtering Meets Mobile Recommendation: A User-centered Approach, *Proceedings of AAAI*, 24(1), 236-241, (2010).

[4] Scheutz, P., Fehr, R., Valerie, B., Geiser, M., Deiss, M., Gomes, F., Kutz, A., Tribolet, P., Bregenzer, T., Braun, N., Hoess, C., Pavlicek, V., Schmid, S.,

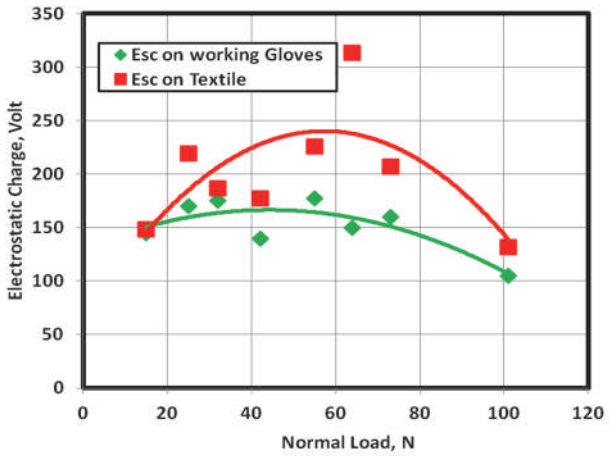

Fig. 13 Electrostatic charges generated from sliding of worker's gloves against yellow clothes for doctor's in operating theatres, dry condition.

Electrostatic charge of doctor's gloves sliding against clothes for doctor's in operating theatres, 65%, Polyester + 35% Cotton, dry condition, as shown in Fig. 14. Static charge decreases with increasing normal loads. This behavior may be related to the increase and decrease in friction between the gloves and textile. The maximum value of static charge was observed on the textile at lower loads. The minimum value of static charge was observed at higher loads.

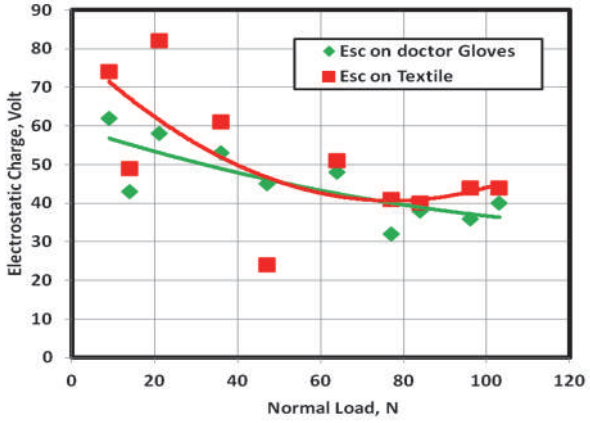

Fig. 14. Electrostatic charges generated from sliding of doctor's gloves against clothes for doctor's in operating theatres, 65%Polyester + 35%Cotton, dry condition

Figure 15 Depicts the relation between electrostatic charge and the normal load for the worker's gloves sliding against clothes for doctor's in operating theatres i.e.,65%Polyester + 35% Cotton, in dry condition. It is evident it as the typical load is increased up to 60 N, the static electricity increases.. Increase normal load over 60 N, shows deduction in the static charge value. The maximum value of static charge was 72 volts observed at 60 N normal load.

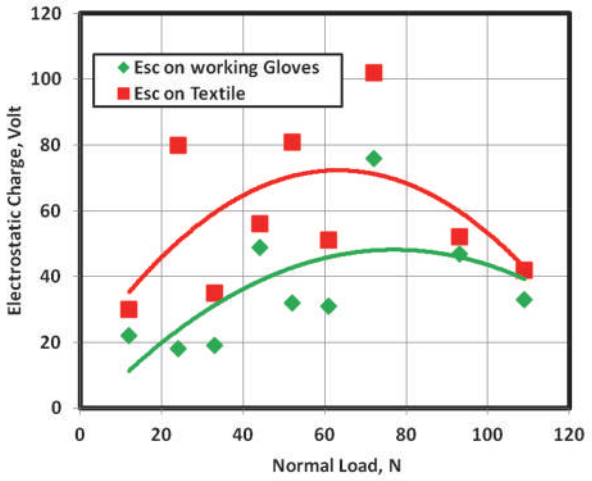

Fig. 15. Electrostatic charges generated from sliding of worker's gloves against clothes for doctor's in operating theatres, 65%Polyester + 35%Cotton, dry condition

Electrostatic charge generated from sliding of doctor**'s** gloves against blue clothes for doctor's in operating theatres, dry condition is shown in Fig. 16. As the typical power is increased, electrostatic charge also rises. The static charge levels represent the heights values on textile materials, this value is may be related to the damage of some devices in the OT's. The maximum value of static charge was 95 volts observed at 120 N normal loads. This study recommends using this type of clothes under light load.

Electrostatic charge of worker**'s** gloves sliding against the blue clothes for doctor's in operating theatres, in dry condition is shown in Fig. 17. As the typical power is increased, electrostatic charge also rises. Even after the maximum static charge on clothing fabric exceeds 70 volts, the static charge values are still significant.

Previous studies have shown that the amount of static charge that is deposited on textile surfaces affects the material's quality. In places with little static electricity, the quality is at its greatest. The fabrics with the largest electrostatic charge, which reached 70 volt, were made of 97 percent cotton and 3 percent

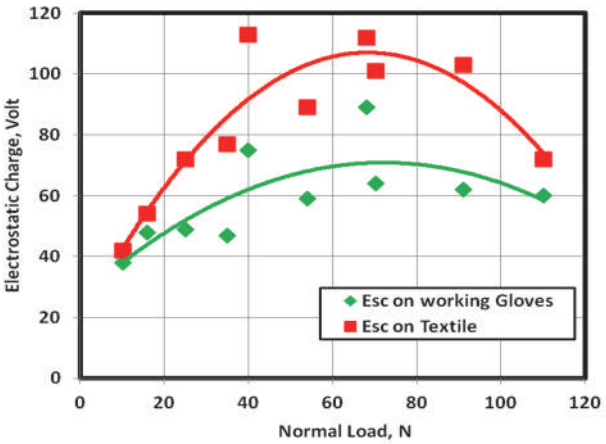

Fig. 9. Electrostatic charges generated from sliding of workrs gloves against clothes for male patients, dry condition

Electrostatic charge of doctor's gloves sliding against the clothes of female patients is shown in Fig. 10. Electrostatic charge increased when normal loads were increaseding normal loads. Increased static charge is related to decreasing friction as the normal load increases; this action increases the gap between gloves and textile. The maximum value of static charge was 67 volts observed at 80 N normal loads. The content of the textile may have generated more static charge.

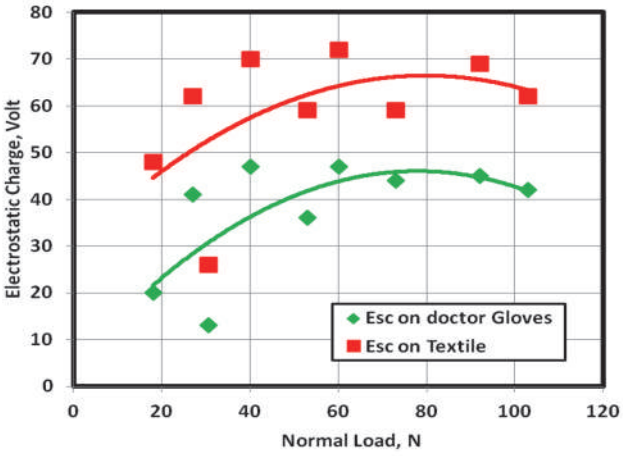

Fig. 10. Electrostatic charges generated from sliding of doctor's gloves against clothes for female patients, dry condition

Fig. 12 Shows the relation between electrostatic charge and normal load, for doctor's gloves sliding against the yellow clothes for doctor's in operating theatres. It can be observed that when the normal traffic rises, its electrostatic charge also does. This behavior may be related to decreasing friction as the normal load increases. The maximum static charge was 230 volts, as observed on the textile at 110 N normal load.

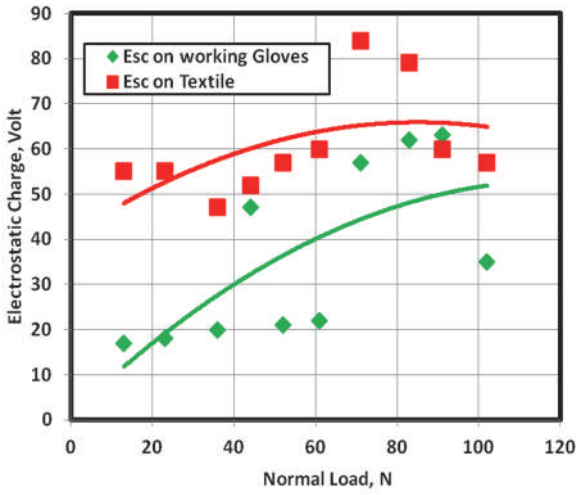

Fig. 11. Electrostatic charges generated from sliding of worker's gloves against clothes for female patients, dry condition

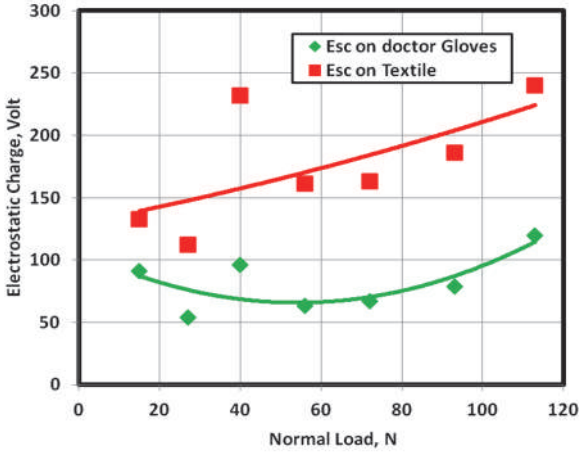

Fig. 12. Electrostatic charges generated from sliding of doctor's gloves against yellow clothes for doctors in operating theatres, dry condition

Electrostatic charge of worker's gloves sliding against dry yellow clothes for doctors in operating theatres is shown in Fig. 13. When the usual load increased to 60 N, the static charge grew a little, then shrank as the normal load increased. 240 volts was the maximum electrostatic charge it was observed at 60 N normal loads. The reason for increasing static charge is the lesser thickness of latex gloves.

load of electrostatic charge. A large value of electrostatic charge is generated from the bed sheet. The maximum value of electrostatic charge was 140 volts at 120 N normal loads. This study recommends not using the bed sheet under a higher load.

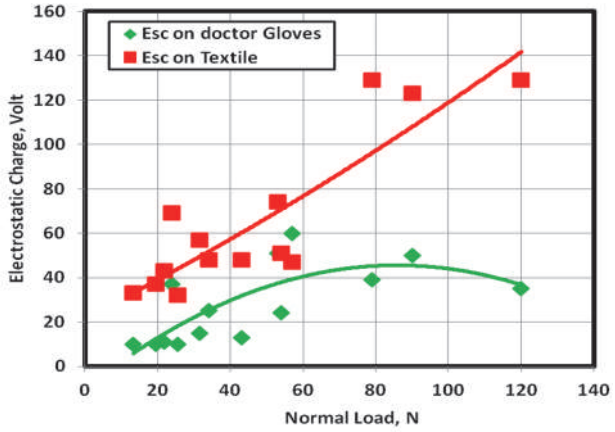

Fig. 6. ESC generated from sliding of doctor's gloves against bed sheet with content 50% cotton + 50% polyester, dry condition

The electrostatic charge of worker's gloves while sliding against the bed sheet in dry conditions is shown in Fig. 7. Electrostatic charge increases when normal load is increased. Worker's gloves generated greater electrostatic charge than doctor's gloves. The maximum value of electrostatic charge was 170 volt at 80 N normal loads. Hence, while using these types of gloves, a light load is beneficial to avoid the danger of static charges.

The electrostatic charge of doctor's gloves sliding against the clothes of male patients in dry conditions is represented in Figure. 8. The graph indicates that electrostatic charge increases with increased normal loads. This behavior may be related to more friction between the gloves and textile. Decreasing friction increases static charge and the gap between gloves and textile increases static charge. The maximum value of static charge was observed on the textile (170 volt).

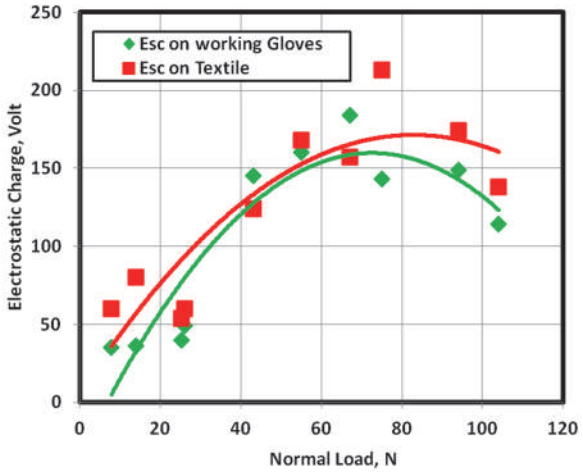

Fig. 7. Electrostatic charge generated from sliding of worker's gloves against bed sheet with content 50% cotton + 50% polyester, dry condition

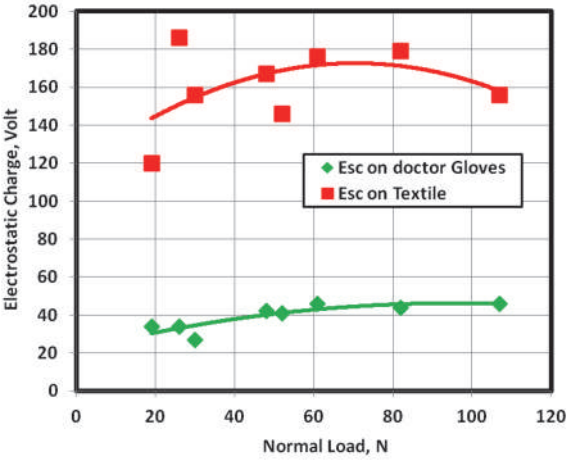

Fig. 8. Electrostatic charges generated from sliding of doctor's gloves against clothes for male patients, dry Conditions.

Figure 9 shows the static charge produced when employees' gloves are pressed to against clothing of male patients. Voltage generated from the sliding of workers gloves against clothes for male patients in dry conditions is illustrated. The static charge increases to maximum values with the increase in normal loads to 70 N. Static charge decreases when normal load is increased above 70 N. The textile accumulated a larger amount of static charge than the gloves.

Bed sheet
50%Polyester + 50%Cotton

Clothes for diseased male

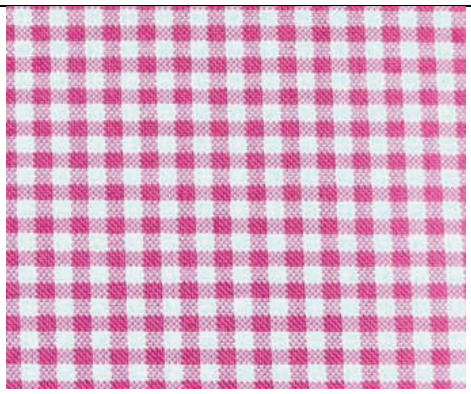

Clothes for diseased female

Yellow clothes for doctors in operating theatres

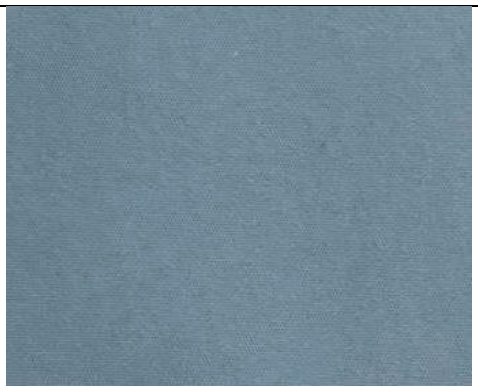

Clothes for doctors in operating theatres, 65%Polyester + 35%Cotton

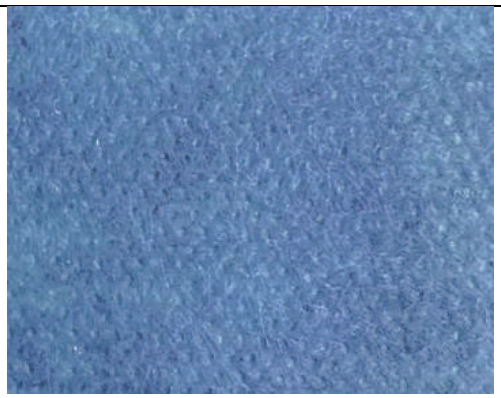

Blue clothes for doctors in operating theatres

Fig. 5 Textiles and clothes used in hospitals

3 Results and discussion

Along with technical specifications, quality evaluation is crucial for identifying materials. The integration of relevant of textiles vary from one another in that a fabric must be strong and function well while also being supple, stretchy, simple to form and pleat, and comfy in terms of sensory perspective. The term "fabric hand" is frequently to use when discussing a technique for evaluating textiles based only on their tactile qualities. Figure 6 shows the relation between electrostatic charge and the normal load on sliding the doctor's gloves against a bed sheet in dry condition. It is depicted in Fig. 6 with increasing the normal

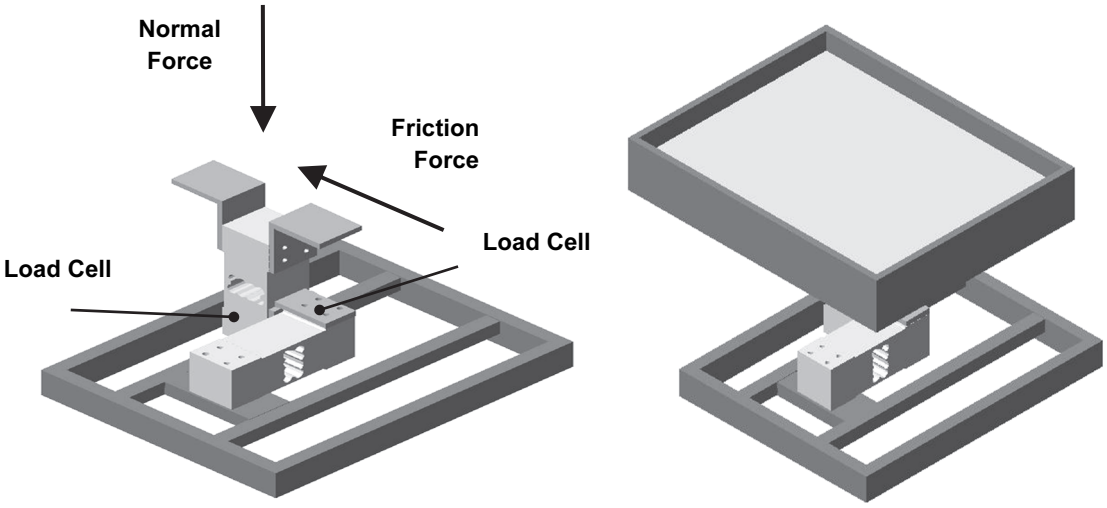

Fig. 2 Sliding test rig

Fig. 3. Gloves sliding against textile specimens.

Latex gloves for workers in hospitals

Latex gloves for doctors and nurses in hospitals

Fig. 4. Gloves used in hospitals

Fig. 1 Electrostatic charge (voltage) measuring device.

Using a test setup created and produced to measure friction, the normal load while rubbing the gloves against the textile of clothes, and between cotton and clothes. Two load cells are used to quantify the horizontal force (friction force) and vertically force applied to the tested textiles, which are put in a base (normal load). Figure. 2 depicts the test rig's configuration.

Sliding gloves of doctor and nurses in the hospital against the textile is shown in Fig. 3. The textile specimens were fixed on the table and attached with the load cells. The load cells measure the normal load applied from gloves on the textile. While sliding, the electrostatic charge was generated on the contact surface. The electrostatic charge accumulated on the gloves as well as the textile. Then the static charge was measured on the surfaces of both gloves and textile.

fabrics, and upholstery fabrics) common materials with a reputation for storing electrical charge. Textile materials must be created to have acceptable electrostatic characteristics in order to prevent the aforementioned negative impacts. Textile materials act as an electric fee capacitor because the dielectric substance is composed up of fibers and air voids [14]. There existence of an air gap in fibers and textiles can be described as a mixed-type capacitor dielectric layer to specify the electrical properties of textile materials. As a result, a wide range of electrical properties of fabrics or textile products are affected by topography, compactness, chemical and thermal treatment of the final product, as well as the atmospheric conditions in which the textile products are employed, or electronic conductivity is measured. Fabric material buyers seek out goods created with acceptable electrostatic characteristics. It is essential to measure and evaluate their properties.

The majority of materials used to make textile items are electric insulators, and the primary electric characteristic that is measured is surface resistance, which fluctuates wildly between 1013 and 106 [15]. Highly surface-resistance materials can carry an electrostatic charge, as is common knowledge. A significant electrostatic environment can be generated. be created and maintained by an amassed electric charge. A measurably large surface potential can be used to identify this electric field. When studied, Therefore, the basic electrostatic properties of the textile material can be revealed by the surface voltage and voltage dynamics. The European standards, which specify the test techniques for evaluating surface resistivity, are available here give widely-used techniques for determining the electrostatic characteristics of textile materials [16], Research and assessment facilities for textile materials use Electrically charged deterioration and electric conductivity via a material [17, 18]. The Chinese standards for evaluating static properties, static voltage semi-decay of textile materials, and electrostatic discharge testing of textiles [19] also cover assessments of electrostatic characteristics. Analyzing test procedures in further detail reveals that measurements textile materials are based on methods that, in some cases, cannot provide accurate measurements of electrostatic characteristics. enough details about the tested products. The technique outlined below has a few advantages from measuring the total area voltages plus amount of charges since the samples is affected by the ion flux. at the same time to provide more textile-related data. The technique can be modified to measure the dispersion of contact energy. So, in this post, we'll talk about a method for directly measuring electrostatic variables and how it might be used to look at the electrostatic characteristics of textiles.

The present work aims to investigate the quality of textiles in hospitals based on the electrostatic charge generated from the contact and separation. This is done by studying the sliding of gloves doctors, nurses and workers use in hospitals against textiles of clothes used in dry working conditions.

2 Experimental Work

During operations in hospitals, doctors use anesthetic gases. Some of these gases are explosive. (i.e. oxygen). If the gas escapes into the air, a tiny spark could make it explode. The avoidance of static charge in operating theatres and in the other rooms is necessary.

After measuring the electric static charge (electric static field) with an electrostatic charge meter, the (Ultra Stable Surface Voltmeter), the contact and separation of the specimens against rubber and to measure the generated charge under applied loads; see Fig. 1. This device measures electrostatic charge down to 0.1 volt on a surface, and up to 20 kV. Readings (Volts) are normally done with the sensor 25 mm from the surface being tested.

in place procedures to save products throughout their manufacturing, transportation, and usage, as well as workers in hazardous environments. Every standards body has a system for surveying and reviewing standards on a regular basis. Electrostatic guidelines are updated to reflect technical advancements and changes in our understanding of electrostatics. In order to distinguish between the context of circumstances for secure employment, when dangers to safety, loss, and protection of life and equipment in explosive atmospheres are vital, and regular living settings, the idea of electrostatic rest is offered. However a method which accounts for electrostatic relief necessitates a thorough comprehension of electrostatics and calls for particular answers, electrostatic relief has not been widely acknowledge. Static electricity problems are frequently misunderstood, with electrostatic discharges being blamed depending [2] or the AC magnetic or electric forces, or even the electrical assembly. Unrelieved tension and psychosomatic weariness can be caused by electrostatic discomfort. A technical reference sheet on electrostatic rest connotation might be extremely valuable for designers to utilize as a guide. It may also be suggested in construction codes to avoid situations that are difficult to recover from.

In addition to technical specifications, sensory assessment plays an important part in the correspondence of materials. Textiles differ from one another due to their fabricated structures; a good one should be strong, have good performance qualities, and be pliable, elastic, easy to pleat and shape, as well as pleasing to the eye and the senses [3]. The idea of "fabric hand" is widely employed to come up with a strategy for evaluating fabrics spectacularly. The obsession of the textile industry with "handle," or more broadly, "skin spectacular wear comfort," or "tactile comfort," has given rise to an intriguing field of study known as "handle," or more broadly, "skin spectacular wear comfort," or "tactile comfort."," as a result of current debates on understanding and measuring consumer preferences [4, 5] which also describes the full range of sensations experienced when handling or manipulating a fibers in the hands. Because textile handling is dependent on human tastes, It is obvious that to various people and consumers, it means different things [6]. Confirmed fabric type choices are numerous, and in some cases, even contradicting [7]. Hand has an impact on consumer preferences and perceptions of product utility, as well as the ability of retailers to sell clothing. This fabric specification is having precise criteria for developing and selecting fabric materials, which are mostly textiles prepared for use in apparels, for manufacturers, wear designers, and merchandisers [8].

When identifying materials and technical specifications, sensory evaluation is crucial. Textiles integration of relevant must be strong enough to fulfil their intended functions while also being flexible, elastic, simple to pleat and form, and pleasing to the eye and the senses. The term "fabric hand" is frequently used to identify a technique for the sensational appraisal of textiles [9]. Current textile industry research has focused on terms like as "handling," "skin sensational wear comfort," and "tactile comfort" [7, 10], that relate to the total feelings felt when a fabric is stroked or handled in the hands. have become important fields of interest. Identifying and quantifying consumer preferences has become one of these topics. Fabric handles clearly have different meanings for different persons and consumers from various ethnicities. because they are based on people's subjective tastes. There are many different and, in some cases, even opposing preferences for particular fabric types [11]. Hand has an impact on consumers' tastes and how useful they perceive a product to be, which in turn affects retailers' ability to sell the clothing. When creating and choosing textile materials, particularly those intended for use in clothes, manufacturers, garment designers, and merchandisers must take this fabric feature into consideration [12].

It is well-known that electrostatic discharge's unintended effects can result in major issues in a variety of circumstances, including product damage during electronic assembly, item quality problems, issues with worker numerous others [13]. Textiles (textiles,

JKAU: Eng. Sci., Vol. **32** No. 2, pp: 63 – 75 (1444 A.H. / 2022 A.D.)
Doi: 10.4197/Eng. 32-2.5

Evaluating the Quality of Clothes and Gloves Used in the Hospitals in Saudi Arabia

Samy A. M.[1], Al Owad A. M. M.[2]

[1] *Department of production engineering and mechanical design, f aculty of Engineering, Minia University, El-Minia, EGYPT.*
[2] *Department of industrial engineering, faculty of Engineering, Jazan University, Jazan, Saudi Arabia*

Abstract. In a hospital, doctors use anesthetic gases during operations. Some of these gases are explosive. If the gas escapes into the air, a tiny spark from static charge could make it explode. The reduction or avoidance of static charge in operating theatres and other rooms is necessary. The present work aims to investigate the quality of textiles in hospitals in terms of the electrostatic charge generated from the contact and separation. This can be achieved by studying the sliding of latex gloves of doctors, nurses, and other workers in hospitals against the textiles of clothes in dry working conditions.
Based on the results, the amount of static charge collected on the textile surface determines its quality. The finest grade textiles have the lowest static charge values. The static charge is created when sliding the gloves accumulates charge on the material and clothing. In dry conditions, the larger value of static charge was 240 volts, as shown on yellow clothing worn by physicians in operating theatres. For safe working in various workplaces, It's indeed necessary that pay careful attention to the particulars that impact performance in order to enhance the working environment of health care professionals. The following quality management policies and selection of textiles and clothing based on electrostatic charge is strongly advised. Hand and glove performance is extremely important for health care professionals. Glove makers, hospital administration, and health-care personnel all need to be more aware of the issues surrounding gloves. There is a need for procedures and tools that can detect issues with medical gloves.
Keywords: quality, textile, gloves, electrostatic charge

1. Introduction

Texts on learning the fundamentals of electrostatic phenomena, learning how to regulate electrostatic risks, and manufacturing and designing goods to defend against electrostatic hazards may be found in the literature of national and international standards across the world. Adoption and implementation of electrostatic norms are critical for the safety of life [1]. The criteria in this study enable businesses and people to put

تقييم تجربة أخصائي الأشعة مع جرعة المريض في القسم

طارق المجادعه [1]، مجدي النويمي [1]، عصام بانقيطة [1]

[1] قسم الهندسة النووية، كلية الهندسة

جامعة الملك عبد العزيز، جدة ٢١٥٨٩ ،المملكة العربية السعودية

مستخلص. سعت هذه دراسة في قسم الأشعة بمستشفى عام إلى تحديد أسباب تكرار / رفض صور الأشعة السينية وعلاقتها بخبرة الموظفين بقسم الأشعة. كان السبب وراء هذه الدراسة تعظيم سلامة المرضى من جرعات الأشعة الزائدة / غير المبررة في القسم. كان الهدف من الدراسة هو التوصل إلى آلية لمراقبة الجودة للقسم لجعل الأشعة السينية الرقمية آمنة قدر الإمكان في المنشأة. وبالنظر لنتائج هذه الدراسة فقد تبين أن المنشأة والموظفين مسؤولون بشكل جماعي عن جرعات الإشعاع الزائدة للمرضى. ومن هذه الأسباب نقص الخبرة لدى بعض الموظفين وأيضا عدم مراقبة الصيانة الدورية لمعدات التصوير الطبي. وتشير النتائج أيضا إلى أن العاملين بالقسم لا يلتزمون بتطبيق المعايير المطلوبة التي يجب على المرافق الصحية والموظفين العمل بها في اقسام الأشعة التشخيصية. ومن ضمن النتائج تبين أيضا إلى أن الموظفين الذين تقل خبرتهم عن ثمان سنوات سجلوا أعلى أعداد من الصور المعادة وهذا دليل على أن الخبرة تلعب دورا مهما في مجال التصوير الطبي. وهذه قضية مهمة يجب على المنشأة والقسم تكريس جهودهم لحلها والأهم من ذلك ضمان سلامة المرضى من جرعات الأشعة السينية التي يمكن تجنبها.

بالنظر إلى النتائج، توصي الدراسة بتنفيذ أساليب مراقبة الجودة بشكل أكثر قوة، وتحسين تدريب الموظفين أثناء العمل لضمان حماية المرضى من الإشعاع غير الضروري.

5. Conclusion

The goal was to determine the relationship between the technologist experience and the extra x-ray dose caused by retake images and what causes General hospitals in Saudi Arabia to reject or repeat imaging procedures. The rejection of radiographs and repeat procedures was due to a lack of technologist expertise. The construction of an in-house quality control drives aimed at radiology technicians at the department to build staff abilities that will allow proactive prevention of reject and repeat procedures at the radiologic department is recommended in this study. The high rejection/repeat radiology rates were caused by quality control difficulties in radiology at the hospital facility. Even though the study only had a limited sample size and was conducted in a tiny facility in southern Saudi Arabia, the findings are significant for radiology departments worldwide. To attain a higher level of patient safety, radiology departments should prioritize quality control procedures and in-house staff training to make personnel aware of circumstances that predispose patients to excessive ionizing radiation doses.

Acknowledgments

The authors would like to thank the Ministry of Health hospital and the radiology department for permission to access the facility and gather the data used in this article.

References

[1] **Lee, C. I., Elmore, J. G., & MD M**. Radiation-related risks of imaging. 2019;2019:1-24.

[2] **Fernandez R, Ellwood L, Barrett D, Weaver J**. Safety and effectiveness of strategies to reduce radiation exposure to proceduralists performing cardiac catheterization procedures : a systematic review. Published online 2021. doi:10.11124/JBISRIR-D-19-00343

[3] **Stephenson-Smith B, Neep MJ, Rowntree P**. Digital radiography reject analysis of examinations with multiple rejects: an Australian emergency imaging department clinical audit. *J Med Radiat Sci*. 2021;68(3):245-252. doi:10.1002/jmrs.468

[4] **Connor N**. What is ALARA. *Connor, Nick*. Published online 2019:1. https://www.radiation-dosimetry.org/what-is-alara-definition/.

[5] **Society E, Federation E, Societies R**. Patient safety in medical imaging: A joint paper of the European Society of Radiology (ESR) and the European Federation of Radiographer Societies (EFRS). *Radiography*. 2019;25(2):e26-e38. doi:10.1016/j.radi.2019.01.009.

[6] **Akhtar W, Hussain M, Aslam M, Ali A, Faisal A**. ORIGINAL ARTICLE PREDICTORS OF POSITIONING ERROR IN DIGITAL RADIOGRAPHY. 2012;(January 2016).

[7] **Hofmann B, Rosanowsky TB, Jensen C, Wah KHC**. Image rejects in general direct digital radiography. *Acta Radiol Open*. 2015;4(10):205846011560433. doi:10.1177/2058460115604339.

Table 1 Male & Female Retake Images description

Female		Male	
A/P	19	**A/P**	31
Chest	22	**Chest**	38
LE	20	**LE**	19
Skull	4	**Skull**	4
Spine	15	**Spine**	14
UE	12	**UE**	19
Total	92	**Total**	125

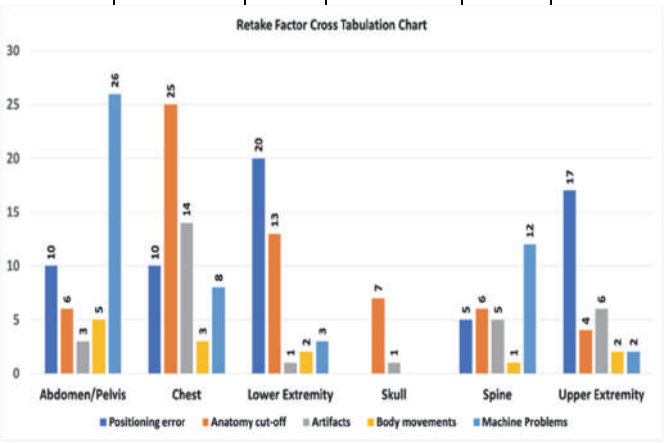

Figure 2 Retake Factor Cross Tabulation Chart

4. Discussion

The results of this study point back to the radiological department. The errors noted in the department are contingent on the competence of the radiological staff. Most of these errors occurred because of staff lack of experience or inadequate understanding of certain predisposing factors to the errors. According to the European Society of Radiology [5], radiologists are responsible for ensuring patient safety when performing radiographic procedures. It means that radiologic technicians and departments oversee keeping patients safe.

A major intervening factor contributing to most of these errors was staff experience and competence. Staff competence/accuracy is a common cause of radiological errors that contribute to rejection and repeat radiation procedures. Lack of experience is a precursor to errors in radiologic procedures. These findings were consistent with the findings of Akhtar et al. [6]; Stephenson et al. [3]; Hofmann et al. [7]. From the findings of this research, staff experience at the facility and quality control elements requires greater commitment dedicated to positively improving the conditions for improving staff competence and know-how to minimize the errors.

Kingdom Saudi Arabia
Ministry of Health
General Directorate of Health Affairs in
Asir Region

المملكة العربية السعودية
وزارة الصحة
المديرية العامة للشؤون الصحية بمنطقة
عسير

Retake X-ray

Notebook

File No.	Gender	Radiographic Procedures*1	KVp	mAs	Dose	Retake Factor*2	Experience

*Factors affecting image retake: -
1) Positioning error 2) Anatomy Cutoff 3) Artifacts
4) Body movements 5) Machine Problems
*Skull – Upper Extremity – Chest – Abdomen & Pelvis – Spine – Lower Extremity.

Figure 1 Data Collection Instrument.

participants, in this case, all the x-ray rejects on the clusters mentioned it was considered the reject rates. Retake factors influenced image retakes in this study. These retake factors include anatomy cutoff, positioning error, artifacts, body movement, and machine problems. The data collected from influences of these factors involved the skull, upper extremity, abdomen, pelvis, chest, lower extremity, and spine. Figure 1 was an essential tool for data collection in the research. Categories used in this data collection instrument were Gender, Radiographic Procedures, kVp, mAs, Dose, Retake Factor, and Technologist experience.

3. Results

From the data collected, reasons for rejection of images included positioning error, artifacts, anatomy cutoff, machine problems, and body movements. The sample size in this study was made up of all the rejected x-rays. The basis for tracking the rejected radiographs included gender, radiographic procedure, technologist experience, retake factor, dose, kVp, and mAs. The distribution of radiography procedures for male and female genders for the procedures that made up the study's data is shown in Table 1.

Figure 2 illustrates a chart of the study's data, demonstrating that positioning error was the most common reason for repeat factors in the radiology department. Positioning error was responsible for the most significant dose of ionizing radiation in the patients that visited the institution. The anatomy cutoff was the second most common cause of reject/repeat procedures at the hospital. The third reason cause for rejection/repeat at the facility was machine problems, while the fourth reason was the artifacts. Body movements accounted for the minor reject/repeat procedures in this study. One groundbreaking finding in this study that pinned the rejection and repeated procedures on the radiology technologist indicated that technologists with eight years of working experience as junior technologists contributed to the highest repeat rates. The data shows that junior staff contributed to 87.5% of the repeat procedures. In comparison, the senior technologists with more than eight years of experience in the department only contributed to 12.4% of the errors, validating the finding of a greater likelihood of the errors originating from staff in the department.

JKAU: Eng. Sci., Vol. **32** No. 2, pp: 57 – 62 (1444 A.H. / 2022 A.D.)
Doi: 10.4197/Eng. 32-2.4

An evaluation of Radiology Technologist Experience with Patient Dose in the Radiology Department

Tariq Almojadah[1*], Majdi Alnowaimi[1], Essam Banoqitah[1]
[1] *Nuclear Engineering, King Abdulaziz University,*
P.O. Box 80204, Jeddah 21589, Saudi Arabia

Abstract: An evaluation study of x-ray image doses at the Public Hospital Radiological Department sought to determine the causes of the repeat/rejected images and how it is related to the staff expertise. The reasoning behind this study was the maximization of patient safety from excess/unwarranted radiology doses at the department. This article will help develop a mechanism for quality control for the department to make digital x-ray as safe as possible at the facility. This study revealed that positioning error, machine problems, anatomy cutoff, artifacts, and body movement were the reasons for frequent repeat/reject x-ray procedures at the department. This article revealed that these errors had a strong relationship with staff causes. The leading cause of the errors coming up in the radiologic department is directly related to the radiology technologists' causes/competencies. Technologists with less than eight years of experience were directly/indirectly responsible for 87.5% of repeat radiation procedures. Technologists with over eight years of experience contributed to 12.4% of the repeat/rejected procedures. This study recommends implementing quality control methods more aggressively and improving on-the-job staff training to protect patients from unnecessary radiation.
Key Words: X-ray, Reject/repeat images, ALARA, Technologist experience.

1. Introduction

Patients are exposed to ionizing radiation during diagnostic x-rays, accounting for approximately half of all ionizing radiation fields to which ordinary people are exposed [1]. Multiple ionizing radiation exposures put people at risk for harmful doses of radiation, which can lead to issues like cancer later in life [2]. Despite these inherent dangers, the maximum dose of radiation that might cause or not create issues later in life is unknown, making it critical to protect patients from any unnecessary radiation as much as possible [3]. The responsibility will be greater on the radiology technologist to maintain patient safety and keep the dose at the low range of risks while ensuring good quality images.

The radiology technologists should keep in their mind "As Low As Reasonably Achievable (ALARA) standards when they perform an x-ray image [4]. This retrospective study investigates causes that may obstruct this goal at one of Saudi Arabia's public hospitals. The study focused on a range of objectives, including understanding the underlying causes of extra doses of irradiation to patients, creating guidelines for reducing digital x-ray retakes at the department, and coming up with recommendations and strategies for minimizing rejects at the department.

2. Methodology

The study was cross-sectional with data collected for rejected upper extremities, lower extremities, chest, skull, abdomen, pelvis, and spine radiographic images. Data collection occurred over three months in 2021 at General Hospital. Exclusion and inclusion criteria are the basis of selecting participants. After selecting study

* Corresponding Author: tsaadalmojadah@stu.kau.edu.sa

خوارزمية جديدة للكشف عن الحرائق باستخدام نهج التعلم العميق

أحمد الشيخي

كلية الهندسة، جامعة الحدود الشمالية، عرعر

المملكة العربية السعودية

مستخلص. النار تدمر كل شيء في طريقها. إنه أكبر خطر يسبب الكوارث. يمكن أن تبدأ من اشتعال صغير ويمكن أن يؤدي إلى خسارة كبيرة أو كارثة غير مرغوب فيها. يفقد الناس حياتهم من الحرائق. وفقا للرابطة الوطنية للحماية من الحرائق(NFPA) ، بلغت حالات الحرائق المبلغ عنها حوالي ١٤٠٠٠٠٠ في عام ٢٠٢٠ بينما تسببت هذه الحالات في ما يقرب من ٣٥٠٠ حالة وفاة مدنية. بالإضافة إلى ذلك، فإن عدد المدنيين المصابين من الحرائق حوالي ١٥٠٠٠ وتبلغ الكلفة التقديرية للخسائر في العقارات حوالي ٢١ مليار دولار أمريكي. وبالتالي، أصبح الكشف عن الحرائق موضوعا مهما للغاية خاصة بسبب التكنولوجيا السريعة والمتوسطة.

في هذه الورقة، يتم اقتراح طريقة بسيطة وسريعة ودقيقة للكشف عن الحرائق باستخدام التعلم العميق. تم تطوير هذه الطريقة بناء على تقنيات معالجة الصور والشبكة العصبية. إذا لم يتم الكشف عن الحريق مبكرا، فإن مستوى الأكسجين ينخفض وقد يؤدي ذلك إلى الاختناق. لذلك، يمكن أن تساعدنا هذه الطريقة من خلال اكتشاف الحرائق في مرحلة مبكرة. يقوم هذا النهج بتقسيم الصور وترشيحها على شكل بكسل بناء على عدة شروط ومحددات ومميزات وخصائص لهذه الصور مثل الألوان وشدة سطوعها ووضوحها والملمس باللهب مع انعكاسها.

يستخدم MATLAB كأداة محاكاة لإجراء العديد من التجارب للتحقق من فعالية الطريقة المقترحة. تظهر النتائج التي تم الحصول عليها أن الدقة كانت أكثر من ٩٧٪ عند تطبيقها على أكثر من ٧٠٠ صورة لأغراض التدريب والاختبار. أخيراً تم توفير نتائج دراسة مقارنة مرجعية بين النهج المقترح وبعض الدراسات المقدمة سابقاً للكشف عن الحرائق.

[11] **K. Angayarkkani, N. Radhakrishnan,** "An Intelligent System for Effective Forest Fire Detection Using Spatial Data," International Journal of Computer Science and Information Security (IJC-SIS2010), vol. 7, no. 1, pp. 202-208, 2010.

[12] **M. Ahrens, B. Evarts,** "Fire Loss in the United States During 2020," NFPA Research, 2021.

[13] **J. Zhou, Y. Lou, Z. Li, C. Kang,** "Analysis of Forest Fire Surveillance and Prewarning Application System Based on Power Grid Gis," International Information and Engineering Technology Association, vol. 1, no. 1, pp. 23-28, 2014.

[14] **D. Wu, C. Zhang, L. Ji, R. Ran, H. Wu, Y. Xu,** "Forest Fire Recognition Based on Feature Ex-traction from Multi-View Images," International Information and Engineering Technology Association, vol. 38, no. 3, pp. 775-783, 2021.

[15] https://medium.datadriveninvestor.com/simple-speech-recognizer-using-tensorflow-1c63efa7cc7b, available online. Accessed on 27/6/2022.

[16] https://www.slideshare.net/GauravMittal68/convolutional-neural-networks-cnn, available online. Accessed on 27/6/2022.

[17] https://livebook.manning.com/book/grokking-deep-learning-for-computer-vision/chapter-5/v-3/34, available online. Accessed on 27/6/2022.

between small and big smoke, however, the computation time is bigger than other approaches in the literature, thus, it needs to be minimized. The comparison results in Table 2 clearly show that the proposed method in this research outperforms other methods from the literature since it reaches over 97% of accuracy for fires and smoke detection.

5. CONCLUSION AND FUTURE WORK

Detection of fire at the early stage has become more crucial as people lose their lives, resources and properties because of the fire hazard. The proposed algorithm for fire detection in this paper provides excellent support to humans by detecting fires as its accuracy is over 97%. Several experiments were conducted using MATLAB to prove its accuracy and performance. Numerous images with fires ranging from small to huge, fire-free, and images with smoke only were tested. All obtained results from this approach show that it can detect fires properly.
The future work is to test it under severe and extreme environmental conditions such as dusty weather, foggy and high winds.

REFERENCES

[1] **N. Ya'acob, M.S.M. Najib, N. Tajudin, A.L. Yusof, M. Kassim,** "Image Processing Based Forest Fire Detecting Using Infrared Camera," Journal of Physics: Conference Series, vol. 1768, no. 1, pp. 1-14, 2021.

[2] **P. Barmpoitis, P. Papaioannou, K. Dimitropoulos, N. Grammalidis,** "A Review on Early For-est Fire Detection Systems Using Optical Remote Sensing," MDPI: Journal of Sensors, vol. 20, no. 6442, 2020.

[3] **T.W. Hsu, S. Pare, M.S. Meen, D.K. Jain, D.L. Li, A. Saxena, M. Prasad, C.T. Lin,** "An Early Flame Detection System Based on Image Block Threshold Selection Using Knowledge of Local and Global Feature Analysis," MDPI: Journal of Sustainability, vol. 12, no. 21, pp. 8899, 2020.

[4] **R. Sandhiya, S. Arulvallal, L. Shree, D. Dhina,** "Fire Recognition Based on Image Processing Using Raspberry Pi," International Journal of In-novative Technology and Exploring Engineering (IJITEE), vol. 9, no. 11, pp. 143-149, 2020.

[5] **L.S. Ravi, H.L. Harsha, C. Sushma, M. Swaroop, K. Thimme,** "Flame Detection Using Image Processing Techniques," International Journal of Engineering Research and Technology (IJERT), vol. 8, no. 13, pp. 115-117, 2020.

[6] **C. Shrimantrao, S.K. Mahesh, V.M. Bonal,** "Fire Detection System Using Matlab," International Journal for Research in Applied Science and Engineering Technology (IJRASET), vol. 5, no. 7, pp. 191-195, 2017.

[7] **K. Poobalan, S.C. Liew,** "Fire Detection Algorithm Using Image Processing Techniques," In Proceeding of the 3rd International Conference on Artificial Intelligence and Computer Science (AICS2015), pp. 160-168, 2017.

[8] **S. Gharge, S. Birla, S. Pandey, R. Dargad, R. Pandita,** "Smoke and Fire Detection," International Journal of Scientific and Research Publications, vol. 4, no. 7, pp. 498-502, 2014.

[9] **T. Hongda, L. Wanqing, W. Lei, O. Philip,** "Smoke Detection in Video: an Image Separation Approach," International Journal of Computer Vision, vol. 106, no. 2, pp.192-209, 2014.

[10] **B. He, X. Zhao, Z. Zhou, Z. Fan,** "Implementation of a Fire Detection Algorithm on TMS320DM642 DSP using MATLAB/Simulink," International Conference on Computer, Networks and Communication Engineering (ICCNCE2013), pp. 626-629, 2013.

Fig. 24: Detected image

The proposed algorithm can detect fires whether they are small or big as shown in the previous Figures. In addition, it has the feature to detect and distinguish the smoke early as in Figs.23 and 24, or if the smoke forms a huge cloud as shown in Fig.21.

Table 1 lists values for all evaluated performance parameters by the proposed approach when applying it to a dataset that contains 1400 images. The dataset is divided into three parts. Part one is used for the training purpose and it has 980 images which are equal to 70% of the dataset. Part two contains 220 images which nearly represent 15% of the dataset and are used for the testing while the last part is used for validation. This dataset contains fires and fires-free images.

A comparison study between the proposed method and other approaches in the literature is conducted and illustrated in Table 2. This comparison focuses on three performance metrics which are precision, recall, and accuracy. However, many approaches that were developed earlier and mentioned in the literature did not consider the three performance parameters.

Table 1: Evaluated performance parameters

Performance parameter	Evaluated value
TP	186
FP	3
TN	29
FN	2
PREC	98.41%
REC	98.94%
Accuracy	97.73%

Table 2: The comparison study results

WORK CONDUCTED	PRECISION	RECALL	ACCURACY
L.S. RAVI ET AL. [5]	NOT MENTIONED	NOT MENTIONED	90%
K. POOBALAN AND S. C.LIEW [7]	NOT MENTIONED	NOT MENTIONED	93.61%
THE PROPOSED ALGORITHM	98.41%	98.94%	97.73%

The proposed algorithm is capable to detect fires and smoke correctly with an accuracy of over 97% as shown in Table 1. In addition, it has the ability to distinguish

Fig. 21: Smoke detecting image

Scenario 5: an image with a small smoke only.

Fig. 22: The original image

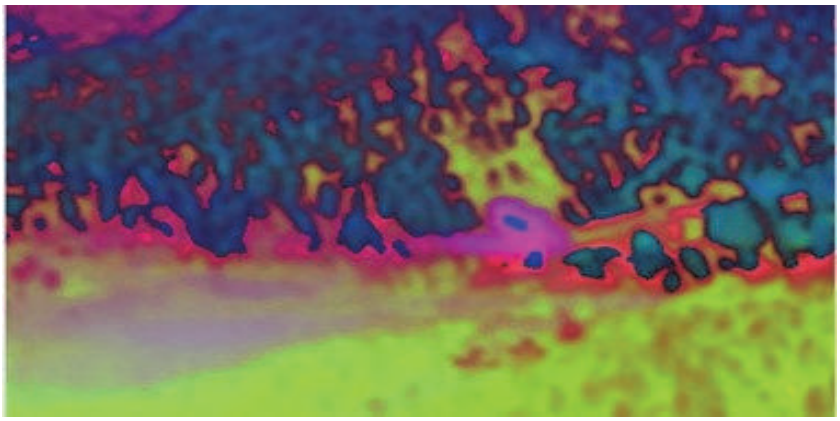

Fig. 23: HSV image

Fig. 18: Detecting fire image

Scenario 4: an image with a huge cloud of smoke only.

Fig. 19: The original image

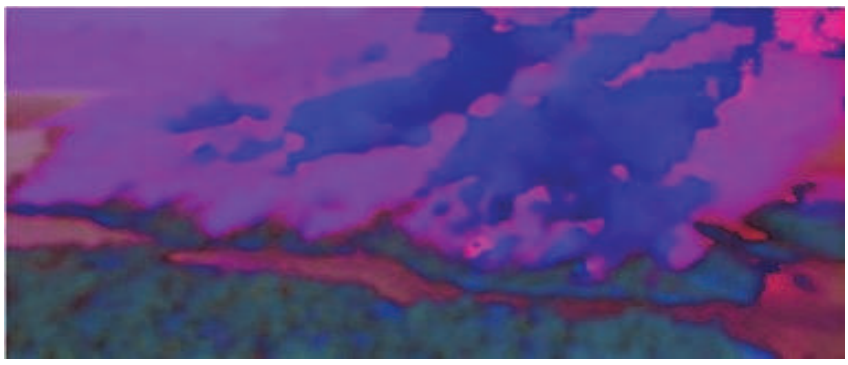

Fig. 20: HSV image

Fig. 15: No fire is detected

Scenario 3: an image with a small fire.

Fig. 16: The original image

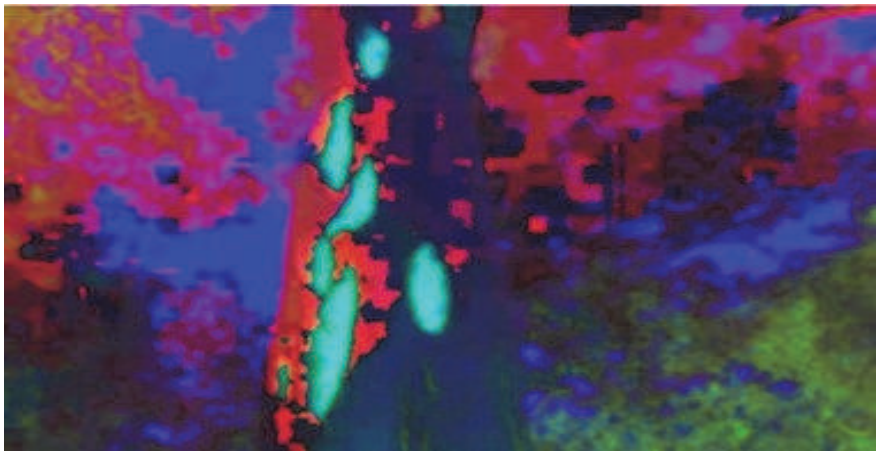

Fig. 17: HSV image

Fig. 12: Detecting fires image

Scenario 2: an image with fire-free.

Fig. 13: Fire-free image

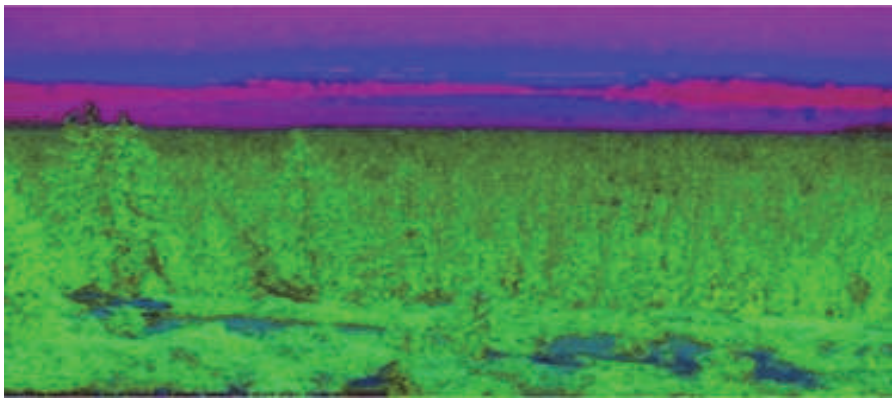

Fig. 14: HSV image

uploaded by a team in 2018 for NASA Space Applications Challenge. This dataset contains 999 images in total and among them 244 are fire-free. The following figures illustrate the resultant images from the proposed approach for several scenarios. Fig.11 depicts HSV image of the original one after converting it by the proposed method. Fig.12 illustrates the detected fires from the presented algorithm

Scenario 1: an image with huge fires.

Fig.10: The original image

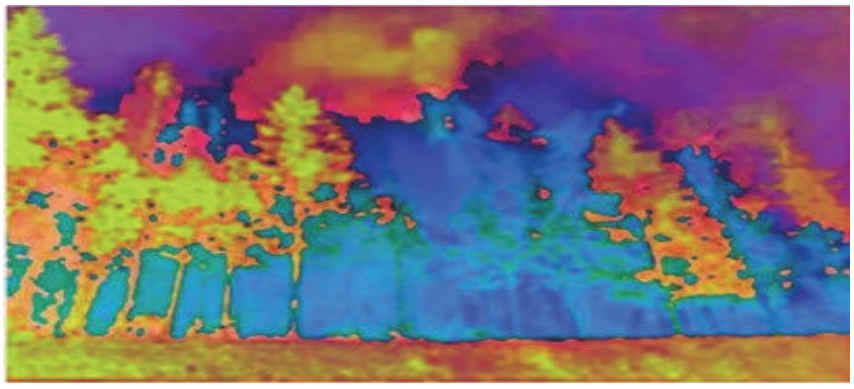

Fig. 11: HSV image

.

AlexNet is used to perform the deep learning technique to extract required features such as color intensity and mean. Furthermore, eight features are extracted in this algorithm.

The last step of the algorithm is to detect fires. It is determined by removing all objects, also known as components, except the pixels that have values larger than the threshold as shown in Fig.8. Fig.9 illustrates the resultant image where pixels that contain fires are isolated and displayed.

Fig. 9: The resultant image with fire detection

Keep in mind that all calculations are determined using an image processing toolbox that is already built-in inside MATLAB and this is the main reason that this simulation tool is picked and utilized.

Various performance parameters are computed and evaluated in the developed and proposed algorithm. These parameters are as follows:

1- True Positive (TP): this parameter measures a number of correctly identified images in the given dataset during the testing stage.

2- False Positive (FP): it measures a number of predicted types of images incorrectly.

3- True Negative (TN): it gives an indication about a figure of the negative images that are correctly identified by the proposed approach.

4- False Negative (FN): it measures a number of negative samples that are identified incorrectly.

5- Precision (PREC): it shows the ratio of the truly identified samples over the summation of the classes that were identified incorrectly plus the true samples that were correctly classified as shown in the following equation

$$PREC = TP / (TP + FP) \quad \textbf{(1)}$$

6- Recall (REC): it gives the ratio of the truly identified sample over the summation of the true samples plus the number of negative samples that were classified incorrectly as depicted in equation (2).

$$REC = TP / (TP + FN) \quad \textbf{(2)}$$

7- Accuracy: this parameter shows the percentage of the summation of the true samples and the negative ones that were classified correctly by the proposed method over the summation of all metrics that were mentioned from 1 to 4 earlier as depicted in equation (3).

$$Accuracy=(TP+TN)/(TP+TN+FN+FP) \quad \textbf{(3)}$$

4. SIMULATION EXPERIMENTS

MATLAB has a powerful tool for the purpose of imaging processing, visualization, and analysis. This tool is called Image Processing Toolbox and it helps users and developers to perform numerous operations. Those operations include but are not limited to: noise removal, segmentation, enhancement, and geometric transformation. This toolbox supports 2D and 3D images. Due to those features, MATLAB was selected to conduct several experiments to prove the correctness and effectiveness of the proposed method. The dataset was collected from the Kaggle website and it was

Fig. 6: The gray image

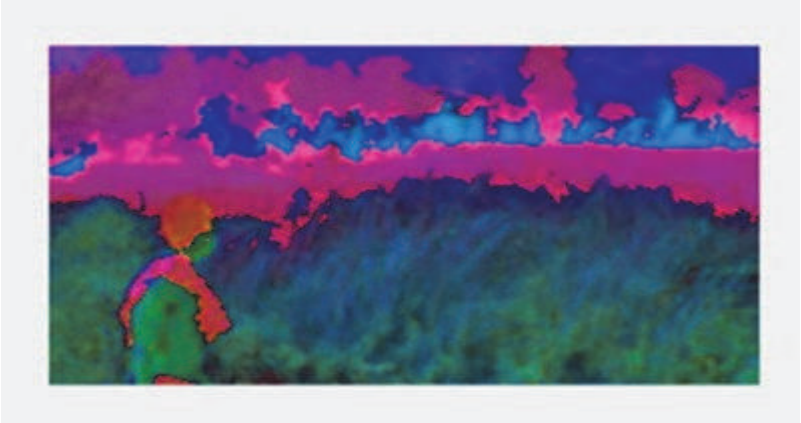

Fig. 7: The resultant HSV image

Fig. 8: Edge detection image

The next step of the proposed algorithm is to compute Y, Cr and, Cb for the considered image or images. YCrCb is another color space that is used in digital media to describe colors. Y is referred to the brightness component of colors which the human eyes are very sensitive to it while Cr and Cb are represented the red and blue components relative to the green component. This procedure is performed by a built-in function inside the simulation tool. After that, the algorithm computes the values of HSV using the built-in function.

Removing the connected objects that have values less than a predefined threshold is determined by the proposed algorithm from the binary images. This process is performed by using the built-in functions inside the simulation.

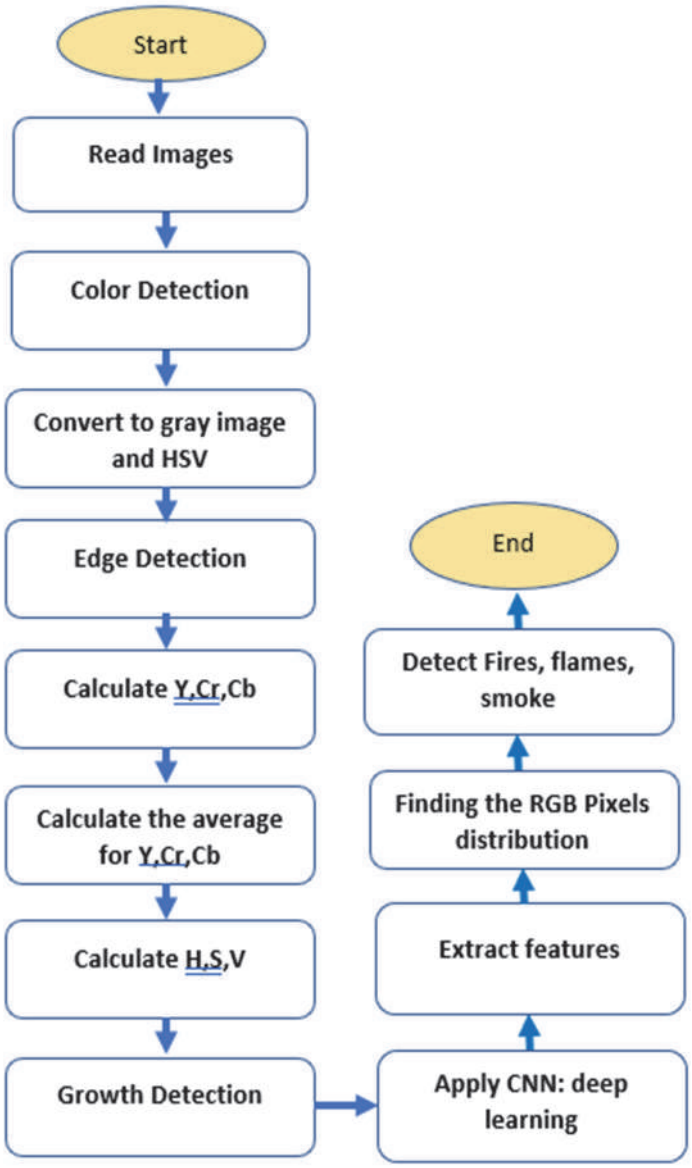

Fig. 4: Flowchart of the proposed approach

Fig. 5: The original image

management. Lastly, the authors proposed a solution based on the power grid. Herein, the proposed approach detects fires at the early stage. In addition, detection only smoke is provided too.

D. Wu et al. in [14] developed a Graph Neural Network (GNN) method to detect forest fire based on the feature similarity method. Extracting features similarities was performed by establishing the correlations features of nodes between multi-view images and their libraries. After that, detecting forest fire was performed by setting a threshold in the HSV method. Interested readers can refer to [14] for more information.

3. THE PROPOSED ALGORITHM

The main goal of this method is to detect fires at an early stage so that saving lives, resources, and properties from damage is possible before the fires grow and cause disaster. Hence, the proposed algorithm is developed using the deep learning approach based on the convolutional neural network tool which is AlexNet. Fig.4 depicts the proposed system. The algorithm starts by reading the images either from a file or a video by extracting them into a simulation tool. Herein, MATLAB is used as the simulation tool. Then, the algorithm detects the needed colors which are Red, Green, and Blue. After that, the images are converted to gray ones, Fig.5 shows an example of an image while Fig.6 displays that image after being converted to the gray image by the proposed approach. Fig.7 displays the original image after the algorithm converts it to an equivalent HSV where H stands for Hue, S represents Saturation and V refers to Value.

Image segmentation is a technique used in image processing and it is performed by detecting edges as illustrated in Fig.8. This process is used in the proposed algorithm to identify the illumination and intensity in the images. it aims to find the discontinuity of regions in the images being tested to observe a major and considerable change in the gray color. In this paper, the Gradient technique for edge detection is sued. Three operators are used and these operators namely: Sobel, Prewitt, and Robert

distinguish the pixels that contain the fire and then take them out from the background. After that, the images were filtered using MATLAB. Lastly, Wavelet analyzer 5.0 was used to perform some calculations on the fire image after generating 15 parts from that image which implies that it requires a heavy computation. Herein, the proposed approach uses the RGB technique to find the fires if exist by performing several computations, more information is presented in the next section. This method gives accurate results, and the accuracy is over 97%. In addition, this approach is light as it just requires a few computations.

P. Barmpoutis et al. in [2] presented a general overview of fire detection based on optical remote sensing. They provided deep details about the algorithms that were used to detect flame and smoke. The authors identified three systems that were named terrestrial, airborne, and spaceborne respectively. Lastly, a discussion of the strengths and weaknesses of each system was performed by showing a comparison between numerous factors such as accuracy, the volume of works and minimum fire size to be detected. Interested readers can refer to [2] for more information.

In [3], T. W. Hsu et al. proposed a general framework to detect fire based on filtering images to blocks. This process is performed according to predefined thresholds for different features. These features referred to the temporal and the spatial of the images. The process started by dividing an image into blocks, then, the flames were isolated and analyzed to identify several features such as the flickering of the flames, their colors, and immobility source. Furthermore, additional analyzing procedures were done on the surrounding blocks to extract the texture and reflections of the flames. The authors claimed that their approach was consistent with the real evidence, more information is found in [3]. In this paper, the proposed method is fast and accurate as its success rate exceeds 95% of all test scenarios.

R. Sandhiya et al. in [4] developed a method that used color and motion information that were obtained from video sequences for fire detection. It worked indoors and outdoors, and it had the capability to detect fires at the starting phase of the scorching process. This approach worked based on the segmentation of the growing region of fires to identify colors on pixels. After that, identifying moving pixels were extracted according to a ratio of their height and width. Readers can get more information in [4].

In [5]. L. S. Ravi et al. utilized shading location, movement identification, and region scattering to create a joint methodology for fire detection from information that was captured by a video. It used handling methods of a picture to detect fires. YCbCr has a powerful feature to isolate luminance from chrominance, so it was used along with the RGB shading method for fire detection.

C. Shrimantrao et al. in [6] developed a novel approach to detect fires from an image sequence that was captured by a camera. The authors used a method to identify fires based on finding the foreground moving object by using the adaptive background subtraction approach. Then, the identified objects were verified according to a color-based method to detect fires. Lastly, the authors conducted several experiments to verify their approach on two groups of videos that contained fires. These groups were fire-colored objects and non-fire color objects. However, it did not consider detecting the smoke and this lacking is a sign of weakness since the smoke can refer to an early fire warning. In addition, this method lacks detection of fires if they are not clearly noticeable to the camera.

Z. Jing et al. in [13] presented a power grid GIS-based analysis and application for forest fire surveillance and prewarning. The developed system worked based on performing several operations as it started with querying of basic information and ended with forest fire thematic map and its

Fig. 2: General CNN layers

AlexNet was developed and implemented in 2012 by a group of three developers. It is a type of convolutional neural network tool that employs the deep learning technique. Typically, AlexNet contains eight layers as illustrated in Fig. 3 from [17]. These layers are classified into two classes which are five convolutional layers and three fully connected layers. The convolutional layers are denoted by convx in Fig. 3 where x refers to the assigned number for each layer which starts from 1 to 5 while the fully connected layers are represented by FCx in the same Fig. x refers to the given number for every layer and it starts from 6 to 8.

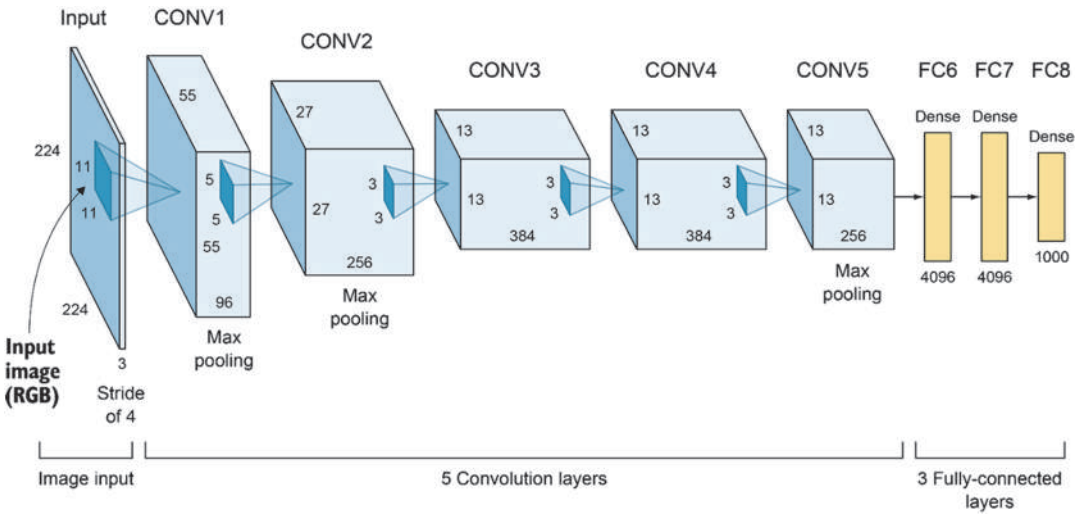

Fig. 3: AlexNet structures

The presented algorithm herein uses image segmentation techniques and CNN to form intelligent and deep learning method to detect fires. Numerous examples are conducted and illustrated in MATLAB to validate and verify how the proposed approach works and demonstrate its correctness and effectiveness as well.

In this paper, the contribution is done by proposing the fast and accurate algorithm to detect smoke and fire early to save lives and properties. This algorithm uses colors to identify smoke and flames along with their reflections. The rest of the paper is organized as follows: a literature review is covered in section 2 while section 3 provides details about the proposing approach. Discussion and results are presented in section 4 and the conclusion is provided in section 5.

2. Related Work

N. Ya'acob et al. in [1] proposed a method for forest fire detection based on image processing using an infrared camera. Their motivation was to capture fire during nighttime since other methods lacked that. Their infrared camera was treated as a satellite to capture from above. Their method used RGB and YCbCr colors to

detect smoke, flame, and heat are required since their ranges are quite small [2]. Thus, these sensors are costly and need to be effectively placed and installed to cover huge areas adequately.

Recently, researchers from academic and industrial fields focus their attention on the benefits of using deep learning approaches to real problems. These methods automatically extract required features and have capabilities to learn about new complex feature interpretations [2, 5], [7]-[10]. Thus, deep learning methods are the most rapidly evolving technologies that are widely used, utilized, and employed on numerous Computer Vision (CV) applications.

Due to evolving technologies, including Machine Learning (ML) and Computer Vision (CV), the detection of fire has acquired researchers' attention. To detect fires, two categories need to be identified: flame and smoke [3]. In general, smoke is visible before flames, hence, this feature helps us detect early fire and reduces the damage cost [1]-[3]. However, smoke detection is not possible at night without using lights [3]. Fire detection systems should be placed almost everywhere to minimize the risk of fire and its impact on nature and human properties [4]-[6].

Convolutional Neural Network (CNN) is an approach of deep learning to manage information that has various features which are represented in either 2D or 3D model. This approach takes its inputs through an image or a sequence of images which can be in colors or in grayscale modes. Fig. 1 illustrates a typical and general CNN structure, and it was downloaded [15].

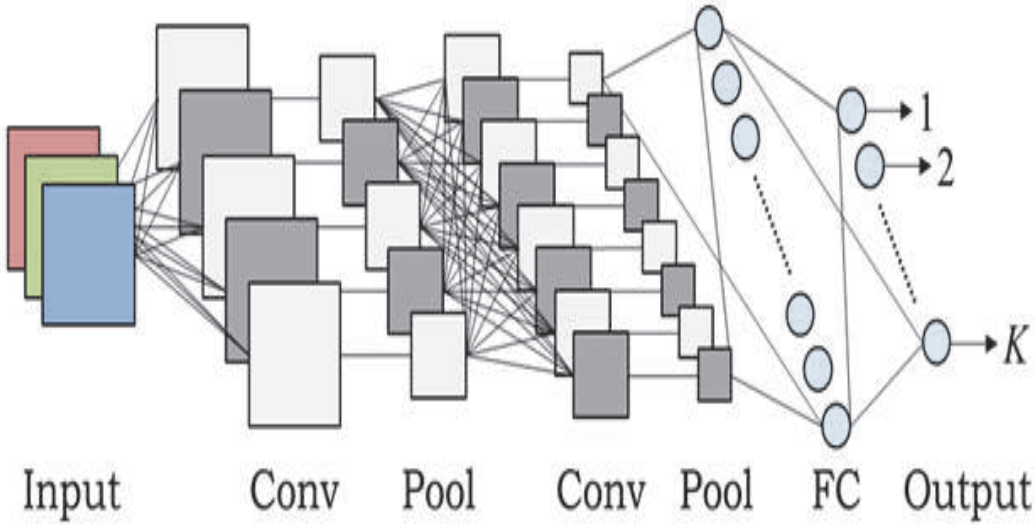

Fig. 1: Typical CNN structure

The convolutional neural network is composed of a series of components which are named layers. These layers form Kernels components which are utilized to learn and extract required features. In general, the convolutional neural network has five layers as depicted in Fig. 2 from [16]. Every layer is differentiated in a unique color except the first and the last layers. However, the last layer is considered one of the five layers.

JKAU: Eng. Sci., Vol. **32** No. 2, pp: 39 – 55 (1444 A.H. / 2022 A.D.)
Doi: 10.4197/Eng. 32-2.3

A Fire Detection Algorithm Using Convolutional Neural Network

Ahmed A. Alsheikhy [1]
Electrical Engineering, Northern Border University, Arar, Saudi Arabia

Abstract. Fire destroys everything on its way. It is the most dangerous hazard that causes disasters. It can be started from a small ignition which could lead to a big loss or unwanted disaster. People lose their lives from fires. According to National Fire Protection Association (NFPA), the reported fire cases were nearly 1,400,000 in 2020 while those cases caused almost 3,500 civilian deaths. In addition, the number of civilians injured from fires is around 15,000 and the estimated properties damage is around 21 billion US Dollars. Thus, the detection of fire has become a very important topic especially due to the rapid and evolving of technology. This paper proposes a simple, fast, and accurate method of fire detection using a deep learning approach. This method is developed based on image processing techniques and a Convolutional Neural Network (CNN) tool. This tool is AlexNet which is a type of convolutional neural network and utilizes the deep learning method. If the fire is not detected early, then the Oxygen level decreases which leads to suffocation. So, this method can help us by detecting fires at an early stage. This approach filters an image into pixels based on thresholds according to features such as colors, immobility source, and flame texture with its reflection. MATLAB is used as a simulation tool to conduct several experiments to verify the effectiveness of the proposed method. A dataset utilized in this research was downloaded from the Kaggle website and is divided into three categories. The obtained results show that the accuracy was over 97% when applied to more than 700 images for training and testing purposes. Lastly, a comparison evaluation between the proposed algorithm and some literature works is provided. This evaluation indicates that the proposed algorithm herein outperforms other works in terms of accuracy, precision, and recall.

Keywords: fire detection; image processing; segmentation; feature extraction; deep learning; artificial intelligence.

1. Introduction

Fire can be a reason for huge and heavy damage to nature including human resources and infrastructure [1], [2]. Furthermore, fire leads to a high rate of civilian deaths according to NFPA [1], [12]. Climate change causes a major effect on the environment such as heatwaves, droughts, and dust storms [2]. The first factor, which is the heat waves, can lead to huge fires that have extreme consequences on human resources, the local, and global economy .On terms of the economical side, fires cause damage to properties such as buildings and increase death rates. On the other hand, a huge number of sensors to [1], [2]. Thus, fire detection has become increasingly important for people to protect their lives and resources as well [2].

Recently, some forest fires are detected by a simple method which is human observations [2]. This method required high towers to be utilized for this purpose. However, it is ineffective and uneconomical since it is susceptible to human errors which may cause a fatigue disaster.

[1] Corresponding Author: aalsheikhy@nbu.edu.sa

الحمل الحراري الطبيعي في حاوية حلقية العمودية ذات زعانف طولية

سرحان المنيعي وعبد اللطيف قارئ

الهندسة الميكانيكية، جامعة الملك عبد العزيز

جدة، المملكة العربية السعودية

مستخلص. يمكن العثور على انتقال الحرارة بالحمل الطبيعي في العديد من تطبيقات الهندسة الحرارية. من أجل تحسين انتقال الحرارة ، يتم استخدام الزعانف لزيادة سطح التلامس وبالتالي معدل انتقال الحرارة. في هذا المشروع ، تمت دراسة أداء انتقال الحرارة بالحمل الطبيعي في الغلاف الحلقي العمودي عدديًا. تم استخدام برنامج الأنسس فلوينت لحل المعادلات الحاكمة لحساب السرعة وتوزيع درجة الحرارة. تم إجراء اختبار الشبكة وتم التحقق من صحة النموذج مع الدراسات التجريبية والرقمية السابقة. أظهرت النتائج أن للزعانف تأثيراً بارزاً في تعزيز انتقال الحرارة مقارنة بالنموذج بدون زعانف. بعد ذلك تم إجراء دراسة بارامترية لدراسة تأثير عدد الزعانف وطولها وسمكها وشكلها. تؤدي زيادة عدد الزعانف إلى زيادة معدل انتقال الحرارة بنسبة ٤٦٪. يتوافق تأثير عدد الزعانف على معدل انتقال الحرارة مع النتائج المذكورة في الأدبيات. زيادة طول الزعانف يزيد من معدل انتقال الحرارة بنسبة ٢٧٪. سمك الزعنفة له تأثير ضئيل على كمية انتقال الحرارة بالحمل الحراري. كما وجد أن الزعانف المربعة لها أفضل النتائج على الزعانف الدائرية والمثلثة. فيما يتعلق بتأثير عدد رالي على انتقال الحرارة، يزداد معدل انتقال الحرارة مع زيادة عدد رالي وهو مايتطابق مع النتائج المذكورة في الأدبيات.

finned cylindrical unit for free cooling application, *Energy Conversion and Management*, 75, 466–473, (2013).

[27] Kumar, R., Three-dimensional natural convective flow in a vertical annulus with longitudinal fins, *International Journal of Heat and Mass Transfer*, 40, 3323-3334, (1997).

[28] Sehgal, B. R., *Nuclear Safety in Light Water Reactors*, Academic Press, (2012).

[29] Grigull, U. and Hauf, W., Natural Convection in Horizontal Cylindrical Annuli, *Proceeding of the 3rd International Heat Transfer Conference*, 2, 182-195, (1966),

[30] Kuehn, T.H. and Goldstein, R. J., An Experimental and Theoretical Study of Natural Convection in the Annulus between Horizontal Concentric Cylinders, *Journal of Fluid Mechanics*, 74, 695-719, (1976).

Journal of Heat and Mass Transfer, 54, 1493–1505, (2011).

[12] Chen, J. C., Chou, G. H. and Hsieh, C. K., The influence of inner-wall motion on the linear stability of natural convection in a tall vertical annulus, *International Journal of Heat and Mass Transfer*, 39, 193- 201, (1996).

[13] Sankar, M., Venkatachalappa, M. and Shivakumara, I. S., Effect of magnetic field on natural convection in a vertical cylindrical annulus, *International Journal of Engineering Science*, 44,1556–1570, (2006).

[14] Husain, S. and Siddiqui, M. A., Experimental and numerical analysis of transient natural convection of water in a high aspect ratio narrow vertical annulus, *Progress in Nuclear Energy*, 106, 1–10, (2018).

[15] Afrand, M., Toghraie, D., Karimipour, A. and Wongwises, S., A numerical study of natural convection in a vertical annulus filled with gallium in the presence of magnetic field, *Journal of Magnetism and Magnetic Materials*, 430, 22–28, (2017).

[16] Abhilash, R. and Lal, S. A., Three dimensional analysis of natural convection in a narrow vertical annulus closed at top and opened at bottom, *International Journal of Thermal Sciences*, 127, 277–287, (2018).

[17] Wang, Z., Liu, Y., Zhang, J. and Dang, N., Study of laminar natural convection in a vertical annulus with inner wall covered by a porous layer by using lattice Boltzmann method, *International Journal of Thermal Sciences*, 135, 386–397, (2019).

[18] Char, M. I. and Lee, G. C., Maximum density effects on natural convection in a vertical annulus filled with a non-Darcy porous medium, *Acta Mechanica*, 128, 217-231, (1998).

[19] Jha, B. K., Babatunde, A. and Muhammad, S., Combined effects of suction/injection and wall surface curvature on natural convection flow in a vertical micro-porous annulus, *Thermophysics and Aeromechanics*, 22, 217-228, (2015).

[20] Rahnama, M. and Farhadi, M., Effect of radial fins on two-dimensional turbulent natural convection in a horizontal annulus, *International Journal of Thermal Sciences*, 43, 255–264, (2004).

[21] Kiwan, S. and Zeitoun, O., Natural convection in a horizontal cylindrical annulus using porous fins, *International Journal of Numerical Methods for Heat and Fluid Flow*, 18, 618-634, (2008).

[22] Nada, S. A. and Said, M. A., Effects of fins geometries, arrangements, dimensions and numbers on natural convection heat transfer characteristics in finned-horizontal annulus, *International Journal of Thermal Sciences*, 137, 121–137, (2019).

[23] Alshahrani, D. and Zeitoun, O., Natural convection in horizontal cylindrical annuli with fins, *Alexandria Engineering Journal*, 44, 825-837, (2005).

[24] Shadlaghani, A., Farzaneh, M., Shahabadi, M., Tavakoli, M. R., Safaei, M. R. and Mazinani, I., Numerical investigation of serrated fins on natural convection from concentric and eccentric annuli with different cross sections, *Journal of Thermal Analysis and Calorimetry*,135, 1429–1442, (2019).

[25] Ramezanpour, M. and Hosseini, R., An experimental study of natural convection in vertical annulus with helical fin, *Experimental Heat Transfer*, 33, 226-244, (2019).

[26] Solomon, G. R. and Velraj, R., Analysis of the heat transfer mechanisms during energy storage in a Phase Change Material filled vertical

q' Heat transfer rate per unit length (W/m)
r Annulus radius (m)
Ra Rayleigh number
T Temperature (K)
Vy Flow velocity components in y-direction (m/s)
W Fin width (mm)

Greek Symbols
α Thermal diffusivity (m^2/s)
β Thermal expansion coefficient (K^{-1})
μ Dynamicviscosity (kg/ m.s)
ρ Density (kg/m^3)
ν Kinematic viscosity (m^2/s)

Subscripts
f Fluid
i Inner
m Modified
o Outer

Acknowledgment

I would like to express my sincere appreciation and my special thanks to my academic supervisor Dr. Abdullatif A. Gari for his great help and precious time, and effort that he provides to help me to upgrade my scientific knowledge and my research skills. Also, my sincere appreciation to King Abdulaziz University's High Performance Computing Center where my study was performed using their supercomputer (Aziz Supercomputer).

LIST OF REFERENCES

[1] Bergman, T. I., Lavine, A. S. and Incropera, F. P., *Fundamentals of Heat and Mass Transfer*, John Wiley & Sons, 7th, (2013).

[2] Rohsenow, W. M., Hartnett, J. P. and Cho, Y. I., *Heat Transfer*, 3rd, McGraw-Hill, N.Y., 11, (1998).

[3] Nada, S. A., Experimental investigation of natural convection heat transfer in horizontal and inclined annular fluid layers, *Heat and Mass Transfer*, 44, 929–936, (2008).

[4] Yeh, C. L., numerical investigation of the three-dimensional natural convection inside horizontal concentric annulus with specified wall temperature or heat flux, *International Journal of Heat and Mass Transfer*, 45, 775-784, (2002).

[5] Kumari, M. and Nath, G., Unsteady natural convection from a horizontal annulus filled with a porous medium, *International Journal of Heat and Mass Transfer*, 51, 5001–5007, (2008).

[6] Yoo, J. S., Prandtl number effect on bifurcation and dual solutions in natural convection in a horizontal annulus, *International Journal of Heat and Mass Transfer,* 42, 3279-3290, (1999).

[7] Wang, W., Li, B. W., Varghese, P. L., Leng, X. Y. and Tian, X. Y., Numerical analysis of three-dimensional MHD natural convection flow in a short horizontal cylindrical annulus, *International Communications in Heat and Mass Transfer*, 98, 273–285, (2018).

[8] Yang, X. and Kong, S. C., Numerical study of natural convection in a horizontal concentric annulus using smoothed particle hydrodynamics, *Engineering Analysis with Boundary Elements*, 102, 11–20, (2019).

[9] Belabid, J. and Allali, K., Effect of temperature modulation on natural convection in a horizontal porous annulus, *International Journal of Thermal Sciences*, 151, 106273, (2020).

[10] Reddy, P. V. and Narasimham, G. S., Natural convection in a vertical annulus driven by a central heat generating rod, *International Journal of Heat and Mass Transfer*, 51, 5024–5032, (2008).

[11] Sankar, M., Park, Y., Lopez, J. M. and Do, Y., Numerical study of natural convection in a vertical porous annulus with discrete heating, *International*

Fig. 25 shows a cross-sectional view of the temperature contour plot with different fin shapes. This section was taken at the horizontal midsection. Using different fin shapes spreads out the temperature profile in the angular direction rather than the radial direction. Moreover, the difference in contact surface is insignificant. Therefore, the improvement among different fin shapes is small.
Fig. 26 shows a vertical side view of the temperature contour plot with different fin shapes. This section was taken at the vertical midsection. The width of hot fluid layers closer to the inner hot wall has small changes when using different shapes of fins.
However, using fins has a great improvement in heat transfer rate compared to cases without fins.

The velocity profile for different fins shapes shows that the velocity profile for the square fins is slightly more than other ones. Also, the velocity profile variations get larger towards the hot surface while closer toward the cold surface as shown in Fig. 27. This is because closer to the hot surface, we will have more dynamic and natural buoyancy movement while closer to the cold surface the fluid is denser and has less movement.

7. Conclusions

This study is for the natural convection of heat transfer in a vertical annulus enclosure where the inner surface is hot and the outer surface is cold. Fins were added to the inner surface to enhance the heat transfer performance. A numerical model was developed using ANSYS Fluent software to solve the governing equations for the model. The numerical model was grid tested and validated by comparing it to results in the literature. Afterward, a parametric study was carried out where one variable is changed while others are kept constants. Parameters chosen in our study are fins number, fins length, thickness, and shape. Results are presented for each parameter. The study results are concluded on the following points:

1- With the increase of fins number, the heat transfer enhanced up to 46% when using 16 fins. Also, it was found that this effect is similar to the one reported in the literature.

2- As the fins length increases, the heat transfer is enhanced up to 27% for 15mm fins length.

3- Fins did enhance the heat transfer by about 28%. Different fins thicknesses had a negligible effect on the heat transfer performance.

4- Square fins have the best results over circular and triangular fins by 5 to 10% respectively.

5- When the Rayleigh number increased, the heat transfer enhanced which is the same compared to the results reported in the literature. Also, when the Rayleigh number increased the temperature and velocity improved.

Nomenclature

g Gravitational acceleration (m/s^2)
Ha Hartmann number, the ratio of electromagnetic force to the viscous force.
K Thermal conductivity, W/(m.K)
k_{eff} Effective thermal conductivity, it is defined as the thermal conductivity of the air at which stagnant air in the annulus can give the same rate of heat transfer , W/(m.K).
L Fin length (mm)
P Pressure (N/m^2)
Pr Prandtl number

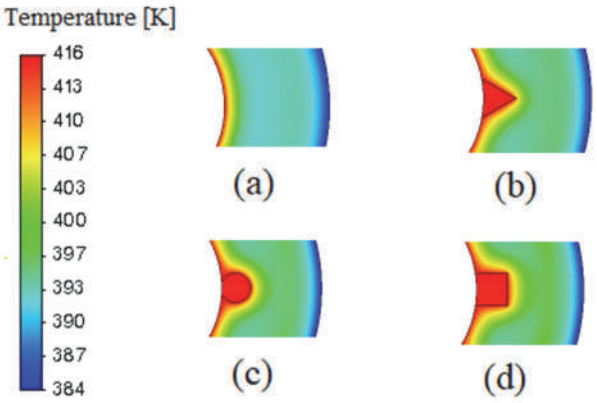

Fig. 25 Cross-sectional horizontal view of temperature contour for (a) no fins, (b) triangular fins, (c) circular fins, and (d) square fins.

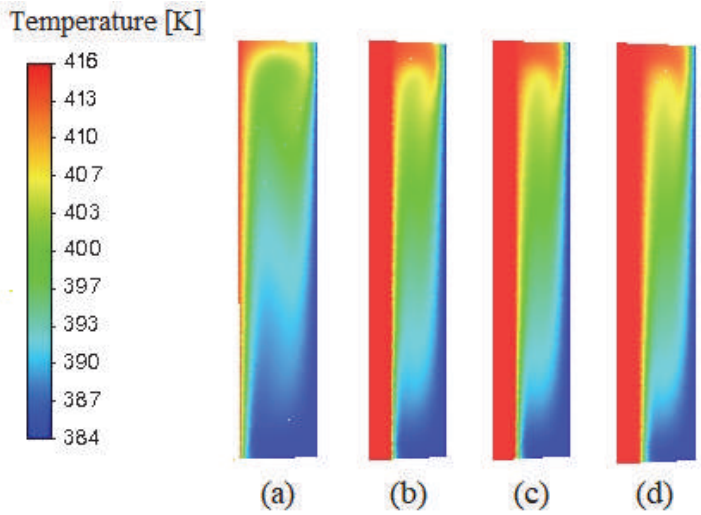

Fig. 26 Cross-sectional vertical view of temperature contour for (a) no fins, (b) triangular fins, (c) circular fins, and (d) square fins.

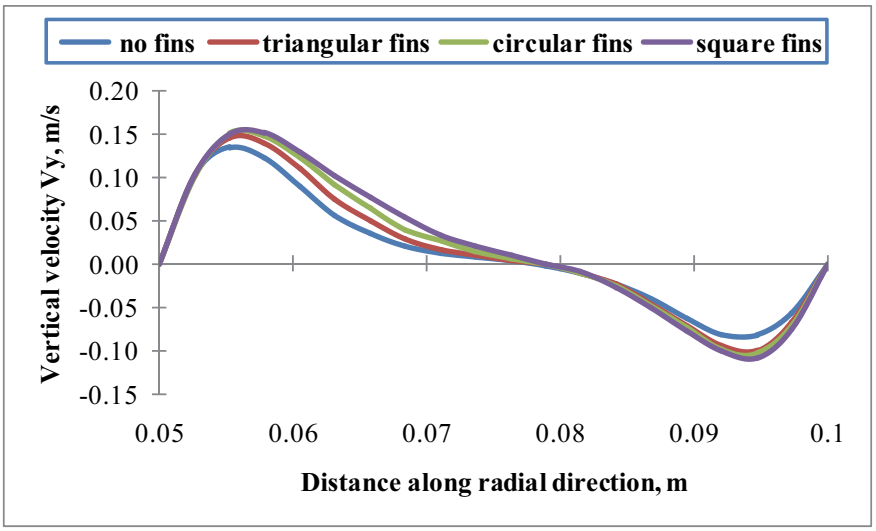

Fig. 27 Vertical velocity profile along the radial direction at the vertical midpoint from the inner hot surface to the outer cold surface at different shapes of the fins.

6.4. Effect of fins shape

Fig. 23 shows the effect of fins shape on heat transfer performance. Three fins shapes were studied and compared to no fins case. These shapes are triangular, circular, and square fins. Results revealed that when using triangular fins, the heat transfer is enhanced by 21% compared to no fins case. When using circular fins, the heat transfer is enhanced by 25% compared to no fins case. When using square fins, the heat transfer is enhanced by 29% compared to no fins case. Square fins would have the largest contact surface area to the working fluid compared to triangular and circular ones. Fig. 24 shows the effect of fins shapes on the temperature profile along the radial direction from the inner hot surface to the outer cold surface. It shows that the temperature profile of the square fins has a slightly better temperature profile than triangular and circular ones.

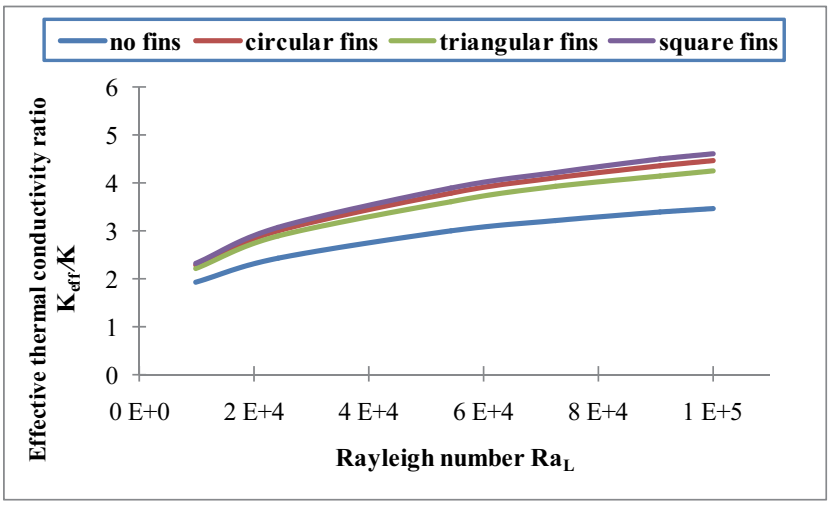

Fig. 23 Effective thermal conductivity ratio vs. Rayleigh number at different shapes of the fins.

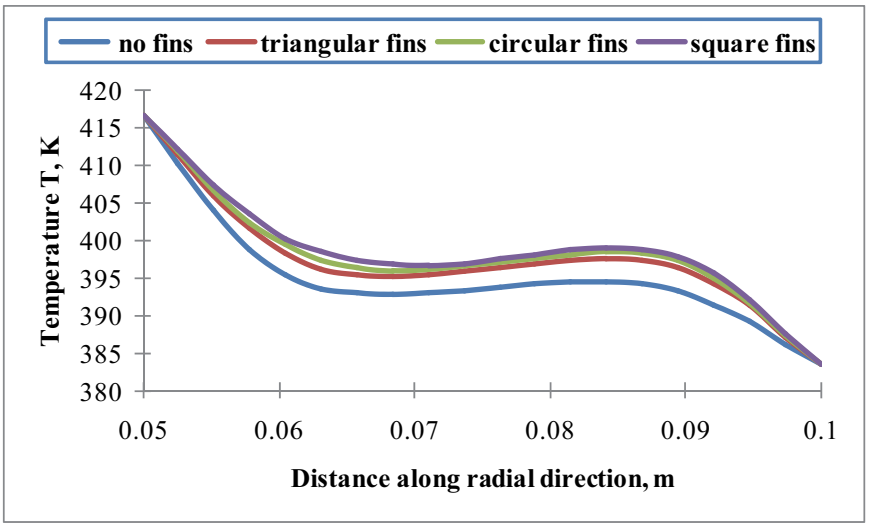

Fig. 24 Temperature profile along the radial direction at the vertical midpoint from the inner hot surface to the outer cold surface at different shapes of the fins.

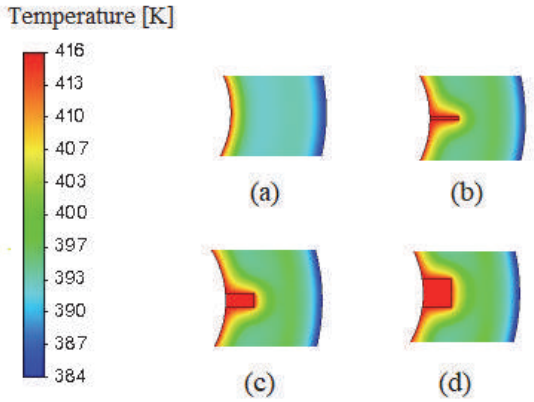

Fig. 20 Cross-sectional horizontal view of temperature contour for (a) no fins, (b) W=2 mm, (c) W=7 mm, and (d) W=15 mm.

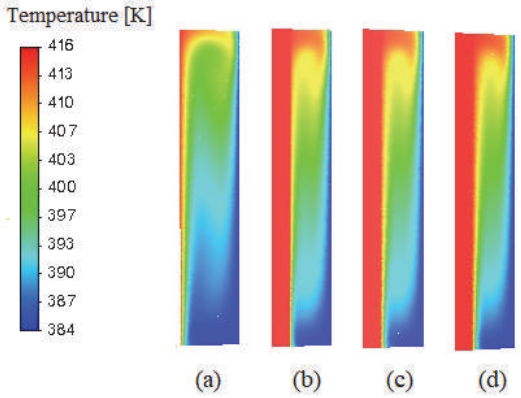

Fig. 21 Cross-sectional vertical view of temperature contour for (a) no fins, (b) W=2 mm, (c) W=7 mm, and (d) W=15 mm

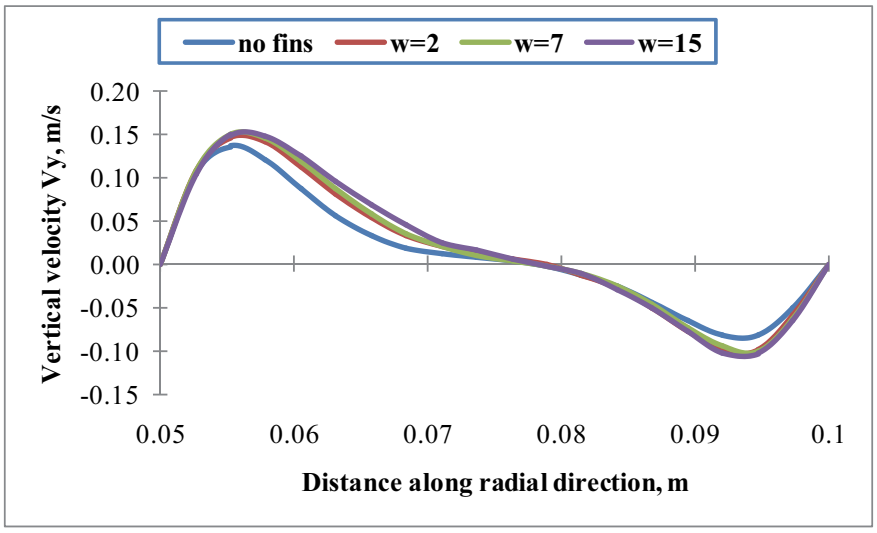

Fig. 22 Vertical velocity profile along the radial direction at the vertical midpoint from the inner hot surface to the outer cold surface at different fins thicknesses

compared to no fins case. When using fins thickness of 15 mm, the heat transfer is enhanced by 29% compared to no fins case. It was noticed that the effect of the increase in fins thickness is negligible. When we increase the fins thickness we increase the area of the fins tip only. The fins tip usually has a lower surface temperature than the base temperature. This means that the temperature gradient at the tip surface is very small which cannot contribute to the total heat transfer to the fluid. This explains why the effect is so small.

Fig. 19 shows the effect of fins thickness on the temperature profile along the radial direction from the inner hot surface to the outer cold surface. It shows that the profile for the three different thicknesses used is very close to each other. This is explained by the same argument addressed above about the small temperature gradient at the fin tip.

Fig. 20 shows a cross-sectional view of the temperature contour plot with different fin thicknesses. This section was taken at the horizontal midsection. With thicker fins, the temperature gradient spreads out in the angular direction. This has little effect on the heat transfer rate in the radial direction.

Fig. 21 shows a vertical side view of the temperature contour plot with different fin thicknesses. This section was taken at the vertical midsection. It can be observed that having fins has a great effect compared to the system without fins. Even though, changing the fins' thickness doesn't change the fluid hot layers much.

The vertical velocity profile is shown in Fig. 22. It can be seen that the increase of fins thickness has little to no effect on the vertical velocity profile. The reason is that increasing the fin thickness doesn't obstruct the movement of the fluid. It doesn't also reduce the cross-sectional area on a scale that will affect the mass flow. Therefore, the fins thickness has little to no effect on the vertical velocity profile.

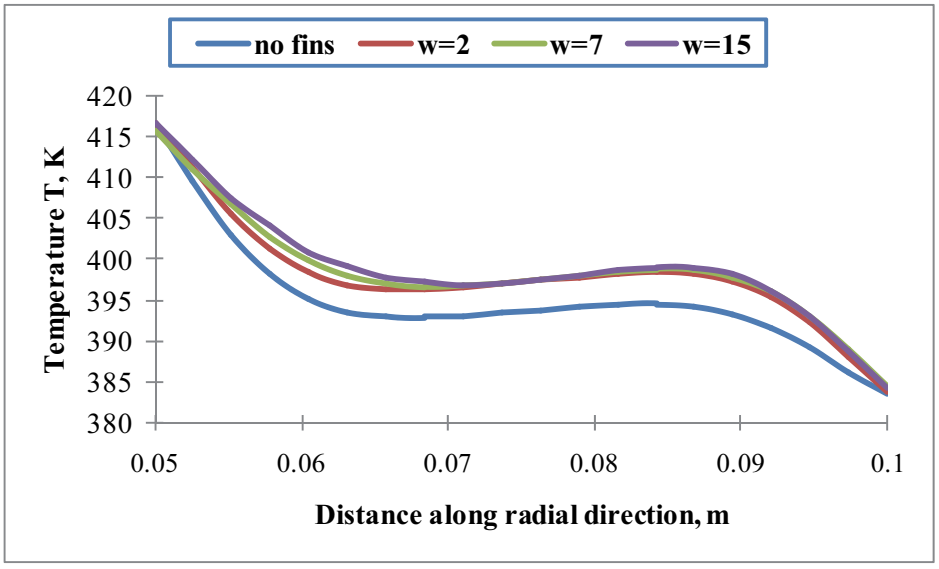

Fig. 19 Temperature profile along the radial direction at vertical mid-point from the inner hot surface to outer cold surface at different fins thickness.

based on the conservation of mass which can be seen clearly in Fig. 17.

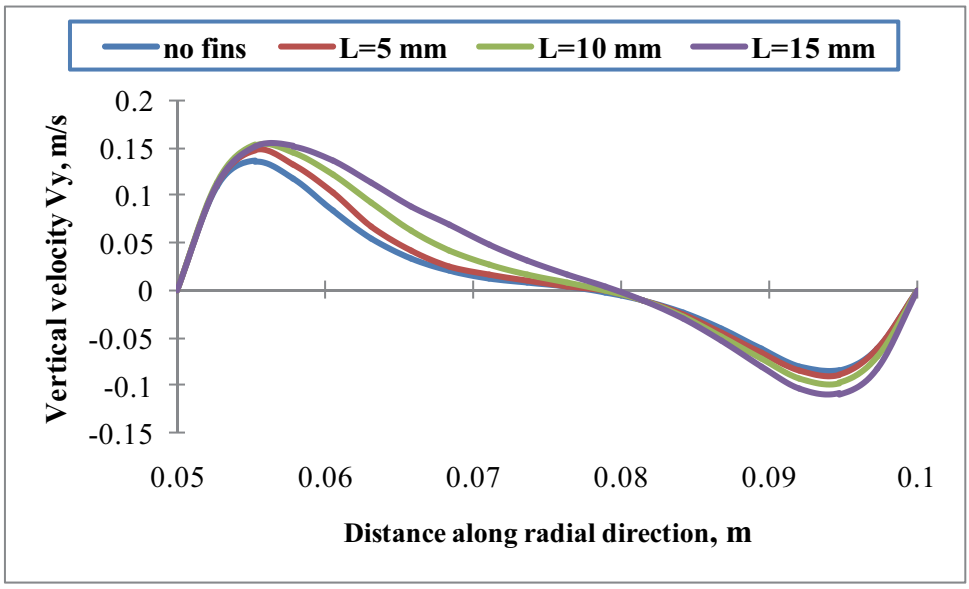

Fig. 17 Vertical velocity profile along the radial direction at vertical mid-point from the inner hot surface to outer cold surface at different fins lengths.

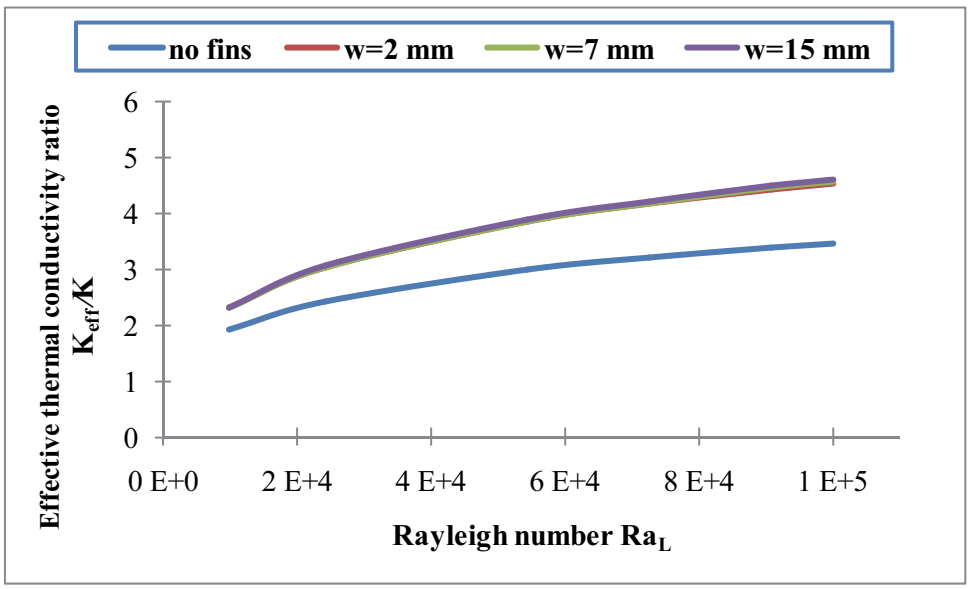

Fig. 18 Effective thermal conductivity ratio vs. Rayleigh number at different fins thicknesses

.

6.3. Effect of fins thickness

Fig. 18 shows the effect of fins thickness on heat transfer performance. when the fins' thickness increases, the contact surface area of total fins exposed to the enclosed fluid increases, and thus, the heat transfer rate increases. When using fins thickness of 2 mm, the heat transfer enhances by about 27% compared to no fins case. When using fins thickness of 7 mm, the heat transfer is enhanced by 28%

Fig. 14 Temperature profile along the radial direction at the vertical midpoint from the inner hot surface to the outer cold surface at different fins lengths.

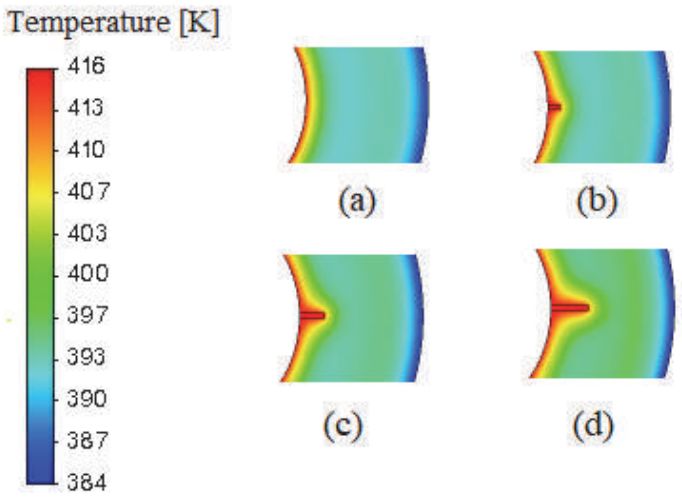

Fig.15 Cross-sectional horizontal view of temperature contour for (a) no fins, (b) L=5 mm, (c) L= 10 mm, and (d) L= 15mm.

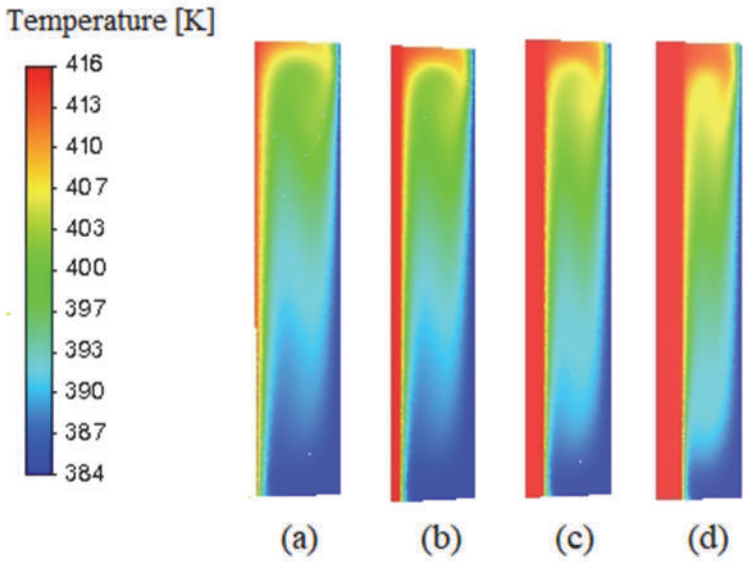

Fig.16 Cross-sectional vertical view of temperature contour for (a) no fins, (b) L=5 mm, (c) L= 10 mm, and (d) L= 15 mm.

Fig. 16 shows a vertical side view of the temperature contour plot with different fin lengths. This section was taken at the vertical midsection. The figure shows wider layers of fluid at a specific range of temperature. This is explained by longer fins, which raise the fluid temperature on the left side.

When the fins length increases, the heat transfer enhances therefore, the velocity profile increases. Moreover, when fins are placed inside the annulus, the volume of the air domain is reduced compared to the annulus without fins hence, the cross-sectional area decreases causing the vertical movement of mass to increase. This is

6.2. Effect of fins length

Fig. 13 shows the effect of fins length on heat transfer performance. When fins length increases, the contact surface area of total fins exposed to the enclosed fluid is increased, and thus, the heat transfer rate increases. When using the fin length of 5 mm, the heat transfer is enhanced by 5% compared to no fins case. When using the fin length of 10 mm, the heat transfer is enhanced by 16% compared to no fins case. When using the fin length of 15 mm, the heat transfer is enhanced by 27% compared to no fins case.

Fig. 14 shows the effect of fins length on the temperature profile along the radial direction from the inner hot surface to the outer cold surface. It shows that the temperature profile generally increases with the increase of fins length. It also shows that the temperature gradient increases toward the inner hot surface while decreasing toward the outer cold surface. Figure 15 shows a cross-sectional view of the temperature contour plot with different fin lengths. This section was taken at the horizontal midsection. For longer fins, the fluid temperature at the inner hot wall (left), which is closer to the fins gets higher in temperature. This clearly enhances the heat transfer rate.

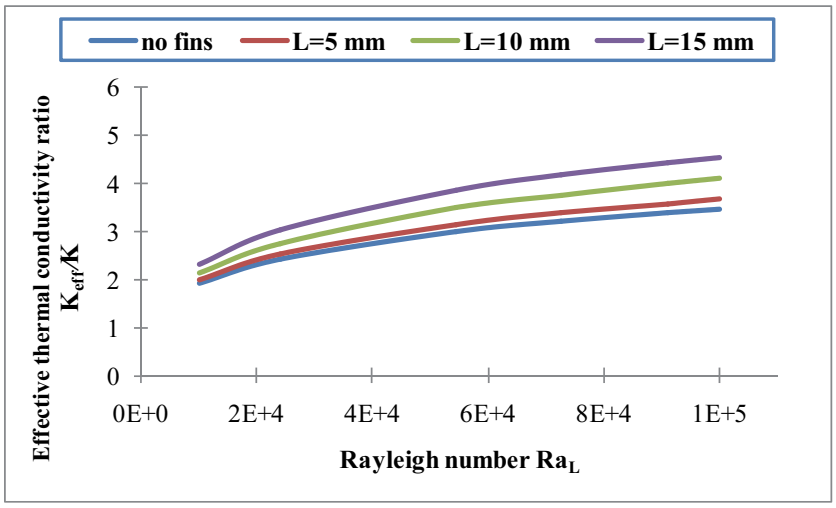

Fig. 13 Effective thermal conductivity ratio vs. Rayleigh number at different fins length.

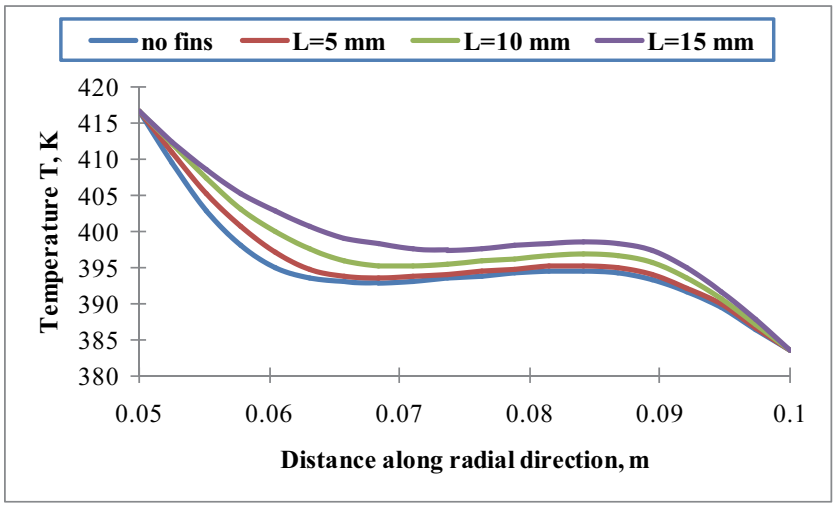

side it becomes cooler and drops down. Adding fins to the inner hot side increases the heat transfer and, hence the velocity in the vertical direction increases. This can be seen clearly in Fig. 12. When the velocity has a positive value, this means the fluid movies to the upper direction and when the velocity has a negative value this means the fluid movies to the lower direction. Note that for the case with no fins, the air is almost stagnant at the midpoint between the two vertical surfaces. This is because vertical fluid movement occurs near the walls. As fins are added, it disturbs the fluid movement at the midpoint and provides extra movement to the fluid.

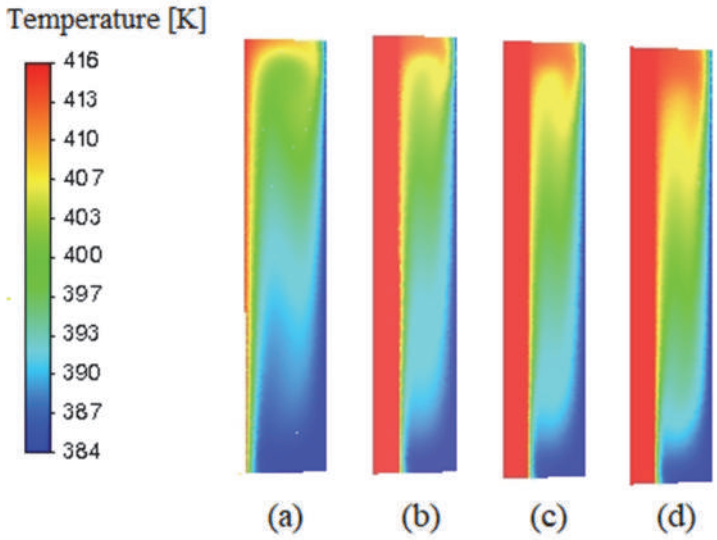

Fig. 11 Cross-sectional vertical view of temperature contour for (a) no fins, (b) four fins, (c) eight fins, and (d) sixteen fins.

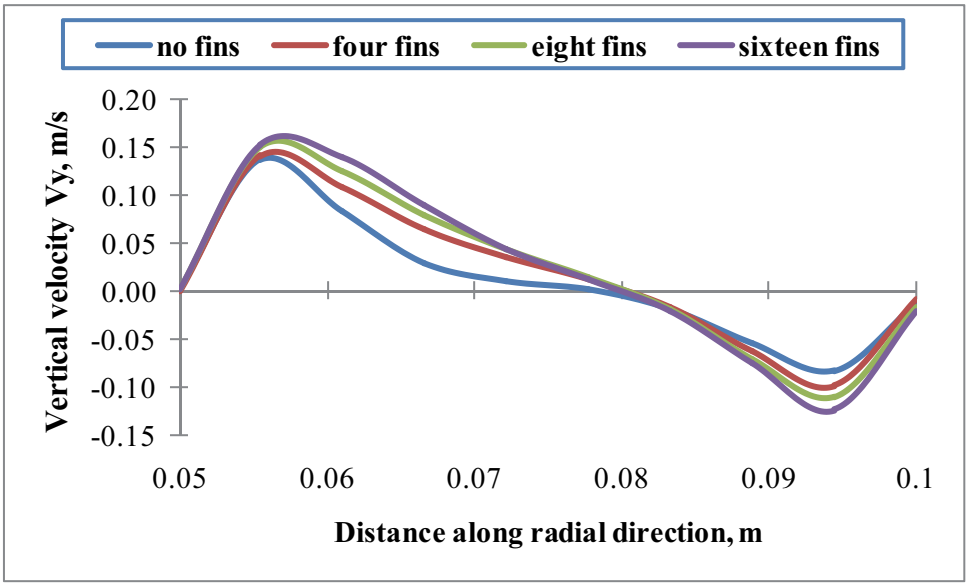

Fig. 12 Vertical velocity profile along the radial direction at the vertical midpoint from the inner hot surface to outer cold surface at different fins numbers.

generally increases with the increase of fins number.

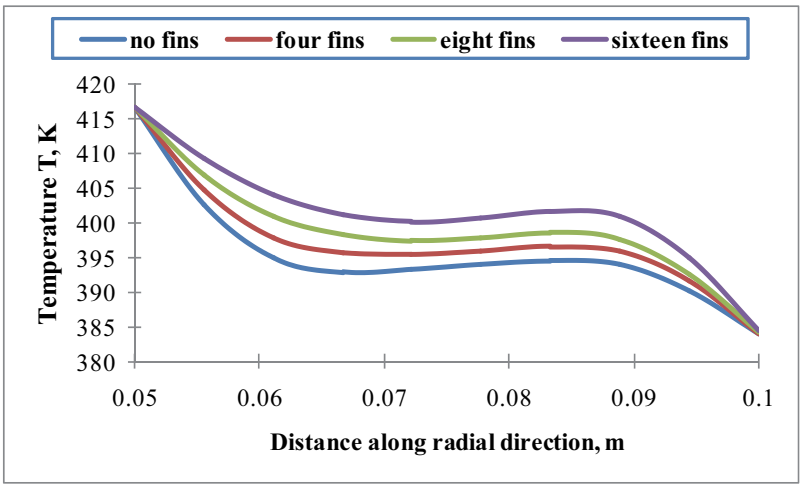

Fig. 9 Temperature profile along the radial direction at the vertical midpoint from the inner hot surface to outer cold surface at different fins number.

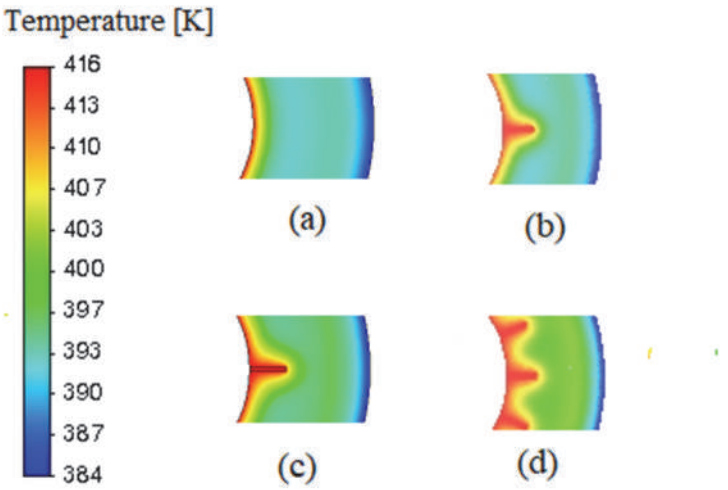

Fig.10 Cross-sectional horizontal view of temperature contour for (a) no fins, (b) four fins, (c) eight fins, and (d) sixteen fins.

Fig. 10 shows a cross-sectional view of the temperature contour plot with the different numbers of fins. This section was taken at the horizontal midsection. It is seen that with more fins, the hot temperature contour lines spread out away from the inner hot surface. This means a higher temperature gradient ($\frac{\partial T}{\partial X}$) and, thus, higher heat transfer.

Fig. 11 shows a vertical side view of the temperature contour plot with the different numbers of fins. This section was taken at the vertical midsection. It can be seen that with more fins, the fluid layers at the inner hot surface (left) become higher in temperature, which means higher heat transfer.

To understand the number of fins' effect on the velocity we should first discuss how the fluid velocity moves inside the annulus without fins. When the vertical inner hot surface (inner side) heats up the adjacent air it will rise up due to the buoyancy effect. When air reaches the top side and moves toward the vertical outer cold

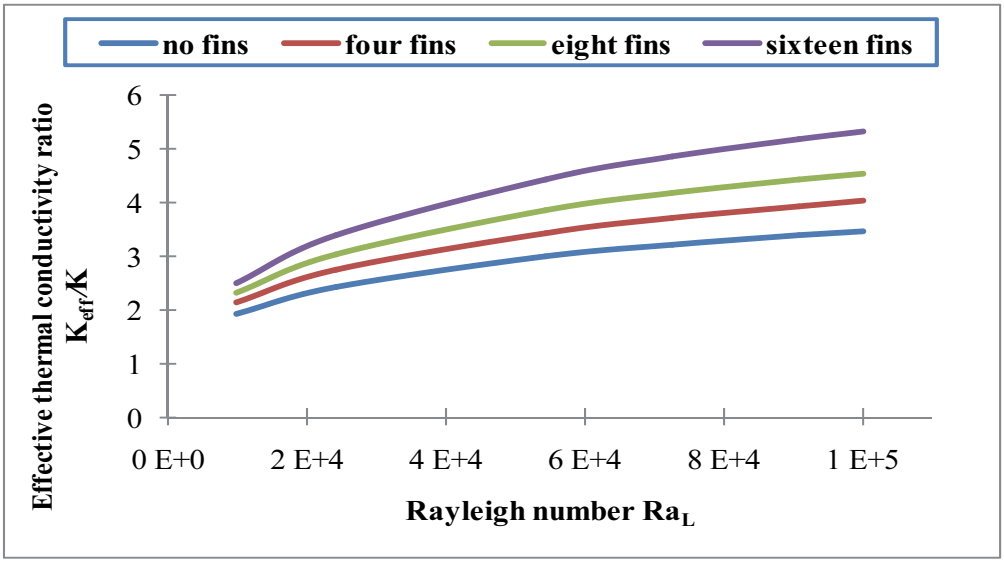

Fig. 8 Effective thermal conductivity ratio vs. Rayleigh number at different fins number

6. Results and Discussions

6.1. Effect of fins number

Fig. 8 shows the effect of fins number on heat transfer performance. When the fins number increases, the contact surface area of total fins exposed to the enclosed fluid increases, and thus, the heat transfer rate increases. When using four fins, the heat transfer is enhanced by 15% compared to no fins case. When using eight fins, the heat transfer is enhanced by 27% compared to no fins case. When using sixteen fins, the heat transfer is enhanced by 46% compared to no fins case.

The effect of fins number in these study correspond with the effect of fins number reported in Nada and Said study [22]. Despite their study being done on a horizontal annulus, the effect is the same which is the increase in natural convection with the increases of fins number which is the same effect in this study. The similarity of the results is because the principle of both studies is the same, which is the increase of fins number, causes an increase in the contact surface area of total fins exposed to the enclosed fluid hence, the rate of heat transfer increases.

The effect of the Rayleigh number on the heat transfer in Rahnama and Farhadi's study [20] shows that the heat transfer increases with the Rayleigh number increases. Although their study was done on turbulent natural convection, it has the same effect compared to our study. Also, Nada and Said's study [22] where their study was done on laminar natural convection in a horizontal annulus. It was found that the natural convection increases with the increase of Rayleigh number which is the same effect in this study.

It can be observed that the Rayleigh number has the same effect on the heat transfer rate in both laminar natural convection and turbulent natural convection, also the Rayleigh number has the same effect on the heat transfer rate in both the horizontal annulus and the vertical annulus.

Fig. 9 shows the effect of fins number on the temperature profile along the radial direction from the inner hot surface to the outer cold surface. It shows that the temperature profile

5.2. Code Validation

Due to the initial conditions and assumptions used in the vertical annulus studies, the validation was found easier with the horizontal annulus studies than with the vertical annulus studies. Therefore, the present study was validated by comparing its output results with four different horizontal annulus studies. Two of the four studies were performed experimentally [29] and [30] and the other two were performed numerically [21] and [23].

In order to compare our results to these four studies, our work was run under the same conditions used in those four studies. The present study results compared with the results of the four studies and showed a good agreement as shown in Fig. 7 We used the effective thermal conductivity ratio (K_e/K_f) to represent the enhancement of the natural convection in a dimensionless form and the modified Rayleigh number (Ra_m) to represent the temperature difference between the hot side and the cold side of the annulus in a dimensionless form.

The relationship between the K_e/K_f and Ra_m is a positive relationship. Hence, when the Ra_m increases, the K_e/K_f increases. We used the effective thermal conductivity ratio (K_e/K_f) vs. modified Rayleigh number (Ra_m) in the validation because it was used in the literature [21,23] Hence, we can compare our results to those in the literature.

Modified Rayleigh number (Ra_m) is given as:

$$Ra_m = Ra_i^{\frac{1}{4}} (0.1389(1-\frac{D_i}{D_o})+0.0927)\ln(\frac{D_o}{D_i}) \quad (7)$$

Where Rai is the Rayleigh number based on the inner diameter and given as:

$$Ra_i = \frac{g\beta(T_h-T_c)(D_i)^3}{\alpha\nu} \quad . (8)$$

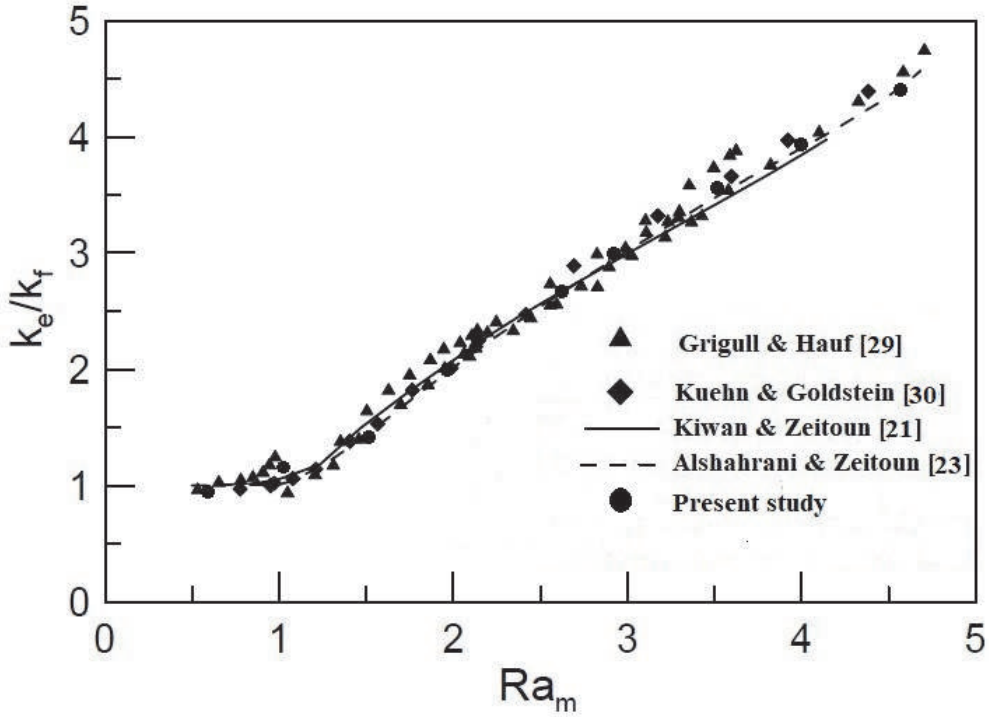

Fig. 7 Numerical model validation: K_e/K_f vs. Ra_m

Table1 Fixed and changed values of the four parameters

Parameter	Original Value	Changed values
number of fins	8	4,8,16
fins length	15 mm	5 mm, 10 mm, 15 mm
fins thickness	2 mm	2 mm, 7mm, 15 mm
fins shape	rectangular	circular, triangular, square

5. Grid Test and Code Validation

5.1. Grid Test

One of the Ansys fluent steps to obtain the solution is to divide the geometry into discrete control volumes or elements. When the mesh size was reduced, the number of elements increased. and the output of the results is more accurate. The effective thermal conductivity ratio (K_{eff}/K) was used as the output results to test the grid accuracy.

The grid test was done at $Ra_L=10^5$ and started by increasing the number of elements from 194275 to 4054716 elements. Table 2 and Fig. 6 show the resulted K_{eff}/K for different numbers of elements. The number of elements Increased until the change in the effective thermal conductivity ratio became minimum. After the number of elements of 3,446,018, the effective thermal conductivity ratio value remains at 3.466 with less than 0.09 % error, hence, the number of elements of 3,446,018 is used in our current project.

Table 2 Effective thermal conductivity ratio for different numbers of elements

Number of elements	K_{eff}/K
194275	4.152
277962	3.544
541394	3.512
1032848	3.491
1421910	3.483
2005578	3.475
2586843	3.472
3009350	3.469
3446018	3.466
4054716	3.466

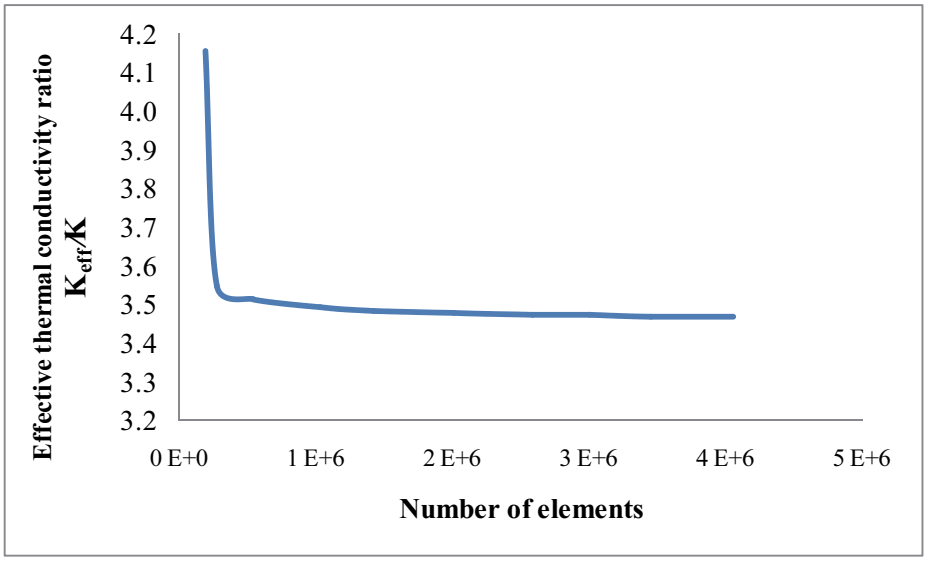

Fig. 6 Effective thermal conductivity ratio vs. number of elements

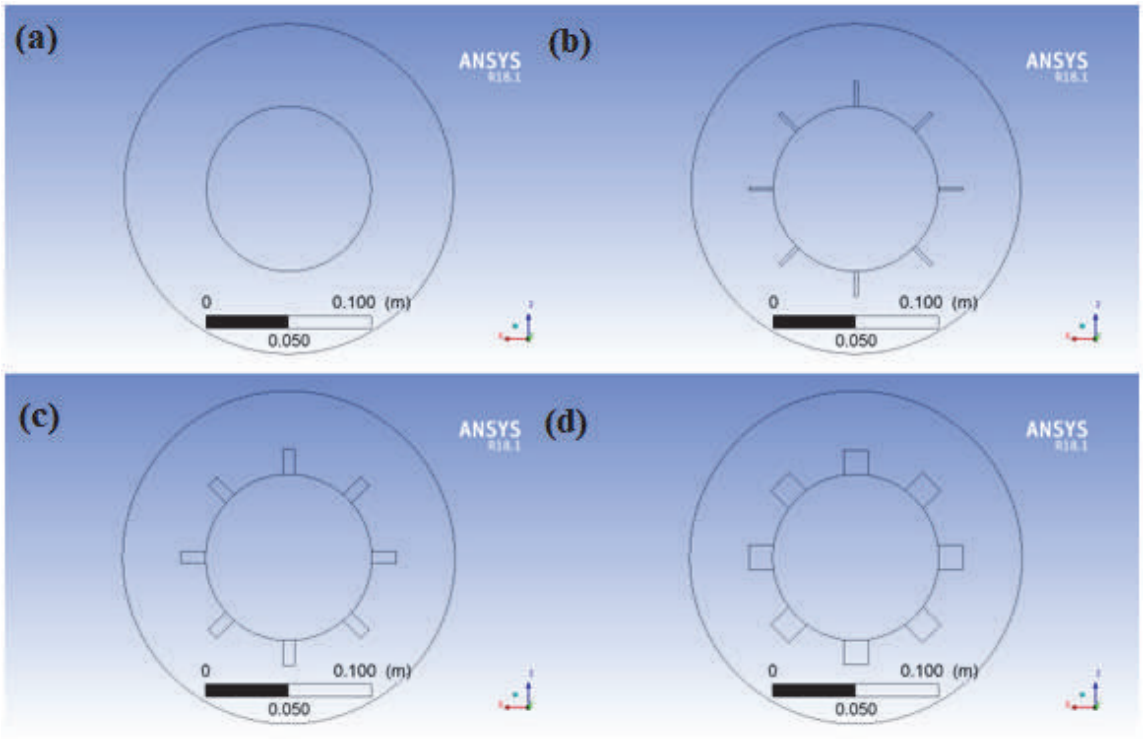

Fig. 4 Vertical annulus with (a) no fins, (b) W=2 mm, (c) W=7mm, and (d) W=15 mm.

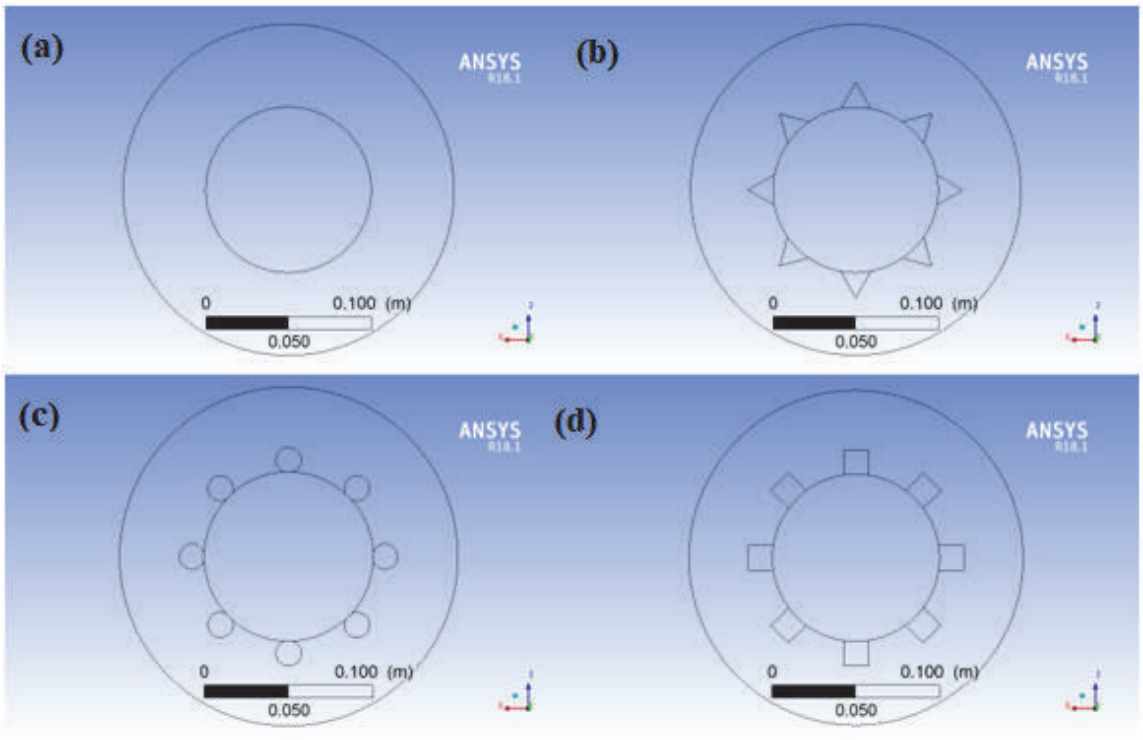

Fig. 5 Vertical annulus with (a) no fins, (b) triangular fins, (c) circular fins, and (d) square fins.

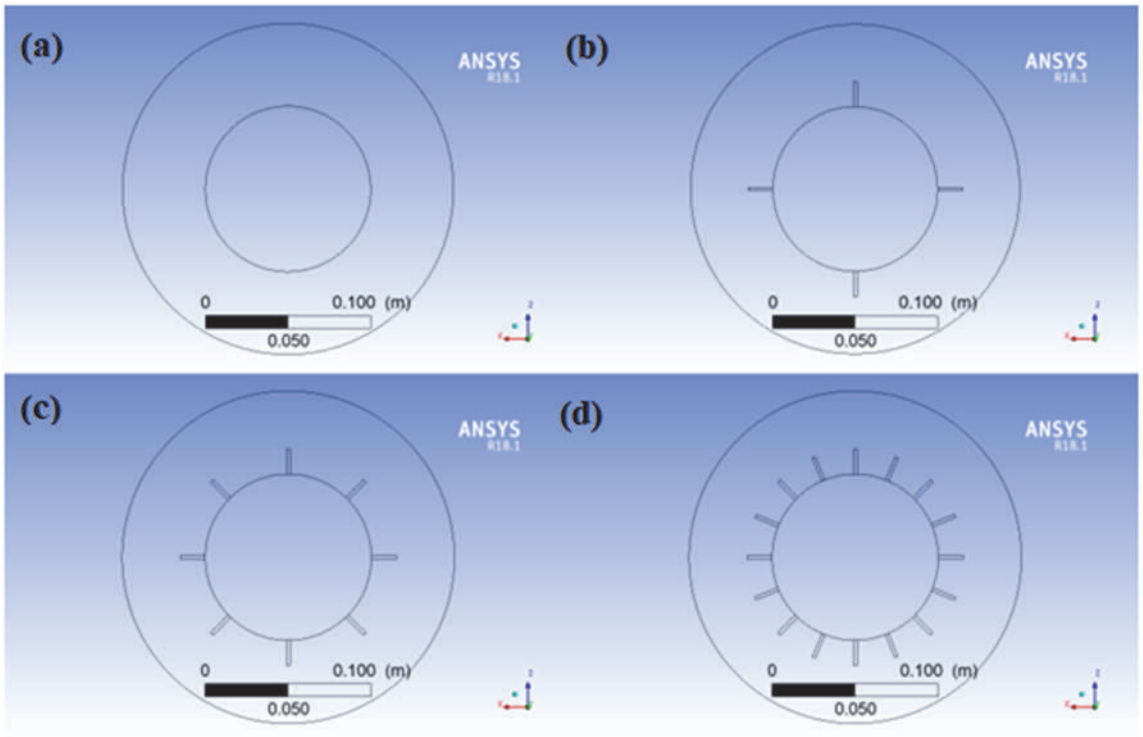

Fig. 2 Vertical annulus with (a) no fins, (b) four fins, (c) eighth fins, and (d) sixteenth fins.

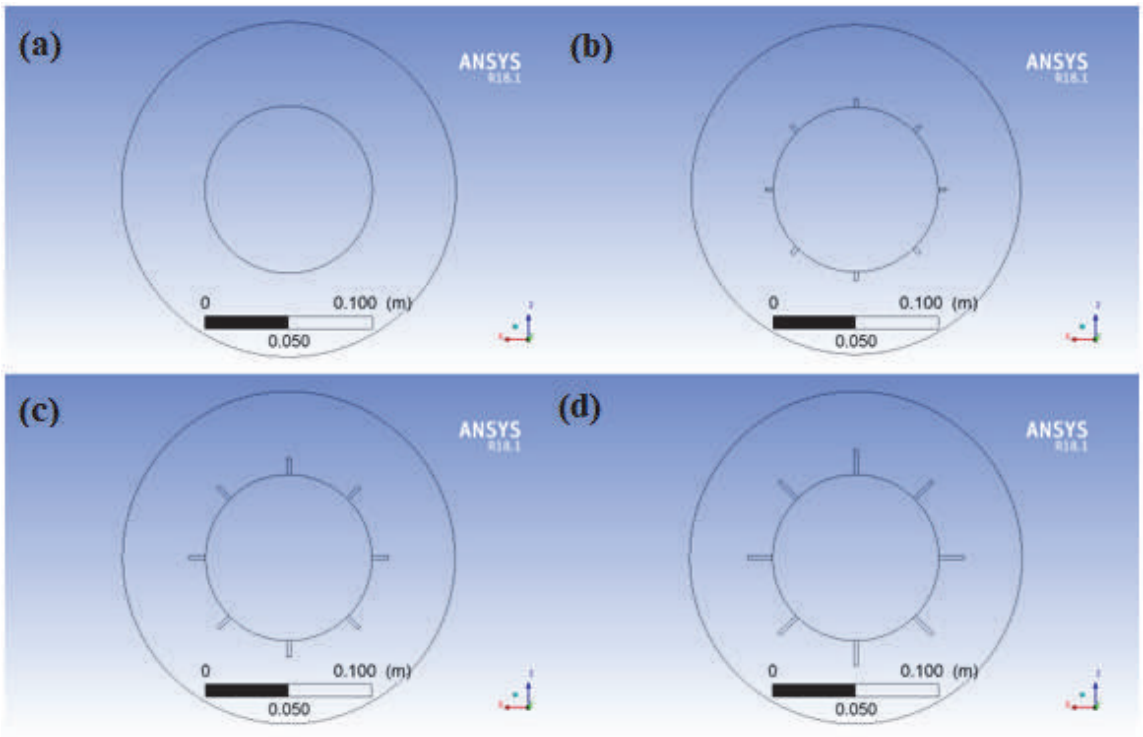

Fig. 3 Vertical annulus with (a) no fins, (b) L=5 mm, (c) L=10 mm, and (d) L=15 mm.

Hence it may also be viewed as the ratio of buoyancy and viscosity forces multiplied by the ratio of momentum and thermal diffusivities, Bergman et al. [1].

In the present study, the Rayleigh number is dependent on the temperature difference between the hot and cold sides of the annulus which means that the other parameters such as r_i and r_o are fixed at 50 mm and 100 mm respectively while the hot inner side temperature and the cold outer side temperature are varied.

The dimensionless groups of the Rayleigh number and Prandtl number are defined as follows, Bergman et al. [1]:

$$Ra_L = \frac{g\beta(T_h - T_c)(r_o - r_i)^3}{\alpha\nu} \quad (4)$$

$$Pr = \frac{\nu}{\alpha} \quad (5)$$

In natural convection in an annulus, the heat transfer coefficient depends on the inner and outer radius of the annulus. Therefore, the free convection heat transfer in the annulus is normally calculated in terms of the effective thermal conductivity of the fluid in the annulus which is defined as the thermal conductivity of the fluid at which stagnant fluid in the annulus can give the same rate of heat transfer. In order to use the effective thermal conductivity in a dimensionless group, we divide it by the thermal conductivity to become the effective thermal conductivity ratio which is considered an indicator of the thermal conductivity enhancement ratio due to natural convection. Hence, when the effective thermal conductivity ratio increases, this means the natural convection is enhanced.

The ANSYS Fluent has many correlations which use to solve the problems. Based on the inputs and the geometry of the problem, the ANSYS Fluent selects a suitable correlation to obtain the results. In our problem, we input the following parameters: the outer diameter (D_o) and inner diameter (D_i) of the annulus, the thermal conductivity of the fluid (K), the temperature difference between the hot inner surface of the annulus (T_h) and the cold outer surface of the annulus (T_c). The numerical method used in ANSYS Fluent to obtain the heat transfer rate is the finite volume method. The ANSYS Fluent will compute the heat transfer rate and we use it in Eq. 3.6 to calculate the effective thermal conductivity ratio (K_{eff}/K).

The equation of the effective thermal conductivity ratio is given as follows, Nada and Said [22]:

$$K_{eff}/K = \frac{q' ln \frac{Do}{Di}}{2\pi K (T_h - T_c)} \quad (6)$$

4.3 Fins Specifications And Parametric Study

Longitudinal fins are added to the inner hot vertical wall inside the 3D annulus enclosure. The fins were made of copper and we used copper because it is easier to maintain than aluminum fins.

A parametric study was conducted to study the effect of four parameters on the heat transfer rate performance. These four parameters are the number of fins, fins thickness, fins length, and fins shape. When we study these parameters, only one parameter was changed while the others remain constant, for example when we study the fins' shape we change the fins' shape while the fins' thickness, number, and length remain fixed. All cases were compared to the model without fins.

The study was done for the number of fins 4, 8, and 16. Fins' length was changed from 5 mm to 15 mm. Fins thickness of 2 mm, 7 mm, and 15 mm were used, and different shapes of square, circular, and triangular shapes were used. The four studied parameters are shown in Fig. 2 to 5 and their dimensions are shown in Table 1.

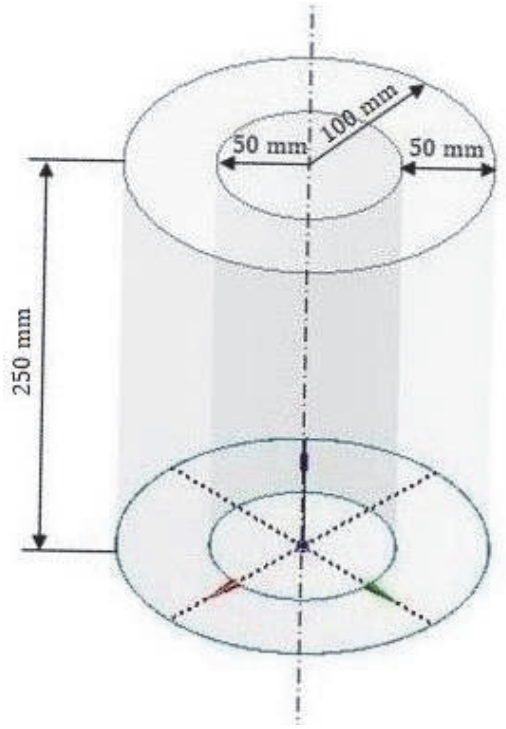

Fig.1 Schematic of the vertical annulus

Buoyancy force was modeled using Boussinesq approximation and taking gravity g=−9.81 m/s^2 in the negative vertical direction. In this project we assumed the following:
1- The variation of the density was taken into account only in the body forces (Boussinesq approximation).
2- Steady-state.
3- No heat generated.
4- No radiation in the enclosure between surface nor fluid particles.

4.2 Ansys Fluent

Ansys Fluent is industry-leading fluid simulation software used to predict fluid flow, heat and mass transfer, chemical reactions, and other related phenomena. Known for delivering the most accurate solutions in the industry, Ansys fluent is based on the finite volume method and works by the following steps:
1. The domain or the geometry in this study is discretized into a finite set of control volumes using a computational domain also known as mesh.

2. The general conservation equations such as mass, momentum, and energy are solved on this set of control volumes.

3. The partial differential equations are discretized into algebraic equations.

4. All algebraic equations are then solved numerically to obtain the solution.

It is important that the computational domain (mesh) is accurate enough to obtain accurate results therefore we decrease the control volumes (mesh size) and run the simulation and record the output results, we repeat this process until the output results become almost the same, this process called the mesh test also known as the grid test.

For the present study, we used Ansys fluent to solve the governing equation to obtain the effective thermal conductivity ratio, temperature distribution, and velocity profile. This is done by iterations through the discretization of the model. The governing equations were solved sequentially using a pressure-based solver. Momentum and energy equations were solved using a second-order implicit scheme. The governing equations for mass, momentum, and energy are defined as follows, Bergman et al. [1]:

$$\boldsymbol{\nabla \cdot V = 0} \quad (1)$$

$$\boldsymbol{\rho(V \cdot \nabla)V = -\nabla P + \mu \nabla^2 V + \rho g} \quad (2)$$

$$\boldsymbol{(V \cdot \nabla)T = \alpha \nabla^2 T} \quad (3)$$

The Rayleigh number is a dimensionless number associated with the buoyancy-driven flow and can be defined as the product of the Grashof number, which describes the relationship between the ratio of buoyancy forces to viscous forces, and the Prandtl number, which describes the relationship between the ratio of the momentum and thermal diffusivities.

inclination angle has a weak effect on the thermal conductivity ratio, where the effective thermal conductivity of the fluid is defined as the thermal conductivity of the fluid at which stagnant fluid in the annulus can give the same rate of heat transfer, and the effective thermal conductivity ratio is the effective thermal conductivity of the fluid divided by the thermal conductivity of the same fluid. Shadlaghani et al.[24] numerically studied the natural convection in a horizontal concentric and eccentric annulus with serrated fins. The results showed that the heat transferred is better in the eccentric annulus case compared to the concentric annulus one.

2.2.2. Vertical annulus

A few studies were performed to study the effect of fins on the natural convection in the vertical annulus. Ramezanpour and Hosseini [25] experimentally studied the natural convection in a vertical annulus with a helical fin and the results show that the helical fin enhances the heat transfer. Solomon and Velraj [26] experimentally studied the natural convection in a vertical annulus with longitudinal fins during the phase change material, where the phase change material is a substance that absorbs or releases large amounts of latent heat when they go through a change in their physical state, the results of the study showed that with the fins used an enhancement occurs in the heat transfer. Kumar [27] numerically studied the natural convection in a vertical annulus with longitudinal fins for various parameters. The results show that the heat transfer rate increases with the increase of the fin width and radius ratio and decreases as the aspect ratio increases beyond one, where the aspect ratio is the annulus height divided by the annulus gap width.

The literature review revealed that adequate studies on natural convection in the annulus were done, but when it's come to natural convection in the annulus with fins, especially on the vertical annulus, few studies were done. Therefore, more studies on vertical annulus with fins are needed.

3. Study Goal

This project will study parameters: fins number, length, thickness, and shape. Their effect on heat transfer rate, temperature distribution, and velocity profile will be studied and presented. The model of a 3-D vertical annulus enclosure was established. It was studied numerically using Ansys fluent.

4. Problem Formulation

4.1 Model Specifications

The mathematical model is a 3-D vertical annulus enclosure with a hot inner wall and cold outer wall, Schematic of the vertical annulus is shown in Fig.1. Boundary conditions of the top and bottom wall are insulated, the inner vertical wall has a hot temperature T_H of 401.65 ℃ to 416.5 ℃ and the outer vertical wall has a cold temperature T_C of 383.5 ℃ to 398.35 ℃. Temperatures of vertical walls were chosen so that R_L values range from 10^4 to 10^5.

Radiation heat transfer becomes important at high temperatures (above 1000 K) [28] and our present study did not reach this limit. Therefore, we can neglect the radiation effect.

increases with the increase in the modified Rayleigh number, and decreases with the increase in the heater length. Chen et al. [12] studied the effect of inner-wall motion on the linear stability of natural convection in a tall vertical annulus using linear theory, the results reveal that the inner wall motion has a significant effect on the stability characteristics. Sankar et al. [13] numerically studied the effect of the axial and radial magnetic field on the natural convection in a vertical annulus. The results indicated that for the shallow cavity, the flow and heat transfer in suppressed is more by the axial magnetic field, while in the tall cavity the radial is more effective. Husain and Siddiqui [14] experimentally and numerically studied the transient natural convection of water in a high aspect ratio narrow vertical annulus. The results showed that the transient period increases gradually as the annulus height increases while decreasing as the heat input increases. Afrand et al. [15] numerically studied the natural convection in a vertical annulus filled with molten gallium in the presence of the horizontal magnetic field. The results revealed that the magnetic field is generating the Lorentz force in the opposite direction of the buoyancy force. Abhilash and Lal [16] numerically studied natural convection in a narrow vertical annulus which is closed at the top and opened at the bottom. They noticed two different modes of flow which are the radial mode and the circumferential mode. Also, the Rayleigh number has an important effect on these modes' stability. Wang et al. [17] numerically studied the natural convection in a vertical annulus with an inner wall covered by a porous layer. The results showed that wrapping with a porous layer is a good tool for both increasing or reducing heat transfer. Char and Lee [18] numerically studied the natural convection in a porous medium saturated with cold water under density inversion. The results revealed that the inversion parameter and the radius ratio have an important effect on the flow and heat transfer, where the radius ratio is the difference between the inner and outer radius divided by the inner radius. Jha et al. [19] analytically studied the effects of suction/injection and wall surface curvature on natural convection flow in a vertical micro-porous annulus. It is found that when the suction/injection on the cylinder walls is increased, the velocity and temperature are increased.

2.2. Natural convection in the annulus with fins

2.2.1. Horizontal annulus

The effect of the fins on the natural convection in the horizontal annulus was studied from many aspects. For example, Rahnama and Farhadi [20] numerically studied the radial fins effect on the turbulent natural convection in a horizontal annulus. It was found that the fins arrangement has no significant effect on the heat transfer while its effect on the flow and temperature fields is noticeable in the case of four fins arrangement. Kiwan and Zeitoun [21] numerically studied the laminar natural convection in a horizontal annulus with porous fins. The results revealed that the porous fins provided higher heat transfer rates than solid fins for similar configurationsNada and Said [22] numerically studied the effect of the longitudinal and annular fins on the natural convection in a horizontal annulus. The results showed that longitudinal fins enhance heat transfer better than annular fins. Alshahrani and Zeitoun [23] numerically studied the fin's inclination angle effect on the natural conduction in the horizontal annulus. It was found that the

the parameters are fins number, length, thickness, material, and shape, Bergman et al. [1].

2. Literature Review

In this study, we conduct a study on natural convection in annulus due to its important application such as in heat exchangers, chemical reactors, and nuclear reactors. Therefore the literature review will focus on natural convection in annulus shape.

2.1. Natural convection in the annulus

2.1.1. Horizontal annulus

Many studies were conducted on the natural convection in the horizontal annulus. For example, Nada [3] experimentally studied the effect of the annulus gap widths and the annulus inclination angle on the natural convection in an annulus and the results showed the heat transfer increases with the increase of the annulus gap width and slightly decreases with the increase of the annulus inclination angle. Yeh [4] numerically studied the natural convection in a horizontal annulus with open ends for the adiabatic outer cylinder surface case and isothermal outer cylinder surface case. He found that the maximum inner cylinder surface temperature reported was at the inner cylinder top and that the inner surface cylinder temperature decreased toward the outlet plan in the adiabatic case and remain relatively constant in the isothermal case. Kumari and Nath [5] numerically studied the unsteady natural convection in an annulus filled with a non-Darcy porous medium. The results showed that the annulus completely filled with a porous medium has the best insulating effectiveness. He also found that most of the natural convection in the horizontal annulus is confined at the top and bottom places, therefore, only these places should be insulated. Yoo [6] numerically studied the bifurcation and dual solutions for natural convection in the horizontal annulus. He found that when the value of the Prandtl number is ranged from about 0.3 to 1.0, two different fluid motion shape types were noticed. The first one is the crescent-shaped eddy in the annulus top. The second one is two counter-rotating eddies in a half annulus. Wang et al. [7] numerically studied the Magnetohydrodynamics effect on the natural convection in a horizontal annulus in terms of the uniform axial magnetic field impacts. It was noticed that a spiral flow arises and the symmetry breaking occurs under a weak magnetic field when Hartmann's number is less than ten. Yang and Kong [8] numerically studied the natural convection in a horizontal annulus. The smoothed particle hydrodynamics method was used and the results showed that the flow stability is increased by increasing the Rayleigh number. Belabid and Allali [9] numerically studied the temperature modulation effect on the natural convection in a horizontal porous annulus, the study is time-dependent and the time-dependent modulation is periodic with frequency and amplitude. It was found that the system became stable at moderate frequency values.

2.1.2. Vertical annulus

Regarding the natural convection in the vertical annulus, several studies were conducted in that area. For instance, Reddy and Narasimham [10] numerically studied the natural convection in a vertical annulus driven by a central heat generating rod. The results showed that with the increase of the Grashof number, the average Nusselt numbers of the inner and outer boundaries increased. Sankaret at.[11] numerically studied the natural convection in a vertical porous annulus with discrete heating for the inner wall, the results indicate that the heat transfer

JKAU: Eng. Sci., Vol. **32** No. 2, pp: 13 – 37 (1444 A.H. / 2022 A.D.)
Doi: 10.4197/Eng. 32-2.2

Natural Convection in a Vertical Annulus Enclosure with Longitudinal Fins

Sarhan Almaneey*, Abdullatif A. Gari*

* Mechanical Engineering King Abdulaziz University, Jeddah 21589, Saudi Arabia
E-mail address: salmaneey@stu.kau.edu.sa

Abstract. Heat transfer by natural convection can be found in many thermal engineering applications. In order to improve the heat transfer, fins are used to increase the contact surface and thus the heat transfer rate. In this project, natural convection heat transfer performance in the vertical annulus enclosure was studied numerically. Software Ansys fluent was used to solve the governing equations to arrive to velocity and temperature distribution. A grid test was performed, and the model was validated with previous experimental and numerical studies. The results showed that the fins have a significant effect on the heat transfer enhancement compared to the model without fins. Afterward, a parametric study was performed to study the effects of fins number, length, thickness, and shape. Increasing fins number increases the heat transfer rate by 46%. The effect of the number of fins on the heat transfer rate corresponds with the results in the literature. Increasing fins length increases the heat transfer rate by 27%. The fin thickness has a little effect on the amount of the convection heat transfer. It was also found that square fins have the best results over circular and triangular fins. Regarding the Rayleigh number effect, increasing the Rayleigh number increases the heat transfer rate, which corresponds with the results reported in the literature.

Keywords: Keywords: Natural convection; Vertical annulus; Longitudinal fins

1. Introduction

There is an increase in energy demand worldwide for industrial use. The rapid development of electronic devices for personal and industrial use and thermochemical processes led to the rise of technical and financial challenges. One of these challenges is the ability to enhance the heat transfer in these applications to reduce energy consumption and cost.

Sometimes the heat is not transferred adequately which can cause serious problems in the thermal systems. For example, when the heat generated from nuclear reactor rods is needed to be transferred regularly to maintain the temperature under control, therefore, enhancing the heat transfer is needed. Bergman et al. [1].

The heat transfer enhancement techniques are mainly classified into two groups. The first one is the active technique where an external source of power is required to maintain the heat transfer enhancement such as mechanical aids, surface vibration, fluid vibration, electrostatic fields, injection, suction, spray, and jet impingement. The second one is the passive technique where the external power source is not needed such as treated surfaces, rough surfaces, smooth surfaces, use of additives such as nanofluids, and extended surfaces such as fins, Rohsenow et al. [2].

The fins are used to enlarge the surface area, hence increasing the contact area resulting in increasing the heat transfer rate. It's important to mention that the effect of fins on the natural convection depends on several parameters. Some of

تقييم معرفة معلومات التصوير المقطعي بين مصوري الأشعة وطلاب البكالوريوس في المدينة المنورة، المملكة العربية السعودية

عبد العزيز قرشي[١]، وولاء الشريف[١]، وسلطان الشعبي[١]، وناصر المحسن [١]، و سعيد الجهني [١]، وعصام بانقيطة[٢٢]، وأحمد سبحي [٣،٤]، وشروق الظاهري[٥]، وخالد الشمراني[٤،٦]

١- قسم تقنية الأشعة التشخيصية، كلية العلوم الطبية التطبيقية، جامعة طيبة، المدينة المنورة، المملكة العربية السعودية

٢- قسم الهندسة النووية، كلية الهندسة، جامعة الملك عبد العزيز، ص.ب. ٨٠٢٠٤، جدة ٢١٥٨٩

٣- كلية العلوم والمهن الصحية، جامعة الملك سعود بن عبد العزيز للعلوم الصحية، جدة، المملكة العربية السعودية

٤- مركز الملك عبد الله العالمي للأبحاث الطبية، جدة، المملكة العربية السعودية

٥- قسم تقنية الأشعة التطبيقية، كلية العلوم الطبية التطبيقية، جامعة جدة، جدة، المملكة العربية السعودية

٦- كلية العلوم الطبية التطبيقية، جامعة الملك سعود بن عبد العزيز للعلوم الصحية، جدة، المملكة العربية السعودية

مستخلص. الهدف من هذه الدراسة هو تقييم فنيي وطلاب الأشعة التشخيصية من حيث معرفتهم بالعوامل المؤثرة على طرق التصوير باستخدام أجهزة الأشعة المقطعية وقياس مدى تأثير ذلك على جودة الصورة والجرعة الاشعاعية. قام المؤلفون بتوزيع استطلاع على الفئات المستهدفة في أربعة مستشفيات في المدينة المنورة واحتوى الاستبيان على ١٢ سؤالا في صيغة خيارات متعددة وكانت متعلقة بالجوانب التقنية المتعلقة باستخدام أجهزة الأشعة المقطعية. تم تزويد المشاركين بشرح تفصيلي عن الهدف من الدراسة وتم التأكيد على الحفاظ على سرية المشاركين وبدون الإفصاح عن هويتهم أو أسماءهم. شارك في هذه الدراسة ٤٠ شخص، ٣١ منهم من فئة الطلاب (١٤ من المستوى الثامن، ١١ من المستوى السادس، ٩ من طلبة الامتياز) بينما كان هناك فقط من فئة فنيي الأشعة. أثبتت النتائج تفوق الطلاب من حيث مقدرتهم على الإجابة على معظم الأسئلة بشكل صحيح وذلك6 بمعدل الضعف مقارنة بفنيي الأشعة بغض النظر عن الفارق في حجم الخبرة الذي يمتلكه الفنيين. السبب الرئيسي في التفاوت بين مستوى الطلاب وفنيي الأشعة فيما يخص الاستطلاع يعود الى الفوارق في مستوى التعليم بين الفئتين حيث أن الفنيين المشاركين في هذه الدراسة لا يحملون سوى درجة الدبلوم.

كلمات مفتاحية: الأشعة المقطعية، الجرعات الاشعاعية، جودة الصورة، تقنية الأشعة، مهارات التحكم بالعوامل التقنية لفحوصات الأشعة المقطعية

[2] ebanoqitah@kau.edu.sa

C) Bone window. D) Lung window. 5) Which of the following describe the relationship between pitch and dose? A) If pitch increase, dose increase. B) If Pitch decrease, dose decrease. C) If pitch increase, dose decrease. D) Nothing happens. 6) What is "ALARA"? A) As Low as Responsibly Acceptable. B) Alarm Loss Activated Radiation Activated. C) As Low as Reasonably Achievable. D) As Low As Really Acceptable.	C) Increasing scan length D) Increasing pitch 11) Reducing kVp in CT results in: A) Better tissue contrast. B) Reduced scan time. C) Metal streak artifacts are improved. D) X-ray penetration improves. 12) Which of the following reduces noise: A) Decrease kVp. B) Decrease mAs. C) High pitch. D) Low pitch.

Radiographers' Knowledge of CT Exposure Parameters. *Insights Imaging*, 2013, *4* (5), 637–646. https://doi.org/10.1007/s13244-013-0282-4.

[12] Kim, M. J.; Park, C. H.; Choi, S. J.; Hwang, K. H.; Kim, H. S. Multidetector Computed Tomography Chest Examinations With Low-Kilovoltage Protocols in Adults: Effect on Image Quality and Radiation Dose. *J Comput Assist Tomo*, 2009, *33* (3), 416–421. https://doi.org/10.1097/rct.0b013e318181fab5.

[13] Radiology, A. C. of. ACR PRACTICE PARAMETER FOR PERFORMING AND INTERPRETING DIAGNOSTIC COMPUTED TOMOGRAPHY (CT) https://www.acr.org/-/media/ACR/Files/Practice-Parameters/CT-Perf-Interpret.pdf (accessed Jul 18, 2020).

[14] Amato, E.; Lizio, D.; Settineri, N.; Pasquale, A. D.; Salamone, I.; Pandolfo, I. A Method to Evaluate the Dose Increase in CT with Iodinated Contrast Medium: Dose Increase in CT with Iodinated Contrast Medium. *Med Phys*, 2010, *37* (8), 4249–4256. https://doi.org/10.1118/1.3460797.

[15] Sigal-Cinqualbre, A. B.; Hennequin, R.; Abada, H. T.; Chen, X.; Paul, J.-F. Low-Kilovoltage Multi–Detector Row Chest CT in Adults: Feasibility and Effect on Image Quality and Iodine Dose. *Radiology*, 2004, *231* (1), 169–174. https://doi.org/10.1148/radiol.2311030191.

Questionnaire

1) What level are you in : A) Level 6. B) Level 8. C) Internship. D) Radiographer. 2) Who decides on the routine CT scan Protocols in your department? A) Radiologists ( ) B) Radiographer ( ) C) Physicist ( ) D) Application specialist ( ) E) Other ( ) 3) Who decides if the patient should take contrast? A) Radiographer. B) Radiologist. C) Physicist. D) Clinical Physician. 4) In Abdomen CT scan what window will be better: A) Narrow window. B) Wide window.	7) Which of the following increase contrast resolution in CT? A) Lower mAs. B) Higher mAs. C) Thin slice thickness. D) Fast gantry rotation. 8) Narrow window width improves: A) Temporal resolution B) Spatial resolution C) Contrast resolution D) All of the above 9) which of the following does not affect noise in CT scan: A) Window level B) mAs C) Slice thickness D) kVp 10) The dose in CT scan can be reduced by which of the following parameters (assuming other factors are constant) A) Increase kVp B) Increase mAs

the employees in this study are technologists with diploma degrees and with lack of continuing professional education. In addition, CT parameters are automated, and this could be a factor further contributing to the respondents' wrong answers. Surprisingly, there is a lack of awareness and knowledge regarding CT parameters among the internship students, despite the fact that they are expected to have the highest level of knowledge among the categories of students. On the other hand, there was a wide range of answers given by Level 6 students who were unable to fully comprehend CT and are still undergoing the CT course. Level 8 students answered fairly well, however there were some limitations that would require more education, more courses, or more online resources. In order to maintain the accuracy of CT parameters, the need for ongoing education is inevitable.

References:

[1] AGENCY, I. A. E. *Dose Reduction in CT While Maintaining Diagnostic Confidence: A Feasibility/Demonstration Study*; TECDOC Series; INTERNATIONAL ATOMIC ENERGY AGENCY: Vienna, 2009.

[2] McCollough, C. H.; Guimarães, L.; Fletcher, J. G. In Defense of Body CT. *Am J Roentgenol*, 2009, *193* (1), 28–39. https://doi.org/10.2214/ajr.09.2754.

[3] Brenner, D. J.; Hall, E. J. Computed Tomography--an Increasing Source of Radiation Exposure. *New Engl J Med*, 2007, *357* (22), 2277–2284. https://doi.org/10.1056/nejmra072149.

[4] Pearce, M. S.; Salotti, J. A.; Little, M. P.; McHugh, K.; Lee, C.; Kim, K. P.; Howe, N. L.; Ronckers, C. M.; Rajaraman, P.; Craft, A. W.; et al. Radiation Exposure from CT Scans in Childhood and Subsequent Risk of Leukaemia and Brain Tumours: A Retrospective Cohort Study. *Lancet*, 2012, *380* (9840), 499–505. https://doi.org/10.1016/s0140-6736(12)60815-0.

[5] Program, N. T. *14th Report on Carcinogens*; Report on Carcinogens; Technical Report 9781523108527; U.S. Department of Health and Human Services, Public Health Service: Research Triangle Park, NC, 2016.

[6] Valentin, J. Managing Patient Dose in Multi-Detector Computed Tomography (MDCT). ICRP Publication 102. 2006, *37*, 1–79, iii.

[7] Amis, E. S.; Butler, P. F.; Applegate, K. E.; Birnbaum, S. B.; Brateman, L. F.; Hevezi, J. M.; Mettler, F. A.; Morin, R. L.; Pentecost, M. J.; Smith, G. G.; et al. American College of Radiology White Paper on Radiation Dose in Medicine. *J Am Coll Radiol*, 2007, *4* (5), 272–284. https://doi.org/10.1016/j.jacr.2007.03.002.

[8] Trattner, S.; Pearson, G. D. N.; Chin, C.; Cody, D. D.; Gupta, R.; Hess, C. P.; Kalra, M. K.; Kofler, J. M.; Krishnam, M. S.; Einstein, A. J. Standardization and Optimization of CT Protocols to Achieve Low Dose. *J Am Coll Radiology Jacr*, 2014, *11* (3), 271–278. https://doi.org/10.1016/j.jacr.2013.10.016.

[9] Foley, S. J.; McEntee, M. F.; Rainford, L. A. Establishment of CT Diagnostic Reference Levels in Ireland. *Br J Radiology*, 2012, *85* (1018), 1390–1397. https://doi.org/10.1259/bjr/15839549.

[10] Hollingsworth, C.; Frush, D. P.; Cross, M.; Lucaya, J. Helical CT of the Body: A Survey of Techniques Used for Pediatric Patients. *Am J Roentgenol*, 2003, *180* (2), 401–406. https://doi.org/10.2214/ajr.180.2.1800401.

[11] Foley, S. J.; Evanoff, M. G.; Rainford, L. A. A Questionnaire Survey Reviewing Radiologists' and Clinical Specialist

recommends that all protocols should be designed by medical physicist, radiographer and radiologist [12]. The base of such designs is to maintain acceptable image quality and appropriate radiation dose [13]. Also, contrast media is widely used in CT scans to improve visualization of vessels [14]. Radiologists are the ones who decide whether the patient should be given contrast or not.

Most students answered the question about the impact of changing pitch factor in CT correctly. However, 28.5% from level eight chose the wrong answer and those, (18.1%) from level six answered wrongly, (44.4%) of interns did not understand how pitch works, while surprisingly four out of six (66.6%) employees showed lack of knowledge when it comes to the relationship of pitch factor in CT. This might be due to the fact that the relation between pitch and dose is relatively complicated to CT users and it is not as straight forward as mAs. Previous published studies have reported the potential harm caused to patients when they are exposed to high radiation doses during angiographic studies [12, 15]. Furthermore, the respondents were asked about certain parameters such as “kVp”, “mAs”, “scan length” and “pitch”. Two out of six employees answered correctly, two out of nine internship students chose the correct answer, eight out of 11 level six students chose the correct answer and 12 out of 14 level eight students answered the question correctly which was the most respondents. This finding might be due to the fact that the dose reduction is confusing and can be implemented using different approaches based on the scan nature. Similarly, Foley et al discovered in their study that (14%) of radiographers believed that there is no reduction in patient dose when kVp is decreased from 120 to 100, and (38%) felt that image noise does not increase, while (48%) said that vessel enhancement does not improve during contrast examinations [11].

The respondents of the study was asked about the optimum scan window of the abdomen. Windowing is tricky question because it is being automated by the system. Although students from level eight should know the impact of changing windowing, they still could not answer this question correctly. This question is another proof that the concept of windowing is confusing. More than half of the respondents answered both of the questions above correctly due to the concept of noise being somewhat complex. These types of questions show lack of fully understanding CT parameter due to the fact that most of the parameters mentioned above are being automated by the system. Furthermore, lack of education or being unfamiliar with CT parameters could be another reason for the variation in the answers given.

The limitation of the study is the small sample size. Employees were not cooperative as much probably due to their duties in the hospital. Also, the duration of the study was not enough to collect as much responses as possible, students were busy with their studies and mid-terms.

A good recommendation for future research would be to repeat the study again with the next cohort of students and same cohort of employees (i.e., radiographers) after conducting continuing professional education training related to CT parameters utilization for various CT procedures in order to evaluate how such continuous training may enhance their knowledge level.

In conclusion, the level of understanding of the CT parameters varied among students and employees, due to the knowledge that most students have from their ongoing undergraduate studies while

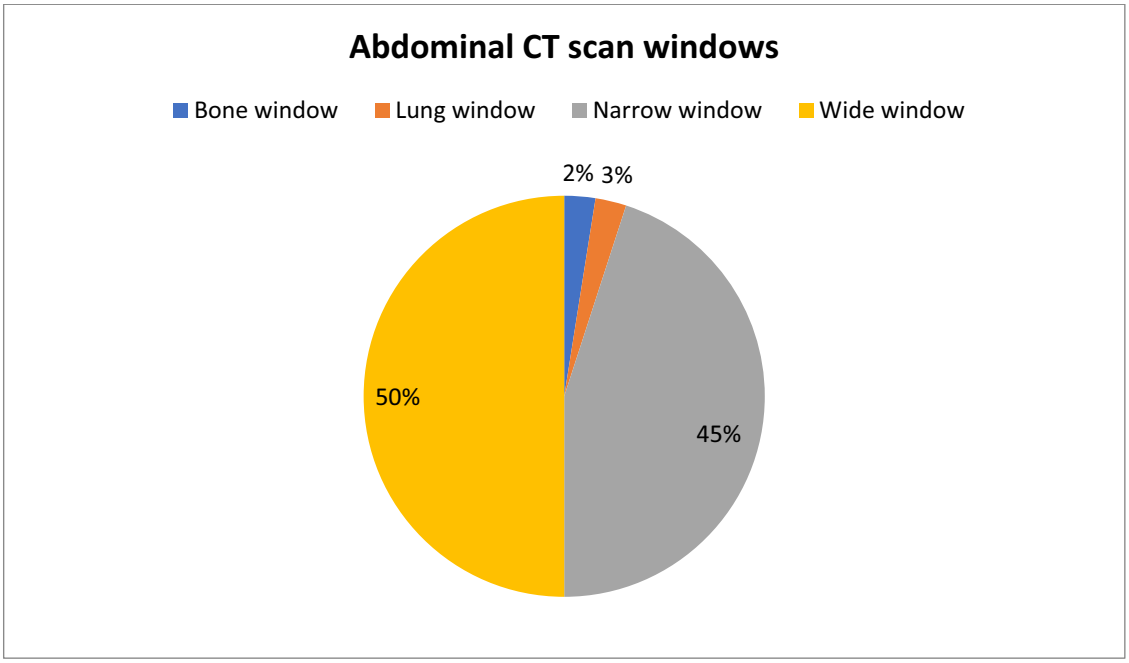

Fig.3. In Abdominal CT scan, what window will be better?

4. Discussion and Conclusion

There was a twofold difference in the answers between undergraduate students and employees despite the experience gap between both groups. Students were able to answer most of the questions correctly. Few of the questions sparked controversy due to the major difference of answers when both groups were compared to each other. Employees' answers greatly varied, most employees answered the ALARA and protocols related question correctly due to the guidelines of the radiology department they are working in. Among radiologists asked about CT protocols, 50% indicated they choose the protocols alone, the rest doing so in cooperation with a physicist (14%), a physicist and radiographer (14%), an applications specialist (7%), a physicist and applications specialist (7%) or with a combination of all (3%) of these individuals [11]. However, when employees were asked about technical parameters such as "optimum scan window", "pitch", "kVp" and "mAs" the majority answered incorrectly probably due to their academic status or most probably due to the fact the CT parameters are automated in the scanners they use. Based on this finding, radiographers should always update themselves and undergo in-house training. Also, raising their awareness about CT parameters can help minimize the radiation dose delivered to the patient. Ongoing education can be a critical point to be recommended to anyone working in the healthcare field especially radiologic technologists or clinical specialist radiographer due to the potential hazards of ionizing radiation.

The understanding of ALARA among the study respondents was almost understandable, due to the fact that the principle of ALARA is one of the radiation protection pillars. Indeed, more than 80% of all categories of respondents answered the meaning of ALARA correctly. The American College of Radiology (ACR)

When the respondents were asked about the optimal window for abdominal CT, one out of six employees chose the correct answer which is narrow window, six out of nine interns chose the correct answer, six out of 11 students from level six also chose the correct answer and finally five out of 14 students from level eight chose the correct answer (Fig. 3).

Also, when respondents were asked about what does narrow window improve, their answers varied, 30 respondents (75%) chose the wrong answer and 10 (25%) chose the correct one. 33.3% of employees chose the correct answer, 77.8% of interns chose the wrong answer, also 81.8% of level 6 chose the wrong answer and level 8 only 28.6% chose the correct answer. "Which of the following increases contrast resolution in CT" 18 (45%) respondents chose "higher mAs" which is the correct answer, 35% chose "thin slice thickness" and 20% chose "lower mAs". 26 (65%) chose "Window level" which is the correct answer when they were asked about "which of the following does not affect noise in CT scan". Similarly when asked about how to reduce noise a significant number of respondents (52.5%) answered "low pitch" would be beneficial. Two question were given to the respondents the first one is "which of the following does not affect noise in CT scan", 26 (65%) respond with "window level". The other question is "which of the following reduces noise", 21 (52.5%) correctly answered "low pitch

Table 4. Results of knowledge about tube potential

Results of reducing kVp			**Frequency**	**Percent (%)**
Employees		Better tissue contrast	4	66.7
		Reduced scan time	1	16.7
		Improved x-ray penetration	1	16.7
		Total	6	100
Students	**Internship (Level 10)**	Better tissue contrast	4	44.4
		Reduced scan time	5	55.6
		Total	9	100
	Level 8	Better tissue contrast	4	28.6
		Improved metal streak artifacts	6	42.9
		Reduced scan time	4	28.6
		Total	14	100
	Level 6	Better tissue contrast	7	63.6
		Improved metal streak artifacts	4	36.4
		Total	11	100

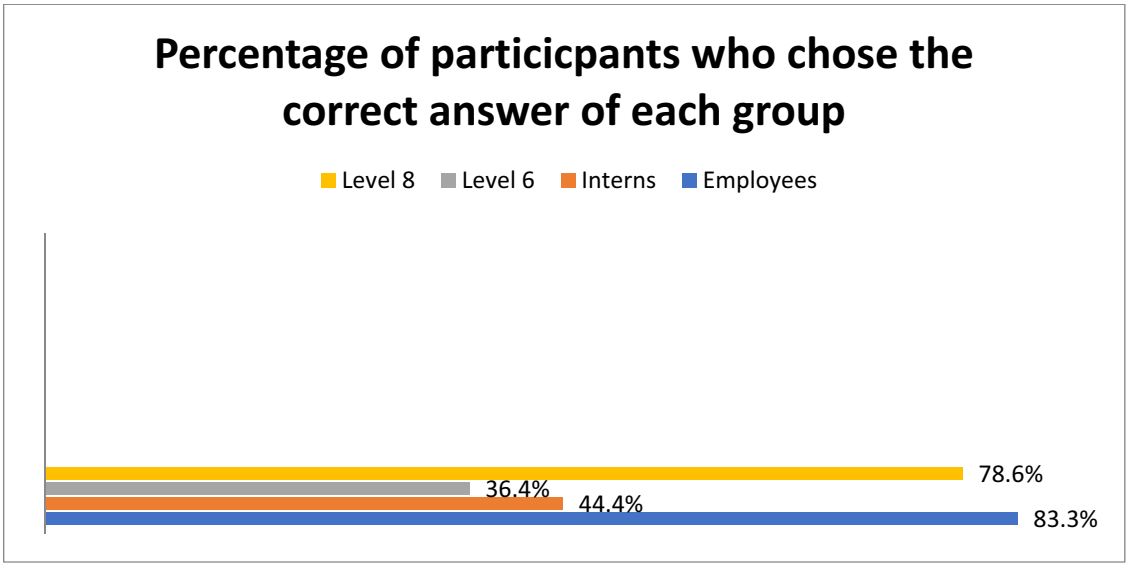

Fig.1. Who decides on the routine CT scan protocols in your department?

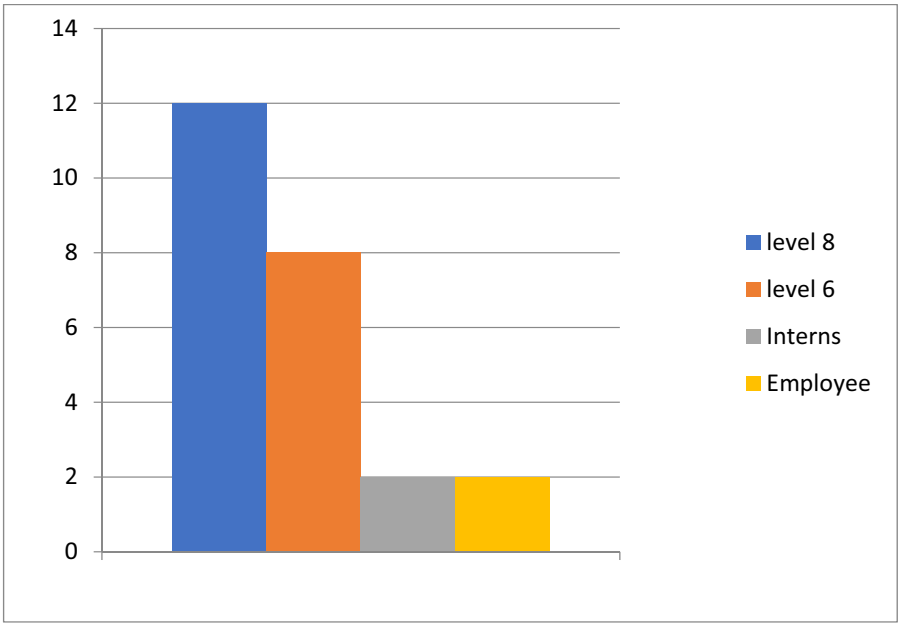

Fig.2. Total number of respondents answering the question correctly regarding ways to reduce dose in CT

They were also asked about what could happen when reducing kVp in CT scan, 47.5% answered “better tissue contrast” and 52.5% chose wrong answers. Table 4 shows the answers of the whole respondents when they were asked" reducing kVp in CT results in", only 47.5% of the whole respondents chose the correct answer which is "better tissue contrast" The answers varied because most CT users confuse kVp with mAs when it comes to which of these two improve tissue contrast.

six) employees were familiar with department protocol and knew that the radiologist is the one who decides if the patient should take contrast or not.

Table 3. Results of knowledge about the responsibility of protocol selection

Who decides on the routine CT scan protocols in your department?			**Frequency**	**Percent (%)**
Employees		Radiologists	6	100
Students	**Internship (Level 10)**	Physicists	4	44.4
		Radiographers	2	22.2
		Radiologists	3	33.3
		Total	9	100
	Level 8	Application specialists	3	21.4
		Others	1	7.1
		Radiographers	2	14.3
		Radiologists	8	57.1
		Total	14	100
	Level 6	Application specialists	2	18.2
		Others	2	18.2
		Radiographers	2	18.2
		Radiologists	5	45.5
		Total	11	100

Only nine respondents chose the wrong answer related to the question of ALARA, one out of six of the employees chose the wrong answer, four out of nine interns chose the wrong answer probably due to the fact that most of the answers were close to each other and almost identical, two out of 11 students from level six missed the correct answer and two out of 14 students from level eight chose the wrong answer (Table 2). The highest percentage of respondents who answered the question correctly are level eight (85.7% or 12 out of 14 students).

The respondents of the survey were asked about CT protocols, 100% or six out of six employees answered "radiologist". Internship students had multiple answers, 44.4% chose "physicist", 33.3% chose "radiologist" and 22.2% chose "radiographer". Level six students 45.4% chose "radiologist", 18.1% chose "radiographer", 18.1% chose "application specialist" and 18.1% chose "other". Level eight students, 64.2% answered "radiologist", 21.4% answered "application specialist", 14.2% answered "radiographer" and 7.1% answered "physicist" (Table 3 and Fig. 1).

Table 1. Demographic distribution

		Frequency	**Percent (%)**
Employees		6	15
Students	**Internship (Level 10)**	9	22.5
	Level 8	14	35
	Level 6	11	27.5
Total		40	100

Table 2. Results of knowledge of the "ALARA" principle

	Frequency	**Percent (%)**
Alarm Loss Activated Radiation Activated	1	2.5
As Low As Really Acceptable	1	2.5
As Low As Reasonably Achievable	31	77.5
As Low As Responsibly Acceptable	7	17.5
Total	40	100

Also, when respondents were asked about "who decides if the patient should take contrast media?", (63.7% or seven out of 11) students from level six had no idea on who decides if the patient should take contrast or not and (21.4% or three out of 14) students from level eight chose different answers. Also, (55.5% or five out of nine) interns had mixed opinions about the question, while (83.3% or five out of

specifically when inappropriately used, in addition to CT carcinogenic risk [5].

All CT examinations must follow the "As low as reasonably achievable" (ALARA) principle, which means that the practice of dose deliverey to patients should ensure that the benefits always outweigh the potential risk [6]. As CT technology has undergone many recent developments, there are some difficulties for CT users to be familiar with all system-specific features, especially if operating multiple scanner models from various manufacturers. Thus, the radiology technologists' knowledge of the various parameters that control the output of CT is important. There are number of CT parameters that the technologist can control to produce images with different quality levels and radiation dose delivery. However, default settings and manufacturers recommended protocols tend to focus on the quality of the image regardless of delivered dose [7].

To ensure optimization, operators must tailor the CT parameters to better match the region being scanned and patient size [8]. The literature showed massive differences in the radiation dose delivered across sites and countries, even for similar-sized patients [9]. This may be attributed to differences in CT equipment and to the scan protocols. Such dose disparities may also point to a lack of knowledge on how to manipulate and adjust CT parameters, especially on an individual basis. A previous study has reported that up to 25% of radiologists are unaware of specific CT parameters used for their routine examinations [10].

In this study, we aim to evaluate employees (i.e., radiographers) and undergraduate students' knowledge about CT parameters to improve healthcare and the outcome that lead to a good practice in the working environment. We further test whether students know more about CT parameters, compared to radiographers. We hypothesize that the respondents will have different levels of knowledge regarding the technicality of CT.

2. Material and Methods

This is a cross-sectional questionnaire study conducted at four hospitals in Medina, Kingdom of Saudi Arabia (KSA); after obtaining ethical approval from the ministry of health (MOH). A copy of the ethical approval was addressed to each hospital manager. The questionnaire used was adapted from previously published and validated survey [11], after obtaining proper permission. The survey consisted of 12 close-ended multiple-choice questions (MCQs) related to computed tomography technical parameters and CT exposure factors such as pitch, slice thickness and reconstruction algorithm. The survey was distributed with a comprehensive explanation to the respondents, and all of the responses remained anonymous with no questions related to identity were asked. Recruitment involved employees, students and interns (i.e., in their fifth year of the study plan "level 10"). Questionnaires were given to each participant via hard copy or online using a web link. All respondents were asked to return the questionnaire with no longer than five days from the day of receipt. Descriptive statistics were generated to show the variations in responses, using SPSS version 22.

3. Results

Out of the 40 questionnaires given to both radiographers and undergraduate students, 35% of the respondents were from level eight, 27.5% were from level six students, 22.5% were from internship students and 15% were from employees (Table 1).

JKAU: Eng. Sci., Vol. **32** No. 2, pp: 1 – 12 (1444 A.H. / 2022 A.D.)
Doi: 10.4197/Eng. 32-2.1

Evaluating the Knowledge of Computed Tomography Parameters between Radiographers and Undergraduate Students in Medina, Saudi Arabia

Abdulaziz Qurashi[1], Walaa Alsharif[1], Sultan Alshoabi[1], Nasser Almohsen[1], Saeed Aljohani[1], Essam Banoqitah[21], Ahmed Subahi[3,4], Shrooq Aldahery[5], Khalid Alshamrani[4,6]

[1] Diagnostic Radiology Technology Department, College of Applied Medical Sciences, Taibah University, Madinah, Saudi Arabia
[2] Nuclear Engineering Department, Faculty of Engineering, King Abdulaziz University, Jeddah, Saudi Arabia
[3] College of Science and Health Professions, King Saud Bin Abdulaziz University for Health Sciences, National Guard, Jeddah, Saudi Arabia
[4] King Abdullah International Medical Research Center, Jeddah, Saudi Arabia
[5] Applied Radiologic Technology, College of Applied Medical Sciences, University of Jeddah, Saudi Arabia
[6] College of Applied Medical Sciences, King Saud bin Abdulaziz University for Health Sciences, Jeddah, Saudi Arabia

Abstract. This study aims to evaluate employees (i.e., radiographers) and undergraduate students' knowledge of Computed Tomography (CT) parameters and their impact on image quality and radiation dose. A cross-sectional questionnaire study was conducted at four hospitals in Medina, KSA. The survey consisted of 12 close-ended multiple-choice questions related to computed tomography technical parameters. The survey was distributed with a comprehensive explanation to the respondents, and all of the responses remained anonymous with no questions related to identity were asked. Forty respondents were included in this study. Of those, 14 students were from level eight, 11 students were from level six, nine were interns and six were employees. There was a twofold difference in the answers between undergraduate students and radiographers despite the experience gap between both groups. Students were able to answer most of the questions correctly. Only few questions sparked controversy due to the major difference of answers when both groups were compared. The understanding level of the respondents varies among students and employees, where most of the correct answers were given by the former. The main reason for this could be due to the variation in the respondents' qualification. The employees in this study were only technicians with diploma degree.

***Keywords*:** Computed Tomography, Exposure parameters, ALARA, Radiation dose, Image quality

1. Introduction

Computed tomography (CT) technology has evolved over the last 50 years making it the modality of choice for different clinical questions. Nevertheless, the radiation dose from diagnostic CT is high owing to the long scan range acquired [1, 2]. As one of the largest contributors of ionizing radiation in the diagnostic medical field; concerns are rising regarding the potential harm that CT may cause on both individuals [3, 4], and respondents

[1] Corresponding Author: ebanoqitah@kau.edu.sa

Contents

Page

Editorial Board

JKAU: Eng. Sci., Vol. **32** No. 2, 100 Pages (1444 A.H. / 2022 A.D.) ISSN 1319-1047 Legal Deposit: 0300/14

Journal of

KING ABDULAZIZ UNIVERSITY

Engineering Sciences

Volume 32 Number 2

1444 A.H. / 2022 A.D.

Scientific Publishing Center
King Abdulaziz University
P.O. Box 80200, Jeddah 21589
Saudi Arbia
http://spc.kau.edu.sa

IN THE NAME OF ALLAH,

THE MOST GRACIOUS,

THE MOST MERCIFUL